UNIVERSITY OF CALIFORNIA

Santa Barbara

Comparative limnology of high-elevation lakes and reservoirs and their downstream effects

A dissertation submitted in partial satisfaction of the requirements for the degree of Doctor of Philosophy in Ecology, Evolution and Marine Biology

by

Adam Patrick Cohen

Committee in charge:

Professor John Melack, Chair

Professor Sally MacIntyre

Professor Scott Cooper

December 2019

The dissertation of Adam P. Cohen is approved.

_____
Scott Cooper

_____
Sally MacIntyre

_____
John M. Melack, Committee Chair

September 2019

Comparative limnology of high-elevation lakes and reservoirs and their downstream effects

ACKNOWLEDGEMENTS

First, I want to thank my partner, Alyssa, for all of her patience, support, kindness, and help over the past five years. I'm immensely thankful to have had her with me through this process, whether I was physically away for fieldwork or mentally preoccupied with graduate work. I am also thankful for the support (and occasional fieldwork help) from my parents, Lew and Kelly, and my sister, Julia.

I'm grateful to everyone who taught me to love the outdoors as I was growing up, especially the Sierra, as I don't think I would have found my way into a graduate degree at all without that passion. For work in the lab and field, I'm lucky to have had a fantastic crew of undergraduate assistants: Patty Hensley, Erik Young and Allyssa Blalock, who all dealt with long days and sometimes less than ideal conditions with good spirits. I am also grateful for the undergraduate students of the courses I TAed each year, who were a pleasure to teach, and helped me learn to better communicate ideas and enthusiasm for science. The graduate students in Noble Hall are a wonderful network of support, and I'm deeply appreciative of their kindness. They have created a supportive environment that is a major asset to EEMB and I hope the tradition endures.

I want to thank each member of my committee for encouraging me to always improve my work. John Melack, who allowed me to design my own projects, and constantly helped me refine my intellectual approach to research questions; Sally MacIntyre, who was an inspiration to myself and undergraduates in spreading the joy of learning and teaching, and taught me valuable skills in the process; and Scott Cooper, whose thorough readings of my dissertation chapters and willingness to discuss them with me vastly improved my work.

VITA OF ADAM P. COHEN

September 2019

Education

PhD	UC Santa Barbara	Ecology, Evolution, and Marine Biology	2019
BA	UC Berkeley	Environmental Earth Science	2014
BS	UC Berkeley	Conservation and Resource Studies	2014

Awards

Worster Award	2017
California Lake Management Society Student Scholarship	2017
Valentine Reserve Fund Graduate Student Scholarship	2016-17
NSF Research Experiences for Undergraduates Supplement	2016

Teaching Experience

Chemical and Physical Methods of Aquatic Environments	2016-19
Lakes and Wetlands	2015, 2017-18
Worster Award Mentor	2017
NSF Research Experiences for Undergraduates Mentor	2016
Introductory Biology Laboratory	2015

Publication

Cohen, A.P., and J.M. Melack. 2019. Carbon dioxide supersaturation in high-elevation lakes and reservoirs in the Sierra Nevada, California. Limnology and Oceanography, doi:10.1002/lno.11330.

ABSTRACT

Comparative limnology of high-elevation lakes and reservoirs and their downstream effects

by

Adam P. Cohen

Reservoirs are abundant worldwide, and have profound effects on downstream flow, water chemistry, and downstream biotic communities. However, studies focused on reservoir effects rarely contrast them with lakes, which provide a comparison of natural climatic conditions without the influence of reservoir management. I compared five high-elevation lakes and five reservoirs in the Sierra Nevada, over three years which encompassed a wide range of snowpacks and flow regimes. I sampled lake, reservoir, and outlet stream water chemistry year-round across the three years to quantify seasonal effects of reservoir management. In addition to outlet water chemistry, I collected benthic macroinvertebrates from lake and reservoir outlets during the ice-free season in conjunction with discharge to determine the effects of reservoir management on downstream invertebrate communities. In 2017, I measured aquatic carbon dioxide and diffusive flux from lakes and reservoirs, beginning under ice and until the end of the ice free season, to determine potential sources of high-elevation aquatic CO_2 supersaturation and characterize ice-free season CO_2 temporal dynamics.

Lake and reservoir nutrient concentrations did not differ in any season or year across the study period. Linear mixed models developed surface and bottom water nutrient concentrations showed that the primary controls were related to basin characteristics and snowpack, but reservoir management in the form of seasonal drawdown was a significant predictor of surface nitrate and both hypolimnetic ammonium and SRP, and indicated that

reservoir water deep-release export diminished hypolimnetic nutrient accumulation. Reservoir mean annual discharge was elevated relative to lakes, which in summer and fall of 2016 and 2017 caused significantly higher export of nutrients from reservoirs. However, elevated ammonium export did not cause divergence of lake and reservoir invertebrate assemblages in those seasons, nor did they differ in any season. Other flow metrics, such as peak annual flow and the recession period, were similar between lake and reservoir outlets across years despite reservoir management. Instead, non-metric multidimensional scaling showed that invertebrate communities were related to elevated flow, but not related to low flow metrics such as baseflow and minimum flows, which were greater below reservoirs. Reservoir management altered flow regimes and nutrient flux, but interannual climactic variability was more important for determining invertebrate community structure.

Carbon dioxide was supersaturated in lake and reservoir surface waters for most of the ice-free season of 2017 despite low rates of ecosystem metabolism. Diffusive flux highest for the first 40 days after ice-off, and did not differ significantly between lakes and reservoirs, but was low relative to other water bodies. Linear mixed modeling indicated that the summer CO_2 concentrations were primarily related to the duration of ice cover, allowing CO_2 to accumulate under ice, which indicates that annual snowpack is a major determinant of summer CO_2 evasion.

.

TABLE OF CONTENTS

CHAPTER ONE

Differences in nutrient chemistry between high-elevation lakes and reservoirs

Abstract

Nutrient concentrations in undeveloped high-elevation lakes results from watershed characteristics and amount of snow, but how reservoir management mediates nutrient levels in these oligotrophic systems is not well understood. This study compares the nutrient concentrations of five lakes and five reservoirs at high-elevation in the Sierra Nevada of California through all seasons in 2015, 2016 and 2017, and is the first study to characterize high Sierra reservoir limnology. Maximum annual snow water equivalent increased from a minimum of 1.3 cm in 2015 to a maximum of 208 cm from 2015 to 2017, to which reservoir management was responsive, providing a gradient of conditions with which to compare lake and reservoir surface, hypolimnion, and outlet nitrate, ammonium, and soluble reactive phosphorus (SRP) concentrations. Lake and reservoir nutrient concentrations were generally low, and not significantly different ($p > 0.05$) in any season. Nutrients accumulated in both lake and reservoir hypolimnia, but they were more often discharged from deep-release reservoirs, resulting in significantly higher outlet concentrations and export in the stratified summer period, and in fall when stratification had weakened. Linear mixed models developed for each nutrient indicated primary controls were related to basin characteristics and snowpack; reservoir drawdown area was a significant predictor of surface nitrate and both hypolimnetic ammonium and SRP, and suggested that reservoir deep-release prevented accumulation of ammonium and SRP to the extent observed in lakes. Mixed models explained most variability of nutrients, strongly for hypolimnetic ammonium (R^2 conditional = 0.82), and nitrate (R^2 conditional = 0.63), but not well for surface ammonium and SRP (R^2 conditional = 0.23, R^2 conditional = 0.24, respectively). Elevated reservoir discharge and

nutrient export late in the ice-free season contributes to disruption of the natural snowmelt-dominated flow regime and may have important implications for downstream ecosystems,

Introduction

Solute concentrations in montane lakes are determined by catchment characteristics and processes, including weathering of the underlying lithology (Brown and Lund, 1991), atmospheric deposition (Blanchard and Tonnessen, 1993; Marchetto et al., 1995; Kamenik et al., 2001; Melack et al., 1997), vegetation (Kopàcöek et al. 2000), landscape position (Sadro et al. 2012), and snowpack levels (Sickman et al. 2003). Snowpack influences variables and processes in high-elevation lakes, including seasonal and interannual patterns in nitrate concentrations and export (Williams et al., 1995, Melack et al., 1998; Brooks and Willams, 1999), temperature (Sadro et al., 2019), phytoplankton productivity (Sadro et al., 2018), and carbon dioxide evasion (Cohen and Melack, 2019). The extent to which reservoir management practices alter the effects of interacting catchment and hydrological characteristics on high-elevation, oligotrophic reservoirs is not well understood. At lower elevations, management practices (e.g., deep water release) and watershed characteristics can influence reservoir water quality (Hannan, 1979; Lee et al., 2009; Park et al., 2014) and primary productivity (Knoll et al., 2003), but limited research on high elevation reservoirs has focused on the biological impacts of water level fluctuations, rather than on water quality and primary production (e.g., Hirsch et al., 2017; Carmignani and Roy, 2017). Reservoir management practices, such as hypolimnetic release, decrease downstream water temperature (Dickson et al., 2012), but their effects on downstream nutrient chemistry are less clear, with one study documenting increases in nitrate concentrations (Kijowska-Strugała et al., 2016),

but others showing no change in nitrate, ammonium, or phosphate concentrations (Voelz and Ward, 1989; Kijowska-Strugała et al., 2016). Across northern latitudes, reservoir total phosphorus concentration is higher and water transparency lower than natural lakes, which reflects greater depth of natural lakes and lower agricultural production in their watersheds (Doubek and Carey, 2017), but these findings will not apply for headwater systems without agricultural production or anthropogenic shoreline development.

In the Sierra Nevada of California, catchment geology, atmospheric deposition, and soil pools are the primary sources of nutrients in high-elevation lakes. Phosphorus in Sierra surface waters is obtained primarily from soils derived from weathered granitic bedrock (Homyak et al., 2014a), and wet and dry deposition (Jassby et al. 1994; Vicars and Sickman, 2010), with lake sediments constituting a minor source (Homyak et al., 2014b). Nitrate is primarily flushed from soil pools and talus during snowmelt, with additional nitrate being derived from the snowpack (Sickman et al., 2003). Ammonium is deposited on Sierra watersheds in both rain and snow and can be produced by remineralization of organic matter, but most is utilized (Melack et al., 1998) or nitrified (Williams et al., 1995) within a basin. Elevated ammonium concentrations have been observed under hypolimnetic anoxic conditions, although these are infrequent in Sierra lakes (Melack et al., 1998).

The high Sierra Nevada (> 2500 m) in California contains 24 reservoirs, which represent 16% of the total lake and reservoir surface area in the range but are <1% of the more than 3,000 lakes and reservoirs found there (> 0.5 ha). Unlike foothill reservoirs, high-elevation reservoirs are usually natural lakes enlarged by a dam, their catchments are undeveloped and are often protected, they are ice-covered for a portion of the year, and hydrological patterns are dominated by snowmelt. After dam construction, reservoirs differ

from natural lakes in several important ways, including deep-water releases from the base of the dam, and large seasonal and interannual fluctuations in water level and discharge. Despite their relatively large surface areas, and importance to downstream ecosystems and as a water supply, little research has been conducted on high Sierra reservoirs. A single study commissioned by one of the dam operators, Southern California Edison (SCE), was conducted from 1985 to 1987 on four Sierra reservoirs (South, Sabrina, Gem, Waugh) where major ions were measured once, and vertical profiles of water temperature, dissolved oxygen (DO) concentration, and pH were measured six times, with one profile conducted under winter ice (Lund, 1987). Seasonal and interannual variability in limnological characteristics of Sierra reservoirs and effects of water management practices on downstream nutrients have not been examined.

Studies on the ecological impacts of water level fluctuations have often focused on initial reservoir filling and subsequent decreases in water quality in young reservoirs (Hirsch et al., 2017); however, physical and chemical fluctuations in reservoirs > 50 years old have been largely unstudied (Zohary and Ostrovsky, 2011). Littoral zones are the most productive areas in oligotrophic montane lakes (Hampton et al., 2011; Sadro et al., 2011b), and are disturbed by water level fluctuations in reservoirs, which can reduce primary productivity, particularly where sediments are exposed to freezing (Hirsch et al., 2016). Nutrient cycling is disturbed by water level fluctuations, because the exposure of sediments to wet-dry cycles can reduce their ability to adsorb phosphorous (Watts, 2000), decrease littoral zone organic matter content by limiting macrophyte growth (Furey et al., 2004), increase nitrate release on rewetting (Cooke et al., 2003), increase ammonium release even under oxygenated

conditions (McGowan et al., 2005), and concentrate nutrients in the hypolimnion as water levels decrease (Zohary and Otrovsky, 2011).

This study compares five reservoirs and five lakes in the high Sierra over three years for two purposes: to characterize the nutrient levels of reservoirs and comparable lakes within and across years and to determine the effects of water management practices on reservoir and outlet nutrient chemistry across years with variable snowpack. I predicted that lake and reservoir surface nutrient concentrations would be comparable given the similarities of their respective watersheds. In contrast, I predicted that hypolimnetic nutrient concentrations and export would differ between lakes and reservoirs because of bottom releases and elevated late-summer flows from reservoirs, resulting in elevated nutrient concentrations in reservoir outlet streams during stratified periods and early fall. Interannual variability in snowpack is expected to alter lake and reservoir characteristics primarily by altering the duration of ice cover and the duration of the subsequent ice-free period.

Methods

I studied five lakes and five reservoirs in the eastern Sierra Nevada, California, within or adjacent to protected wilderness areas. Beginning in summer 2015, three lakes and three reservoirs were sampled, and an additional two lakes and two reservoirs were added in spring 2016, then sampled through fall 2017 (Figure 1). The sites are subalpine to alpine, ranging from 2782 to 3383 m a.s.l., (Table 1) in recently glaciated (<12,000 y.a.) watersheds with poor soil development underlain primarily by granitoids with sporadic metasedimentary and metavolvanic rock. Watershed vegetation is dominated by alpine shrubs, whitebark pine (*Pinus albicaulis*), sporadic wet meadows, and at lower elevations lodgepole pine (*Pinus*

contorta). The five reservoirs are enlarged natural lakes that were constructed in the early 1900s (Ellery, 1927; Tioga, 1928; Saddlebag, 1921; South, 1910; Sabrina, 1908), and are currently managed for recreation, hydropower generation, domestic use, and irrigation. The five lakes were selected for their proximity (Figure 1) and general similarity to the selected reservoirs (Table 1), but surface areas and shoreline development were higher in reservoirs than lakes. Introduced trout (*Oncorhynchus mykiss*, *Oncorhynchus mykiss aguabonita*, *Salvelinus fontinalis*, *Salmo trutta*) were present at all sites, and were stocked annually in all reservoirs as well as one lake (Rock Creek).

Each site was typically sampled at least once per season from summer 2015 through fall 2017 (Supplement 1), where seasons are defined as those typical of dimictic lakes: summer stratification, fall mixing, winter inverse stratification, and spring mixing. Water column profiles of dissolved oxygen (DO) concentration, temperature, and specific conductivity were measured at 1 m intervals during each visit using a Yellow Springs Instruments 2030, DO-temperature-conductivity meter (resolution: ± 0.2 mg DO L^{-1}, ± 0.3 °C, ± 1 μS cm^{-1}). When sites were stratified, thermoclines were identified in the field from each vertical profile, as the depth at which temperature decreased most rapidly. When lakes or reservoirs were thermally stratified, surface water samples were collected at ~0.20 m depth in high density polyethylene bottles and hypolimnetic samples were collected 1 m below the thermocline with a Kemmerer bottle, but only surface samples were taken when the water column was well-mixed (isothermal). For samples taken under ice when inverse stratification was observed, samples were collected from 1 m below the ice bottom and from the upper 1 m of the 4°C water layer. Profiles of photosynthetically active radiation (PAR) were collected

seasonally, using a LI-COR LI-192 underwater quantum sensor. The PAR attenuation coefficient, k_d, was then computed using the Beer-Lambert law.

Dissolved nutrient samples were filtered through 1.0 μm polycarbonate membranes (Nucleopore) < 6 hrs after collection, and frozen for up to 4 months before analysis. Chlorophyll-a (chl-a) samples were collected on 0.45 μm nitrocellulose filters (Millipore) and frozen for up to 1 month prior to analysis, then extracted in 90% acetone for 24 hours prior to analysis on an Abbott V-1100D spectrophotometer (Lorenzen, 1967; detection limit = 0.1 μg L^{-1}). DOC samples were filtered through precombusted (2 hours, 500°C) 0.7 μm nominal pore size Whatman GF/F filters (Wilde et al., 2014) into precombusted (12 hours, 500°C) 40 mL borosilicate vials with Teflon-coated septa. DOC samples were acidified with hydrochloric acid to pH < 2, and analyzed using the high temperature combustion method on a Shimadzu TOC-V (± 1.5% measured concentration; Carlson et al., 2010).

Nitrate, ammonium, and soluble reactive phosphorus (SRP) concentrations were measured on a Lachat Automated Ion Analyzer (Hach Company, Loveland, CO, USA), using cadmium reduction (detection limit = 0.3 μM, ±5%; Strickland and Parsons, 1972), indophenol red ammonia detection (detection limit = 0.3 μM, ±5%; Williason and Johnson, 1986), and phosphomolybdate methods (detection limit = 0.2 μM, ±10%; Grasshoff 1976), respectively. For samples collected between July and August in 2017, the phosphomolybdate and fluorometric o-Phthalaldehyde methods (Taylor et al. 2007) were used to determine SRP and ammonium concentrations within 24 h of sample collection using filtered water that had not been frozen, which reduced the detection limit (ammonium detection limit = 0.1 μM, SRP detection limit = 0.1 μM).

Lake volumes were obtained in three ways: (1) for reservoirs, elevation-storage tables were provided by the reservoir operator, Southern California Edison (SCE); (2) for three lakes (Spuller, Ruby, Crystal), volumes were obtained from Melack et al. 1998; and (3) for the remaining two lakes (Lower Gaylor, Rock Creek), hypsometric curves were generated. A Hook-5 (Lowrance, Tulsa, OK) sonar system was used to record depth and location across transects of each lake, which were then used to calculate hypsometric curves, using QGIS 3.2 (QGIS Development Team, 2019). Reservoir exposed areas were computed from elevation-storage tables and daily water surface level data obtained from SCE. Lake water levels were observed to fluctuate by up to 0.2 m but were not measured fluctuations resulted in little exposure of lake littoral zones, so lakes were treated as "full" for the duration of the study. Watershed areas were calculated from 1/3 arc-second resolution digital elevation models (3D Elevation Program, USGS, https://www.usgs.gov/core-science-systems/ngp/3dep), lake area and lake network number from the California Department of Fish and Wildlife's (CADFW) California Lakes GIS product (https://data.ca.gov/dataset/california-lakes), land cover type from CALVEG (Region 5, Existing Vegetation, https://data.fs.usda.gov/geodata/edw/datasets.php), and basin geology from Jennings et al. (1997), digitized by Saucedo et al. (2000). The shoreline development factor (SDF) was computed using lake perimeters following Wetzel (2001). Watershed, lake, and land cover type areas were calculated using ArcMap 10.4 (Environmental Systems Research Institute, 2016).

Basin April 1 snow water equivalent (SWE), treated as annual maximum SWE, was obtained from California Cooperative Snow Survey (https://cdec.water.ca.gov/snow/) stations nearest to each site (0.25 to 8 km). Ice-on and ice-off dates for all sites were

determined from Landsat 7 and 8 satellite imagery (landlook.usgs.gov). Images were repeated every 16 days, with an offset of 8 days between Landsat 7 and 8 satellites, ice-on and ice-off could be determined within ± 4 day certainty, with sporadic verification by direct field observations. Otherwise, dates were chosen as the midpoint between images before and after ice-on or ice-off.

At reservoir outlets, discharge was recorded by SCE and reported annually to the US Geologic Survey, with the data available in the National Water Information System (NWIS). At each lake outlet, pressure transducers were installed (Solinst Levelogger 3001 M5, ± 0.3 cm), with compensation for atmospheric pressure by the associated deployment of an atmospheric pressure logger (Solinst Barologger, ± 0.05 kPa; Spuller, Gaylor lakes) or by atmospheric pressure data obtained from the US Army Corps of Engineers' Cold Regions Research and Engineering Laboratory and the University of California, Santa Barbara Energy Site at Mammoth Mountain (Bair et al. 2015; Rock Creek, Ruby, Crystal lakes). Discharge also was measured manually during the ice-free season with a measuring rule or tape and a current meter (Marsh McBirney Flo-Mate 2000) to develop rating curves for each lake outlet. Each rating curve was then used to compute discharge from the pressure data.

To measure metabolism, optical dissolved oxygen loggers (D-opto, Zebratech, ±0.02 mg DO L^{-1}) were deployed for 24 h at two lakes and two reservoirs in late July to mid-August and at one lake and one reservoir in late August to mid-September. Instruments were calibrated in 0% and 100% saturation solutions prior to deployment. Loggers were deployed at two to four depths, dependent on maximum lake depth, and recorded DO every 10 minutes. A variation of the mass balance method (Sadro et al. 2011a) was used to calculate metabolic rates from data averaged hourly. Net ecosystem production (NEP) was calculated

for each hourly average as NEP = ΔDO + F_{DO}/MLD, where NEP (g m^{-3}) is the net change in dissolved oxygen that is attributed to biological processes, ΔDO (g m^{-3}) is the change in dissolved oxygen as measured directly by each logger, F_{DO} (g m^{-2}) is flux across the air-water interface, and MLD (m) is the mixed layer depth. Flux of oxygen into or out of the lake or reservoir due to atmospheric gas exchange was calculated as: $F_{DO}= k_{DO}(C_w-C_{aq})$, where k_{DO} (m h^{-1}) is the coefficient of gas exchange of oxygen at given temperature, C_w (g m^{-3}) is the concentration of dissolved oxygen at the water surface, and C_{aq} (g m^{-3}) is the saturation concentration of dissolved oxygen at the water surface. C_{aq} was calculated from measured water surface temperature and local atmospheric pressure, k_{DO} was estimated from k_{600} as modeled from wind speed, and Schmidt numbers, which were used to compute the gas transfer coefficient of oxygen, were calculated based on surface water temperature (Wanninkhof 2014). Wind speeds were obtained from the California Data Exchange Center (CDEC), which included data from California Department of Water Resources meteorological stations ranging from 0.5 km (Rock Creek) to 6 km (Saddlebag) from each study site. At Rock Creek Lake in July, wind speed data from a station 13 km away were used because repairs were being conducted at the nearer station. Wind data from these stations introduce error into my estimates of O_2 flux, but approximate local high-elevation wind conditions.

Calculated NEP hourly averages for each depth layer were summed across each 24 h deployment to determine daily rates of NEP and community respiration (CR) was determined by summing calculated nighttime NEP and dividing by the duration of night to obtain an hourly rate of CR, which was then used for entire deployment duration. GPP was then calculated from the difference of NEP and CR where CR is a negative value. Whole-lake

areal rates of metabolism were computed by multiplying volumetric metabolic rates by the volume of water at each logger depth, summing those rates for all depths, and dividing by the surface area of the lake.

NEP hourly averages were summed across each deployment to determine daily rates of NEP; community respiration was determined by summing calculated nighttime NEP and dividing by the duration of night to obtain an hourly rate of CR. GPP was then calculated from the difference of NEP and CR, where CR was treated as a negative value. Whole-lake areal rates of metabolism were computed by multiplying volumetric metabolic rates by the volume of water at each logger depth, summing those rates for all depths, and dividing by the surface area of the lake. Although horizontal variation in metabolic rates has been observed in mountain lakes (Sadro et al., 2011b), measurements from the lake center provide a reasonable approximation of lake metabolism (Sadro et al., 2011a).

To determine explanatory variables nutrient concentrations across all seasons, mixed models were developed for each 'layer' (surface, hypolimnion). Continuous, measured or computed environmental variables and 'type' (lake or reservoir) were included as fixed effects. Calendar sampling date was treated as a random effect because sites were sampled repeatedly at irregular intervals. Concentrations that were below our limits of detection were entered into the dataset as half of the detection limit. Explanatory variables were checked for collinearity using a Pearson's *r* correlation matrix, where variables with a known mechanistic connection to nutrient concentrations were retained and other variables, correlated with these, were dropped. Elevation and alpine shrub area, as well as maximum reservoir or lake surface area and watershed area, were correlated, thus elevation and surface area were not included in initial models. Explanatory variables were then scaled by centering around an adjusted

mean of zero with a standard deviation of 0.5, and measured nutrient concentrations were square-root transformed, satisfying parametric assumptions. The function 'dredge' in *MuMIn* was used for automated model selection, to test all possible combinations of an initial linear mixed model that included all random and fixed effects. Interactive effects were included where fixed effects were thought to be significant in only some seasons. The initial fixed effects were: type, days since ice-off, shoreline development factor, season, duration of the ice-covered period, maximum depth, watershed area, current area exposed by water level declines, annual maximum exposed area, dissolved oxygen concentration, outlet discharge, water residence time, percent of the watershed that was bare, wet meadow, alpine shrub, montane chaparral, and conifer forest, percent of the watershed that was underlain by granitic rock, hornfels, glacial till, and gabbro, and interactive effects of season*depth and maximum exposed area*season. The final model for each response variable was selected using minimum values of the Aikake information criterion, and no additional models are discussed here because other models had AIC values > 2 over the best model. Model fit was determined with a mixed model pseudo-coefficient of determination (Nakagawa et al., 2017), which produces two values, one which includes random effects (R^2 conditional, 'R^2c'), and one which does not (R^2 marginal, 'R^2m'). A comparison of the two values then indicates the importance of the random effect (sampling date).

I also examined relationships between pairs of variables using Spearman's rank correlations and compared variable values for lakes versus reservoirs using Mann Whitney U tests, and Benjamini-Hochberg adjustment for comparisonwise error. Statistical analyses were performed using R, in RStudio, with the base *stats* package. Linear mixed models were developed in R using the packages *MuMIn* and *lme4*.

Results

Annual peak snowpack increased over the study period, beginning with 5% of the April 1 long-term Sierra average in 2015, 73-88% in 2016, and 163-173% in 2017. Both lakes and reservoirs remained ice-covered for over half of the year, for approximately 7 months (Table 2). Ice-off in 2017 occurred weeks to months later than in 2016 and 2015, in conjunction with substantially higher SWE. There were no significant differences in peak SWE between lakes and reservoirs in any study year (2015: n lake = 3, n reservoir = 3; 2016-2017: n lake = 5, n reservoir = 5). All sites were dimictic: inverse stratification developed in winter under ice and persisted until ice-off, followed by a brief period of isothermy, then the development and persistence of summer stratification until a second, brief isothermal period in late fall before ice cover (Figure 2). Spring surface ($p = 0.038$; n lake = 5, n reservoir = 5) and outlet ($p = 0.007$; n lake = 5, n reservoir = 5), and summer outlet ($p = 0.008$; n lake = 5, n reservoir = 5), temperatures were higher in 2016 than 2017, summer outlet temperatures were higher in 2015 than 2017 ($p = 0.016$; n lake = 5, n reservoir = 5), but temperatures were similar between years for other seasons and layers. After applying Bejamini-Hochberg corrections for comparisonwise error for multiple comparisons, temperatures for different layers and the outlets were not significantly different between lakes and reservoirs for individual seasons, either averaged across years or within individual years.

Hypoxia (DO < 2 mg L^{-1}) and anoxia were observed rarely in bottom waters of both lakes and reservoirs, in winter, summer and fall (Figure 3). Dissolved oxygen remained high in all other cases, and was not different throughout the study period between lakes and reservoirs in any season (n lake = 96, n reservoir = 86). k_d varied by nearly an order of

magnitude over all three years and all sites. A minimum value of 0.04 m^{-1} was obtained in spring 2016 (Saddlebag Reservoir) and a maximum value of 0.56 m^{-1} was obtained in summer 2016 (Lower Gaylor Lake). The lowest values were generally measured in spring and the highest in fall with k_d being positively correlated with water residence time ($r = 0.38$, $p < 0.00001$, n lake = 96, n reservoir = 86). Concentrations of chlorophyll-a (chl-a) were low (80% of samples were below 2 $\mu g\ L^{-1}$). Metabolic rates also were low and ranged from net autotrophy to heterotrophy (NEP: -14.2 to 33.9 $mmol\ m^{-2}\ d^{-1}$) (Table 3).

The extent of water level fluctuations varied across reservoirs (Figure 4). Except for Ellery which fluctuated randomly over the study period, reservoirs generally had low water levels from summer 2015 to spring 2016, associated with a drought, but filled in subsequent springs and early summers with drawdown through the following seasons until snowmelt. Water flowed over the dam at Tioga reservoir for several days in July 2016, and at Tioga, South, Ellery, and Saddlebag reservoirs in July 2017. No data are presented for Tioga reservoir from October 2016 - April 2017, because the reservoir was drained to its minimum storage level during repairs on the dam. Several lake outflows began flowing only intermittently through time in late summer of 2015 and 2016 (Gaylor, Crystal, Spuller), whereas all reservoirs but Ellery continued flowing year-round. Outlet nutrient concentrations could not be collected where and when flow had ceased, and export in those cases was recorded as 0. Ellery discharge was sporadic in 2015 and 2016, but more closely resembled lake flow in 2017. A large flow event occurred at Ruby Lake in winter 2017, associated with an avalanche during a major snowfall event. Mean daily reservoir discharge on sampling dates was nearly three times that of lakes in summer and over eight times greater in fall (Table 4).

Replicates used for nutrient analyses by year, season, layer, and type are presented in Supplement 1. Between summer of 2015 and fall of 2017 concentrations of nitrate, ammonium, and SRP ranged from below detection (0.3, 0.2, 0.2 μM respectively) to 24, 26, and 4.5 μM, respectively, across all water bodies (Figure 5). Surface and hypolimnetic nitrate concentrations generally peaked in winter or spring, then steadily decreased into fall. Seasonal trends of hypolimnetic ammonium and SRP were more variable, occasionally increasing in stratified periods (winter, summer) and during fall. Surface ammonium and SRP were low and near our detection limit throughout the study period. Mean lake and reservoir nutrient concentrations in each season in each water layer and the outlets were not significantly different ($p > 0.05$, Mann Whitney U tests with Benjamini-Hochberg corrections) (Fig. 5).

Seasonal mean outlet export of all three nutrients, the product of concentration and discharge, was significantly higher from reservoirs than lakes in summer 2017 (Figure 6), and ammonium export was also higher in fall of both 2016 and 2017 (all p values < 0.01, Mann Whitney U tests with Benjamini-Hochberg corrections). Nutrient export did not differ between lakes and reservoirs in any other season-years ($p > 0.05$, Mann Whitney U tests with Benjamini-Hochberg corrections).

Associations of nutrient concentrations with environmental variables

Final explanatory models for each nutrient and layer, as selected by minimum AIC values, are presented in Table 5. Models explained 10-82% of the variation in nutrient concentrations in different layers, and were particularly weak where concentrations were low, such as for surface ammonium and SRP concentrations ($R^2c = 0.23$ and 0.24). Final models explained more of the observed surface nitrate variation ($R^2c = 0.73$) than variation in

surface ammonium or SRP concentrations likely due to their low levels, but final models explained more of the variation in hypolimnetic ammonium concentrations ($R^2c = 0.82$) than in hypolimnetic nitrate ($R^2c = 0.63$) or SRP ($R^2c = 0.28$) concentrations.

Watershed characteristics, such as coverage by bare rock, conifer forest, chaparral, alpine shrubland, glacial deposits, and wet meadow, were included in all models, except that for hypolimnetic SRP concentrations. Wet meadow was a significant positive predictor for surface ammonium and SRP concentrations, chaparral was a significant positive predictor of surface SRP and negative predictor of hypolimnetic nitrate concentrations, alpine shrubland, likely a proxy for elevation, was a significant negative predictor for hypolimnetic ammonium concentration, glacial till was a negative predictor for hypolimnetic nitrate concentration, conifer coverage was a positive predictor of surface nitrate concentration, and proportion of bare space was a predictor of surface and hypolimnetic nitrate concentrations. The shoreline development factor, which was significantly higher for reservoirs and ranged from 1.19 to 1.81 across sites (Table 1), was included as a significant negative fixed effect in models for hypolimnetic nitrate concentration. Days since ice-off or ice period were included in four models (surface nitrate; hypolimnetic nitrate, ammonium, SRP). Dissolved oxygen concentration was a significant negative predictor of hypolimnetic concentrations of all three nutrients. 'Type' of water body (lake or reservoir), was a significant negative predictor, indicating lower concentrations in reservoirs, of hypolimnetic ammonium and SRP. Current or maximum reservoir area exposed was included as a term in models for surface nitrate, and hypolimnetic ammonium (in winter) and SRP concentrations. Date, as the sole random effect, had variable explanatory power but was most important in the model for hypolimnetic ammonium concentration.

Discussion

Lake and reservoir nutrient concentrations were not significantly different in any of the seasons, when comparing means across all study years. Watershed and/or climactic characteristics predicted surface nutrient concentrations, but hypolimnetic concentrations were also related to internal processes, which affected dissolved oxygen concentrations and water levels. Although outlet nutrient concentrations were not significantly different between lakes and reservoirs, year-round hypolimnetic release of reservoir water caused higher export of nutrients from reservoirs than lakes in summer and fall. Ammonium and SRP appeared to be produced and accumulated in both lake and reservoir bottom waters under anoxic and hypoxic conditions, but were continuously released from reservoirs while accumulating in stratified lakes. Interannual differences in reservoir and lake discharge were related to snowpack levels (5% to 170% of average snowpack levels over study period). In dry years (2015, 2016), reservoirs were drained slowly throughout the winter then filled during snowmelt, with elevated outlet discharge compared to lakes and reservoir throughout the year. In wet years (2017), reservoir discharge was managed in spring to increase capacity for later runoff, then increased with snowmelt, matching lake outflow patterns, reflecting management to minimize dam overtopping.

Epilimnion

Lake and reservoir surface concentrations of all three nutrients were not significantly different across the study period and were related to coverage by different vegetation types previously known to control surface nutrient concentrations (e.g. Sickman et al., 2003). Surface nitrate concentrations were positively related to bare and conifer watershed cover,

suggesting flushing from soil and talus pools (Sickman et al., 2003). These results differed from those for lakes in the Austrian Alps, where water chemistry variability was only weakly related to vegetation coverage, but strongly related to catchment morphology (Kamenik et al., 2001). In addition, maximum area exposed was positively related to surface nitrate concentration, indicating the importance of the drying and rewetting of the littoral zone for nitrate release (Cooke et al., 2003). Nitrate concentrations also declined with time since ice off, reflecting decreasing inputs from snowmelt and soils as earlier snowmelt was flushed downstream.

The explanatory power of final mixed models was much weaker for surface ammonium and SRP than nitrate concentrations, but catchment characteristics remained significant predictors of both ammonium and SRP concentrations. Wet meadow and chaparral coverages were included as positive but non-significant fixed effects in models for both ammonium and SRP concentrations, possibly reflecting their importance as sources of labile nutrient inputs in the Sierra. Net ammonium production can occur in wet meadow soils above 0 °C (Miller et al., 2007), and in early to late summer during snowmelt (Miller et al., 2009), thus the timing of snowmelt and total SWE will determine, at least partly, surface ammonium concentrations in watersheds with substantial wet meadow cover. Similarly, SRP is partially derived from watershed soil pools (Homyak et al., 2014b). Lake network number, which can partially explain spatial variation in montane lake chemistry (Sadro et al., 2012), was also included as a negative, but non-significant fixed effect in the final surface ammonium model, indicating uptake or nitrification during downstream transport from headwater to downstream lakes, which may be enhanced where nitrification is not photoinhibited, such as under snow (Kopáček and Blažzka, 1994).

Hypolimnion

Nitrate, ammonium, and SRP concentrations in the hypolimnion were not significantly different between lakes and reservoirs. The final mixed model for hypolimnetic nitrate concentration was complex, including predictors that reflected seasonality (ice period, season), source area (watershed area), geologic and vegetation characteristics related to soil flushing (chaparral, bare rock, glacial till), dissolved oxygen concentration, and water body morphology and landscape position (SDF, lake network number). Nitrate inputs come primarily from snowmelt and soil flushing in Sierra lakes (Sickman et al., 2003), but the mixing model suggested additional sources and limitations on inputs. Nitrate was negatively related to dissolved oxygen, and positively related to ice period, suggesting that organic matter decomposition and subsequent nitrification allowed some accumulation of nitrate under ice. Similarly, the negative relationships of nitrate to lake network number and SDF, which reflects the extent of the littoral zone, suggests that biotic uptake in littoral zones and streams removes nitrate that otherwise might reach the hypolimnion, as has been observed in Rocky Mountain stream networks (Brown et al., 2008). Surface area and SDF were greater in reservoirs than lakes (Table 1), which could have contributed to additional nitrate uptake in reservoirs, possibly offsetting inputs from the wetting and drying of reservoir littoral areas.

Hypolimnetic ammonium and SRP concentrations, like nitrate, were positively related to ice period and negatively related to dissolved oxygen, reflecting the accumulations of ammonium and SRP, first under ice and again during summer and fall periods with low DO levels. Final models also suggested that hypolimnetic ammonium and SRP concentrations, after considering DO levels, ice period, and reservoir area exposed, were lower in reservoirs than lakes (Figure 5), suggesting that deep-water discharge from

reservoirs exported hypolimnetic water downstream, removing ammonium and SRP that otherwise accumulate in lake hypolimnia. This is further reflected in the significantly higher export observed below reservoirs than lakes in summer and fall (Figure 6), though this is also an effect of discharge as well. Low hypolimnetic oxygen was not observed in 2015 in either lakes or reservoirs, possibly because of reduced allochthonous inputs and subsequently decreased hypolimnetic decomposition rates. Although k_d values indicated that light should have reached the bottom of water bodies throughout the study period, higher hypolimnetic k_d values in the later ice-free season could have reduced photosynthetic rates in the deep waters of some lakes and reservoirs with associated reductions in DO concentrations (Tioga reservoir, Gaylor Lake), and k_d and DO were negatively related ($r = -0.41$, $p = 0.002$; lake $n = 42$, reservoir $n = 29$). The short ice period in 2015 also may have reduced the accumulation of nutrients under ice, although this was not quantified because sampling did not begin until mid-summer.

In addition, models for both hypolimnetic ammonium and SRP concentrations included terms related to reservoir drawdown, including current exposed area in the SRP model and season x maximum exposed area in the ammonium model. In the latter case, maximum exposed area was only a significant predictor in winter, suggesting the importance of the drawdown area exposed to winter freezing for SRP release. Lake sediment exposure to air and rewetting can also increase ammonium release (Qui and McComb, 1996), suggesting increased remineralization can contribute to hypolimnetic reservoir ammonium production when reservoirs refill, even though some ammonium appears to be lost through reservoir outlet discharge. Ammonium production by decomposition will persist throughout the year, which can then accumulate under anoxic conditions during stratified periods. The final model

also showed that hypolimnetic ammonium concentration was positively related to coverage by alpine shrubs, the dominant vegetation type in study watersheds that lay largely above the tree line, which may be a source of the organic matter in lake sediments where decomposition occurs.

Although the final mixed model showed a positive relationship between hypolimnetic SRP concentration and current exposed area, the explanatory power of this model was lower than that for ammonium and mechanisms of phosphorus loading were less clear. Littoral sediments that are subjected to annual drying and rewetting have a reduced ability to adsorb SRP (Fabre 1988; Watts 2000), thus reservoir sediments may act as P sources. However, Sierra lake sediments have been found to be net P sinks (Homyak et al., 2014b), and watershed soil nutrient pools are expected to be the primary source of phosphorus inputs to lakes and reservoirs. Homyak et al. (2014a) suggested that DOC flushed from watershed soils may transport additional P to lakes, but I found no correlation between DOC and SRP concentrations ($r = 0.02$, $p = 0.81$, hypolimnion $n = 71$, epilimnion $n = 111$). Additionally, SRP concentrations rise in lake and reservoir hypolimnia after peak snowmelt rather than during, suggesting an autochthonous source. High sulfate concentrations may increase P release from sediments during anoxia (Caraco et al. 1993), but sulfate concentrations in the Sierra are rarely sufficient (100-300 $\mu eq\ L^{-1}$) to stimulate P release, except in watersheds dominated by volcanic rock (Melack et al. 1985). Although volcanic lithology was not selected in the final SRP model, the basins of the two sites where anoxia and elevated hypolimnetic SRP were most often observed, Tioga Reservoir and Lower Gaylor Lake, were dominated by volcanic rock. Nearby lakes in basins dominated by volcanic rocks (Parker Pass, Lundy) had SO_4 concentrations >100 $\mu eq\ L^{-1}$ (Melack et al. 1995), indicating that

watershed sulfate may contribute to sediment P release, although there are additional controls on the rate of that release (Hupfer and Lewandowski, 2008; Homyak et al., 2014b).

Outlet

Outlet nutrient concentrations did not differ between lakes and reservoirs across all study years and seasons, but export was significantly higher from reservoirs than lakes for all three nutrients (all p's < 0.001) in summer and fall, which could be attributed to higher discharge from reservoirs than lakes. Lake outlet flows became temporally intermittent in the summer or fall, whereas all reservoirs outlets (except Ellery) continued flowing into the winter. Hypolimnetic water release from reservoirs also may reduce the duration of the stratified period and cause earlier water column mixing relative to natural lakes (Nowlin et al., 2004; Furey et al., 2004), promoting the export of nutrients into the upper water column. Although year-round flows from reservoirs allow introduced fish populations to persist, dams disrupt the natural flow regime in fall dry periods, which may serve as an important ecological filter benefiting native species (Poff and Ward, 1989). Additionally, increased reservoir nutrient export may contribute to downstream productivity (Ward and Stanford, 1979), but this has not been examined in high Sierra outlet streams. Where lake outlets continued flowing into fall, which was more commonly observed in 2017 due to the larger preceding snowpack, nutrients accumulating in lake hypolimnia might be brought to lake surfaces and exported downstream.

Conclusions

Lake and reservoir nutrient concentrations were similar across water layers, seasons, and years, but nutrient export was greater from reservoirs than lakes owing to differences in the levels and timing of outlet discharge. Nutrients could accumulate in lake and reservoir

hypolimnia during stratification, likely caused by the decomposition of organic matter in sediments, then were exported through hypolimnetic releases from reservoirs and, rarely, from lakes during fall mixing, although lake and reservoir nutrient export was similar in spring. Dam construction and management results in the deep-water release of water from the hypolimnion and, in some cases, increased outlet discharge during dry periods, resulting in hypolimnetic nutrient export to downstream areas. Reservoir water level fluctuations were associated with nutrient concentrations, possibly by intensifying the release of nutrients from sediments exposed to repeated wet-dry cycles. Snowpack levels controlled interannual variation in reservoir management and the duration of the ice covered period, with repercussions for nutrient concentrations and export, as nutrient export was elevated in wet years particularly below reservoirs. Compared to lakes, reservoirs alter the timing and amounts of discharge and increase the export of labile nutrients to downstream ecosystems.

References

Bair, E.H., Dozier, J., Davis, R.E., Colee, M.T., Claffey, K.J., 2015. CUES—a study site for measuring snowpack energy balance in the Sierra Nevada. Front. Earth Sci. 3. https://doi.org/10.3389/feart.2015.00058

Blanchard, C.L., Tonnessen, K.A., 1993. Precipitation-chemistry measurements from the California Acid Deposition monitoring program, 1985–1990. Atmospheric Environment. Part A. General Topics 27, 1755–1763. https://doi.org/10.1016/0960-1686(93)90239-U

Brooks, P.D., Williams, M.W., 1999. Snowpack controls on nitrogen cycling and export in seasonally snow-covered catchments. Hydrological Processes 13, 2177–2190. https://doi.org/10.1002/(SICI)1099-1085(199910)13:14/15<2177::AID-HYP850>3.0.CO;2-V

Brown, A.D., Lund, L.J., 1991. Kinetics of weathering in soils from a subalpine watershed. Soil Science Society of America Journal 55, 1767–1773. https://doi.org/10.2136/sssaj1991.03615995005500060044x

Brown, P.D., Wurtsbaugh, W.A., Nydick, K.R., 2008. Lakes and forests as determinants of downstream nutrient concentrations in small mountain watersheds. Arctic, Antarctic, and Alpine Research 40, 462–469. https://doi.org/10.1657/1523-0430(07-052)[BROWN]2.0.CO;2

Caraco, N.F., Cole, J.J., Likens, G.E., 1993. Sulfate control of phosphorus availability in lakes. Hydrobiologia 253, 275–280. https://doi.org/10.1007/BF00050748

Carmignani, J.R., Roy, A.H., 2017. Ecological impacts of winter water level drawdowns on lake littoral zones: a review. Aquat Sci 79, 803–824. https://doi.org/10.1007/s00027-017-0549-9

Carlson CA, Hansell DA, Nelson NB, Siegel DA, Smethie WM, Khatiwala S, Meyers MM, Halewood E., 2010. Dissolved organic carbon export and subsequent remineralization in the mesopelagic and bathypelagic realms of the North Atlantic basin. Deep Sea Research Part II: Topical Studies in Oceanography.;57(16):1433-45.

Cohen, A.P., Melack, J.M., in press. Carbon dioxide supersaturation in high-elevation oligotrophic lakes and reservoirs in the Sierra Nevada, California. Limnology and Oceanography.

Cole, J.J., Caraco, N.F., 1998. Atmospheric exchange of carbon dioxide in a low-wind oligotrophic lake measured by the addition of SF_6. Limnology and Oceanography 43, 647–656. https://doi.org/10.4319/lo.1998.43.4.0647

Cooke, G.D., 1980. Lake level drawdown as a macrophyte control technique. JAWRA Journal of the American Water Resources Association 16, 317–322. https://doi.org/10.1111/j.1752-1688.1980.tb02397.x

Dickson, N.E., Carrivick, J.L., Brown, L.E., 2012. Flow regulation alters alpine river thermal regimes. Journal of Hydrology 464–465, 505–516. https://doi.org/10.1016/j.jhydrol.2012.07.044

Jonathan P. Doubek & Cayelan C. Carey (2017) Catchment, morphometric, and water quality characteristics differ between reservoirs and naturally formed lakes on a latitudinal gradient in the conterminous United States, Inland Waters, 7:2, 171-180, https://doi.org/10.1080/20442041.2017.1293317

Environmental Systems Research Institute, 2016. ArcGIS Desktop: Release 10.4, Redlands, CA.

Fabre, A., 1988. Experimental studies on some factors influencing phosphorus solubilization in connexion with the drawdown of a reservoir. Hydrobiologia 159, 153–158. https://doi.org/10.1007/BF00014723

Furey, P.C., Nordin, R.N., Mazumder, A., 2004. Water level drawdown affects physical and biogeochemical properties of littoral sediments of a reservoir and a natural lake. Lake and Reservoir Management 20, 280–295. https://doi.org/10.1080/07438140409354158

Grasshoff, K., 1976. Methods of Seawater Analysis. Verlag Chemie.

Hampton, S.E., Fradkin, S.C., Leavitt, P.R., Rosenberger, E.E., 2011. Disproportionate importance of nearshore habitat for the food web of a deep oligotrophic lake. Mar. Freshwater Res. 62, 350–358. https://doi.org/10.1071/MF10229

Hannan, H.H., 1979. Chemical modifications in reservoir-regulated streams, in: Ward, J.V., Stanford, J.A. (Eds.), The Ecology of Regulated Streams. Springer US, Boston, MA, pp. 75–94. https://doi.org/10.1007/978-1-4684-8613-1_6

Hirsch, P.E., Eloranta, A.P., Amundsen, P.-A., Brabrand, Å., Charmasson, J., Helland, I.P., Power, M., Sánchez-Hernández, J., Sandlund, O.T., Sauterleute, J.F., Skoglund, S., Ugedal, O., Yang, H., 2017. Effects of water level regulation in alpine hydropower reservoirs: an ecosystem perspective with a special emphasis on fish. Hydrobiologia 794, 287–301. https://doi.org/10.1007/s10750-017-3105-7

Hirsch, P.E., Schillinger, M., Appoloni, K., Burkhardt-Holm, P., Weigt, H., 2016. Integrating economic and ecological benchmarking for a sustainable development of hydropower. Sustainability 8, 875. https://doi.org/10.3390/su8090875

Homyak, P.M., Sickman, J.O., Melack, J.M., 2014a. Pools, transformations, and sources of P in high-elevation soils: Implications for nutrient transfer to Sierra Nevada lakes. Geoderma 217–218, 65–73. https://doi.org/10.1016/j.geoderma.2013.11.003

Homyak, P.M., Sickman, J.O., Melack, J.M., 2014b. Phosphorus in sediments of high-elevation lakes in the Sierra Nevada (California): implications for internal phosphorus loading. Aquat Sci 76, 511–525. https://doi.org/10.1007/s00027-014-0350-y

Hupfer, M., Lewandowski, J., 2008. Oxygen controls the phosphorus release from lake sediments – a long-lasting paradigm in limnology. International Review of Hydrobiology 93, 415–432. https://doi.org/10.1002/iroh.200711054

Jassby, A.D., Reuter, J.E., Axler, R.P., Goldman, C.R., Hackley, S.H., 1994. Atmospheric deposition of nitrogen and phosphorus in the annual nutrient load of Lake Tahoe (California-Nevada). Water Resources Research 30, 2207–2216. https://doi.org/10.1029/94WR00754

Jennings, C.W., Strand, R.G., Rogers, T.H., 1977. Geologic map of California. California Division of Mines and Geology, scale 1:750,000.

Kamenik, C., Schmidt, R., Kum, G., Psenner, R., 2001. The influence of catchment characteristics on the water chemistry of mountain lakes. Arctic, Antarctic, and Alpine Research 33, 404–409. https://doi.org/10.1080/15230430.2001.12003448

Kijowska-Strugała, M., Wiejaczka, Ł., Kozłowski, R., 2016. Influence of reservoirs on the concentration of nutrients in the water of mountain rivers. Ecological Chemistry and Engineering S 23, 413–424. https://doi.org/10.1515/eces-2016-0029

Kleinschmidt, 2019. Pre-Application Document, Volume III- Technical Study Plans: Bishop Creek Hydroelectric Project FERC Project No. 1394. Southern California Edison, Bishop, California.

Kling, G.W., Kipphut, G.W., Miller, M.M., O'Brien, W.J., 2000. Integration of lakes and streams in a landscape perspective: the importance of material processing on spatial patterns and temporal coherence. Freshwater Biology 43, 477–497. https://doi.org/10.1046/j.1365-2427.2000.00515.x

Knoll, L.B., Vanni, M.J., Renwick, W.H., 2003. Phytoplankton primary production and photosynthetic parameters in reservoirs along a gradient of watershed land use. Limnology and Oceanography 48, 608–617. https://doi.org/10.4319/lo.2003.48.2.0608

Kopáček, J., Blažzka, P., 1994. Ammonium uptake in alpine streams in the High Tatra Mountains (Slovakia). Hydrobiologia 294, 157–165. https://doi.org/10.1007/BF00016856

Kopàcöek, J. öå, Stuchlåk&, E.E.N., Strasökrab, V., Psöenàk, P., 2000. Factors governing nutrient status of mountain lakes in the Tatra Mountains. Freshwater Biology 43, 369–383. https://doi.org/10.1046/j.1365-2427.2000.00569.x

Lee, S.-W., Hwang, S.-J., Lee, S.-B., Hwang, H.-S., Sung, H.-C., 2009. Landscape ecological approach to the relationships of land use patterns in watersheds to water quality characteristics. Landscape and Urban Planning 92, 80–89. https://doi.org/10.1016/j.landurbplan.2009.02.008

Lorenzen, C.J., 1967. Determination of chlorophyll and pheo-pigments: spectrophotometric equations. Limnology and Oceanography 12, 343–346. https://doi.org/10.4319/lo.1967.12.2.0343

Lund, L.J., 1987. Water quality of Bishop Creek and selected eastern Sierra Nevada lakes. University of California at Riverside. Department of Soil and Environmental Sciences, Riverside, CA, USA.

Marchetto, A., Mosello, R., Psenner, R., Bendetta, G., Boggero, A., Tait, D., Tartari, G.A., 1995. Factors affecting water chemistry of alpine lakes. Aquatic Science 57, 81–89. https://doi.org/10.1007/BF00878028

McGowan, S., Leavitt, P.R., Hall, R.I., 2005. A whole-lake experiment to determine the effects of winter droughts on shallow lakes. Ecosystems 8, 694–708. https://doi.org/10.1007/s10021-003-0152-x

Melack, J., Sickman, J.O., Leydecker, A., Marrett, D., 1998. Comparative analyses of high-altitude lakes and catchments in the Sierra Nevada: susceptibility to acidification, final report (No. 032–188). University of California, Santa Barbara, California Air Resources Board.

Melack, J.M., Cooper, S.D., Jenkins, T.M., Barmuta, L., Hamilton, S., 1989. Chemical and biological characteristics of Emerald Lake and the streams in its watershed and the responses of the lake and streams to acidic deposition. Final report (No. A6-184–32). University of California, Santa Barbara, California Air Resources Board.

Melack, J.M., Sickman, J.O., Setaro, F., Dawson, D.R., 1997. Monitoring of wet deposition in alpine areas in the Sierra Nevada. Final report (No. Contract A932-081). California Air Resources Board.

Melack, J.M., Stoddard, J.L., Ochs, C.A., 1985. Major ion chemistry and sensitivity to acid precipitation of Sierra Nevada lakes. Water Resources Research 21, 27–32. https://doi.org/10.1029/WR021i001p00027

Miller, A.E., Schimel, J.P., Sickman, J.O., Meixner, T., Doyle, A.P., Melack, J.M., 2007. Mineralization responses at near-zero temperatures in three alpine soils. Biogeochemistry 84, 233–245. https://doi.org/10.1007/s10533-007-9112-4

Miller, A.E., Schimel, J.P., Sickman, J.O., Skeen, K., Meixner, T., Melack, J.M., 2009. Seasonal variation in nitrogen uptake and turnover in two high-elevation soils: mineralization responses are site-dependent. Biogeochemistry 93, 253–270. https://doi.org/10.1007/s10533-009-9301-4

Nakagawa, S., Johnson, P.C.D., Schielzeth, H., 2017. The coefficient of determination R^2 and intra-class correlation coefficient from generalized linear mixed-effects models revisited and expanded. J R Soc Interface 14. https://doi.org/10.1098/rsif.2017.0213

Nowlin, W.H., Davies, J.-M., Nordin, R.N., Mazumder, A., 2004. Effects of water level fluctuation and short-term climate variation on thermal and stratification regimes of a British Columbia reservoir and lake. Lake and Reservoir Management 20, 91–109. https://doi.org/10.1080/07438140409354354

Park, Y.-S., Kwon, Y.-S., Hwang, S.-J., Park, S., 2014. Characterizing effects of landscape and morphometric factors on water quality of reservoirs using a self-organizing map. Environmental Modelling & Software 55, 214–221. https://doi.org/10.1016/j.envsoft.2014.01.031

Poff, N.L., Allan, J.D., Bain, M.B., Karr, J.R., Prestegaard, K.L., Richter, B.D., Sparks, R.E., Stromberg, J.C., 1997. The natural flow regime. BioScience 47, 769–784. https://doi.org/10.2307/1313099

Poff, N.L., Ward, J.V., 1989. Implications of streamflow variability and predictability for lotic community structure: a regional analysis of streamflow patterns. Can. J. Fish. Aquat. Sci. 46, 1805–1818. https://doi.org/10.1139/f89-228

Power, M., Eloranta, A.P., Amundsen, P.-A., Brabrand, Å., Charmasson, J., Helland, I.P., Hirsch, P.E., Sánchez-Hernández, J., Sandlund, O.T., Sauterleute, J.F., Skoglund, S., Ugedal, O., Yang, H., 2017. Effects of water level regulation in alpine hydropower reservoirs: an ecosystem perspective with a special emphasis on fish. Hydrobiologia 794, 287–301. https://doi.org/10.1007/s10750-017-3105-7

QGIS Development Team (2019). QGIS Geographic Information System. Open Source Geospatial Foundation Project. http://qgis.osgeo.org

Qui, S., McComb, A.J., 1996. Drying-induced stimulation of ammonium release and nitrification in reflooded lake sediment. Mar. Freshwater Res. 47, 531–536. https://doi.org/10.1071/mf9960531

Sadro, S., Melack, J.M., MacIntyre, S., 2011a. Depth-integrated estimates of ecosystem metabolism in a high-elevation lake (Emerald Lake, Sierra Nevada, California). Limnology and Oceanography 56, 1764–1780. https://doi.org/10.4319/lo.2011.56.5.1764

Sadro, S., Melack, J.M., MacIntyre, S., 2011b. Spatial and temporal variability in the ecosystem metabolism of a high-elevation lake: integrating benthic and pelagic habitats. Ecosystems 14, 1123–1140. https://doi.org/10.1007/s10021-011-9471-5

Sadro, S., Melack, J.M., Sickman, J.O., Skeen, K., 2019. Climate warming response of mountain lakes affected by variations in snow: Climate sensitivity of mountain lakes. Limnology and Oceanography Letters 4, 9–17. https://doi.org/10.1002/lol2.10099

Sadro, S., Nelson, C.E., Melack, J.M., 2012. The influence of landscape position and catchment characteristics on aquatic biogeochemistry in high-elevation lake-chains. Ecosystems 15, 363–386. https://doi.org/10.1007/s10021-011-9515-x

Sadro, S., Sickman, J.O., Melack, J.M., Skeen, K., 2018. Effects of climate variability on snowmelt and implications for organic matter in a high-elevation lake. Water Resources Research 54, 4563–4578. https://doi.org/10.1029/2017WR022163

Saucedo, G.J., Bedford, D.R., Raines, G.L., Miller, R.J., Wentworth, C.M., 2000. GIS Data for the Geologic Map of California. California Department of Conservation, California Geological Survey, Sacramento, CA. https://maps.conservation.ca.gov/cgs/metadata/GDM_002_GMC_750k_v2_metadata.html

Sickman, J.O., Leydecker, A., Chang, C.C.Y., Kendall, C., Melack, J.M., Lucero, D.M., Schimel, J., 2003. Mechanisms underlying export of N from high-elevation catchments during seasonal transitions. Biogeochemistry 64, 1–24. https://doi.org/10.1023/A:1024928317057

Strickland, J.D., Parsons, T.R., 1972. A practical handbook of seawater analysis. Fisheries Research Board of Canada Bulletin 157, 2nd Edition, 310 p.

Taylor, B.W., Keep, C.F., Hall, R.O., Koch, B.J., Tronstad, L.M., Flecker, A.S., Ulseth, A.J., 2007. Improving the fluorometric ammonium method: matrix effects, background fluorescence, and standard additions. Journal of the North American Benthological Society 26, 167–177. https://doi.org/10.1899/0887-3593(2007)26[167:ITFAMM]2.0.CO;2

Vicars, W.C., Sickman, J.O., 2011. Mineral dust transport to the Sierra Nevada, California: Loading rates and potential source areas. Journal of Geophysical Research: Biogeosciences 116 G01018. https://doi.org/10.1029/2010JG001394

Voelz, N.J., Ward, J.V., 1989. Biotic and abiotic gradients in a regulated high elevation Rocky mountain river. Regulated Rivers: Research & Management 3, 143–152. https://doi.org/10.1002/rrr.3450030114

Wanninkhof, R., 2014. Relationship between wind speed and gas exchange over the ocean revisited. Limnology and Oceanography: Methods 12, 351–362. https://doi.org/10.4319/lom.2014.12.351

Ward, J.V., Stanford, J.A., 1979. Ecological factors controlling stream zoobenthos with emphasis on thermal modification of regulated streams, in: Ward, J.V., Stanford, J.A. (Eds.), The Ecology of Regulated Streams. Springer US, Boston, MA, pp. 35–55. https://doi.org/10.1007/978-1-4684-8613-1_4

Watts, C.J., 2000. Seasonal phosphorus release from exposed, re-inundated littoral sediments of two Australian reservoirs. Hydrobiologia 431, 27–39. https://doi.org/10.1023/A:1004098120517

Wetzel, R.G., 2001. Limnology: lake and river ecosystems. Academic Press, San Diego, CA. 1006 pgs.

Wilde, F.D., .Sandstrom M.W., and Skrobialowski S.C., 2014, Selection of equipment for water sampling: U.S. Geological Survey Techniques of Water Resources Investigations, Book 9, Chap. A2, , 78 p. https://doi.org/10.3133/twri09A2

Willason, S.W., Johnson, K.S., 1986. A rapid, highly sensitive technique for the determination of ammonia in seawater. Mar. Biol. 91, 285–290. https://doi.org/10.1007/BF00569445

Williams, M.W., Bales, R.C., Brown, A.D., Melack, J.M., 1995. Fluxes and transformations of nitrogen in a high-elevation catchment, Sierra Nevada. Biogeochemistry 28, 1–31. https://doi.org/10.1007/BF02178059

Zohary, T., Ostrovsky, I., 2011. Ecological impacts of excessive water level fluctuations in stratified freshwater lakes. Inland Waters 1, 47–59. https://doi.org/10.5268/IW-1.1.406

Table 1: Basic characteristics of study lakes and reservoirs, and comparisonwise error adjusted p-values comparing lake and reservoir characteristics. ‘L’ and ‘R’ correspond to lake and reservoir; ‘LNN’ is lake network number and ‘SDF’ is shoreline development factor.

Site	***Latitude***	***Longitude***	***Elevation (m)***	***Max. Depth (m)***	***Surface Area (ha)***	***Watershed Area (ha)***	***LNN***	***SDF***
Crystal (L)	37° 35' 39" N	119° 01' 07" W	2932	19	5	95	0	1.39
Spuller (L)	37° 56' 55" N	119° 17' 05" W	3124	5.5	1.9	137	0	1.31
Lower Gaylor (L)	37° 54' 50" N	119° 16' 06" W	3155	13	9.5	99	1	1.33
Rock Creek (L)	37° 27' 14" N	118° 44' 13" W	2957	24	23	3116	9	1.29
Ruby (L)	37° 24' 55" N	118° 46' 01" W	3383	34	15	449	1	1.19
Sabrina (R)	37° 12' 35" N	118° 36' 50" W	2782	19	76	4334	6	1.53
Saddlebag (R)	37° 58' 01" N	119° 16' 06" W	3068	22	124	1801	4	1.58
South (R)	37° 10' 07" N	118° 34' 12" W	2977	10	69	3277	5	1.67
Tioga (R)	37° 55' 35" N	119° 15' 10" W	2937	16	29	980	0	1.5
Ellery (R)	37° 56' 07" N	119° 14' 07" W	2901	4	25	4139	5	1.81
Adjusted p-values			0.34	0.67	**0.035**	0.095	0.68	**0.036**

Table 2: Dates of ice-on and ice-off for lakes and reservoirs as determined by remote sensing (see Methods). Corresponding ice period duration and local peak (April 1) snow water equivalent (SWE) are listed.

							Ice period (days)			SWE (cm)		
	Ice-on 2014	***Ice-off 2015***	***Ice-on 2015***	***Ice-off 2016***	***Ice-on 2016***	***Ice-off 2017***	***2015***	***2016***	***2017***	***2015***	***2016***	***2017***
Crystal (L)	12/5	4/25	11/16	5/17	12/2	6/30	141	183	210	3.8	103	208
Spuller (L)	11/24	6/14	11/18	6/25	10/15	8/1	202	220	290	5.1	69	164
Lower Gaylor (L)	11/24	6/7	11/18	6/17	11/24	7/22	195	212	240	3.8	72	138
Rock Creek (L)	12/9	3/27	12/1	5/4	12/11	6/1	108	155	172	1.3	19	80
Ruby (L)	12/9	6/1	12/1	6/17	12/2	7/14	174	199	224	12.7	49	132
Sabrina (R)	1/27/15	2/23	12/25	4/23	12/23	5/10	27	120	138	2.5	34	61
Saddlebag (R)	12/17	5/30	11/30	6/9	12/10	7/22	164	192	224	5.1	69	164
South (R)	12/13	3/27	12/1	5/2	12/23	6/3	104	153	162	2.5	34	61
Tioga (R)	12/5	5/30	11/30	5/29	11/24	7/4	176	181	222	3.8	72	138
Ellery (R)	11/24	4/25	11/8	5/17	11/24	6/12	152	191	200	15.2	70	160

Table 3: Areal net ecosystem productivity (NEP), community respiration (CR), gross primary productivity (GPP) rates (mmol O_2 m^{-2} day^{-1}), and the ratio of gross primary productivity to community respiration during the ice-free season of 2017, by site and date.

Site	***Date***	***Areal NEP*** *(mmol m^{-2} day^{-1})*	***Areal CR*** *(mmol m^{-2} day^{-1})*	***Areal GPP*** *(mmol m^{-2} day^{-1})*	***GPP:CR***
Rock Creek (L)	Jul. 26	1.2	-73.7	74.9	1.0
Gaylor (L)	Aug. 18	-11.8	-32.6	20.8	0.6
Rock Creek (L)	Sept. 18	-13.1	-96.4	80.3	0.8
Tioga (R)	Aug. 17	-14.2	-83.7	69.5	0.8
Saddlebag (R)	Aug. 19	8.9	-8.3	17.2	2.1
Tioga (R)	Aug. 24	33.9	-16.3	50.2	3.1

Table 4: Mean flows (m^3 s^{-1}) on sampling dates within each season, pooled across years. Significant differences between lakes and reservoirs are shown in bold.

Season	***Type***	***Mean flow***	***Standard error***
Winter	Lake	0.117	0.058
	Reservoir	0.745	0.356
Spring	Lake	0.716	0.2805
	Reservoir	1.424	0.6401
Summer	Lake	**0.409**	0.141
	Reservoir	**1.105**	0.293
Fall	Lake	**0.045**	0.021
	reservoir	**0.377**	0.099

Table 5: Final mixed models for lake and reservoir nutrient concentrations based on AIC values (see Methods). R^2 marginal is the coefficient of determination for fixed effects only, whereas R^2 conditional includes both fixed and random effects. Asterisks denote p-values, where: * = $p < 0.05$, ** = $p < 0.01$, *** = $p < 0.001$. Effects without asterisks are were not significant. Positive and negative coefficients are denoted with (+) and (-).

Nutrient	*Layer*	*Fixed effects*	*Random effects*	*R^2 marginal*	*R^2 conditional*
NO_3	surface	Season (-) Days since ice-off (-)*** P. Bare (+)*** P. Conifer (+)** Max. area exposed (+)***	Date	0.58	0.73
	hypolimnion	Season (+)*** Dissolved oxygen (-)*** Ice period (+)*** Lake network number (-)*** P. Bare (-)*** P. Chaparral (-)*** P. Glacial (-)*** Shoreline develop. factor (-)*** Watershed (+)***	Date	0.57	0.63
NH_4	surface	Lake network number (-) P. Bare (+) P. Chaparral (+) P. Meadow (+) ***	Date	0.19	0.23
	hypoliminion	Depth (+) Dissolved oxygen (-) *** Ice period (+) ** P. Alpine shrub (-) * winter x max. exposed area(-)*** Type, reservoir (-)*	Date	0.52	0.82
SRP	surface	Dissolved oxygen (-) P. Chaparral (+) ** P. Meadow (+) * Water residence time (-)	Date	0.10	0.24
	hypolimnion	Dissolved oxygen (-)* Ice period (+) Current exposed area (+) *** Type, reservoir (-)*	Date	0.27	0.28

Supplement 1: Number of replicates used in analyses, where *epi* = epilimnion (surface), *hyp* = hypolimnion (bottom), and *out* = outlet.

Year	*season*	*layer*	*Type*	*n*
2015	summer	epi	lake	4
		epi	reservoir	3
		hyp	lake	4
		hyp	reservoir	2
		out	lake	4
		out	reservoir	3
	fall	epi	lake	4
		epi	reservoir	5
		hyp	lake	2
		hyp	reservoir	1
		out	lake	4
		out	reservoir	5
2016	winter	epi	lake	2
		epi	reservoir	3
		hyp	lake	5
		hyp	reservoir	2
		out	lake	2
		out	reservoir	3
	spring	epi	lake	4
		epi	reservoir	5
		hyp	lake	4
		hyp	reservoir	3
		out	lake	5
		out	reservoir	5
	summer	epi	lake	4
		epi	reservoir	5
		hyp	lake	5
		hyp	reservoir	5
		out	lake	5
		out	reservoir	5
	fall	epi	lake	5
		epi	reservoir	5
		hyp	lake	5
		hyp	reservoir	3
		out	lake	5
		out	reservoir	5
2017	winter	epi	lake	3
		epi	reservoir	4
		hyp	lake	2
		hyp	reservoir	2
		out	lake	1
		out	reservoir	2
	spring	epi	lake	5
		epi	reservoir	4
		hyp	lake	2
		hyp	reservoir	1
		out	lake	5
		out	reservoir	4
	summer	epi	lake	5
		epi	reservoir	5
		hyp	lake	5
		hyp	reservoir	5
		out	lake	5
		out	reservoir	5
	fall	epi	lake	5
		epi	reservoir	5
		hyp	lake	2
		hyp	reservoir	1
		out	lake	5
		out	reservoir	5

Figure 1: Study site locations in the eastern Sierra Nevada, California, USA. Topography was obtained from USGS digital elevation models, park boundaries from the US Forest Service, roads from Tiger Roads, and water bodies from the National Hydrography Dataset.

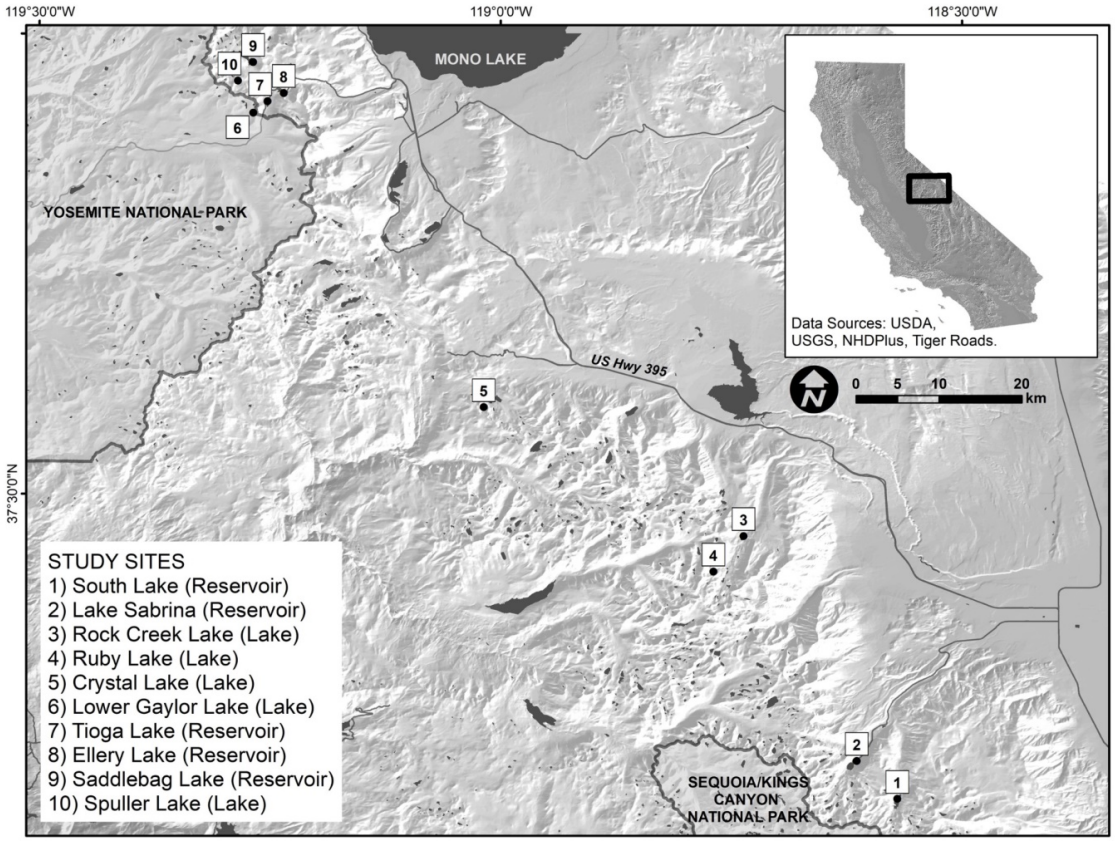

Figure 2a: Mean lake and reservoir temperatures ± 1 SE grouped by layer and separated by year, across all four seasons. No significant differences were observed ($p > 0.05$, Mann Whitney U tests with Benjamini-Hochberg corrections).

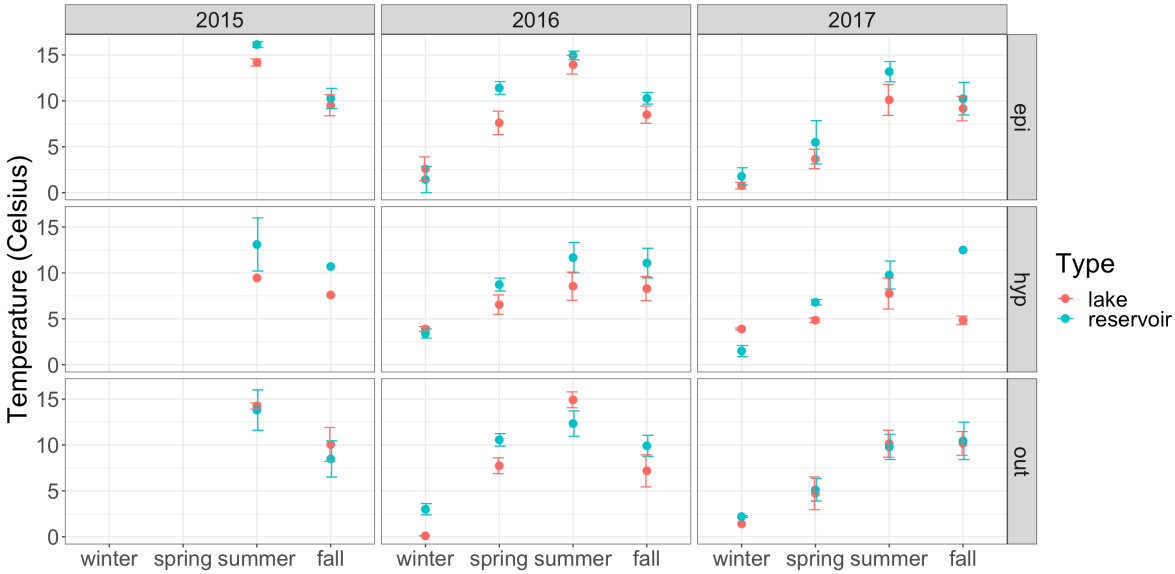

Figure 2b: Mean lake and reservoir temperatures ± 1 SE for each layer, type, and season. Bars indicate standard error. No significant differences were observed ($p > 0.05$, Mann Whitney U tests with Benjamini-Hochberg corrections).

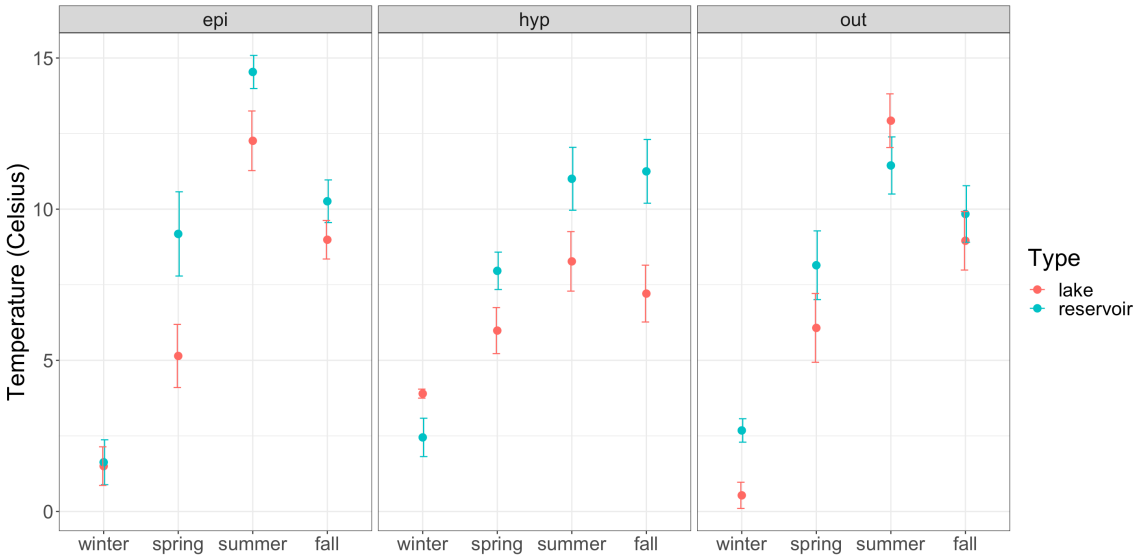

Figure 3: Relationship of hypolimnetic ammonium concentrations and hypolimnetic dissolved oxygen content, pooled across years.

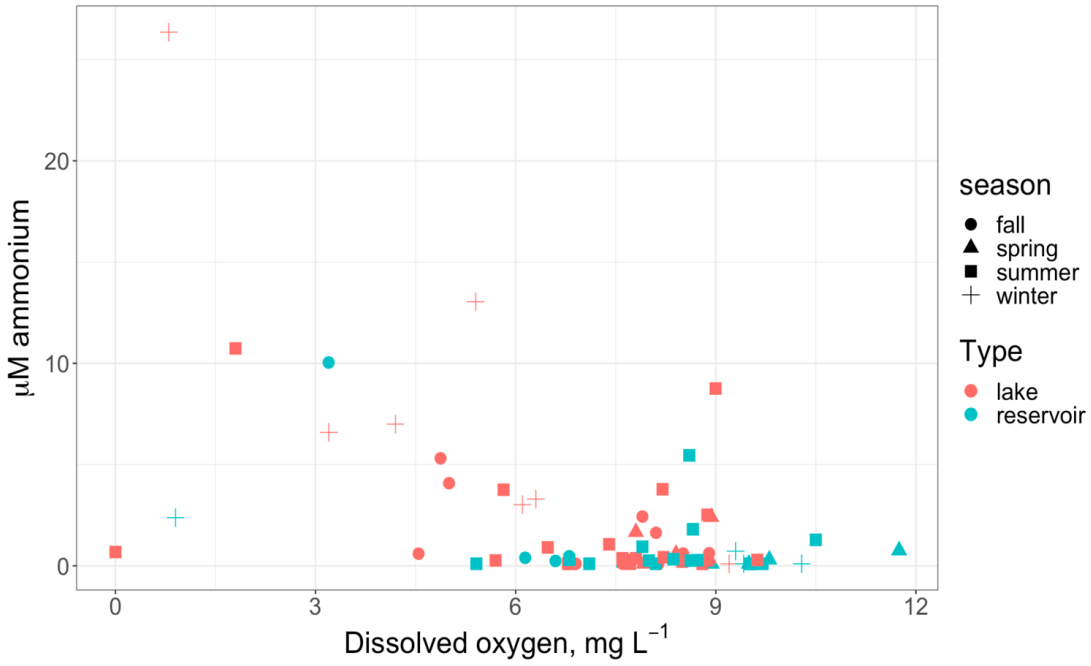

Figure 4: Mean daily discharge for each lake (top panel) and reservoir (middle panel) through the study period, obtained from USGS for reservoirs and computed from rating curves for lakes. The bottom panel presents reservoir area exposed over time. Lake levels did not vary appreciably through the study period.

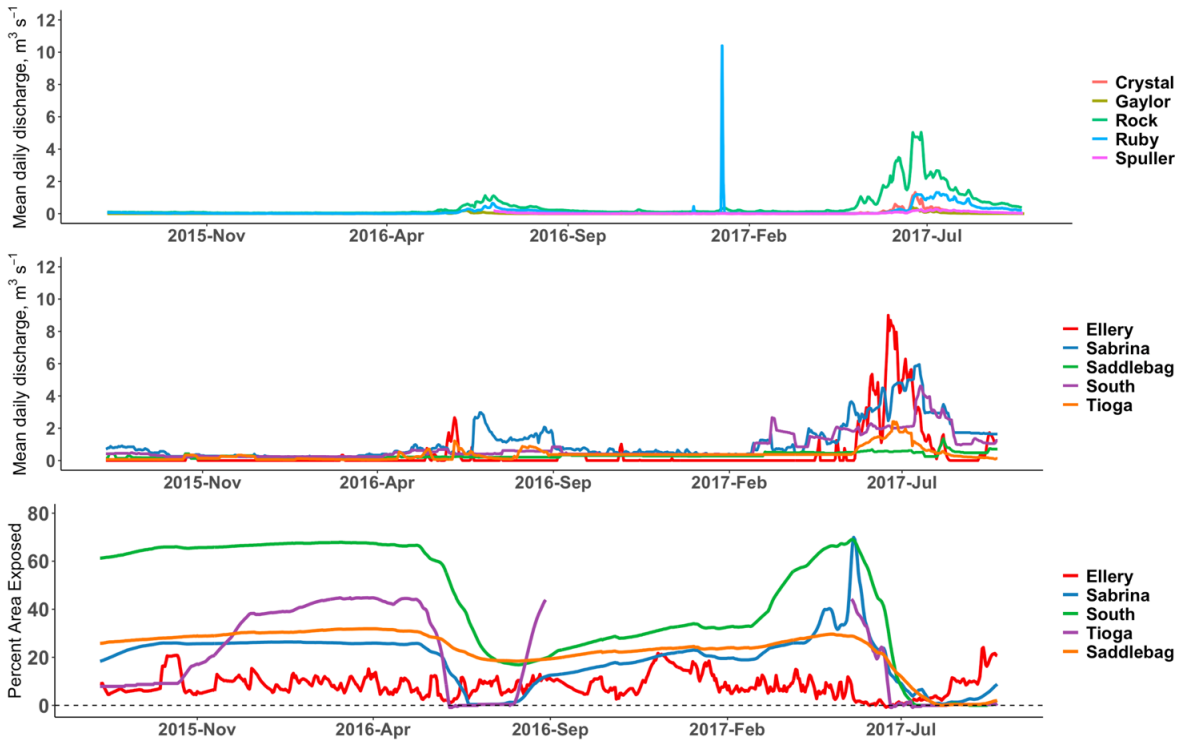

Figure 5: Mean lake and reservoir nutrient concentrations ± 1 SE for each water layer (epilimnion, hypolimnion, outlet) for each season and year over the study period (summer 2015 through fall 2017). Top panel: nitrate concentration; middle panel: Ammonium concentration; bottom panel: soluble reactive phosphorus concentration.

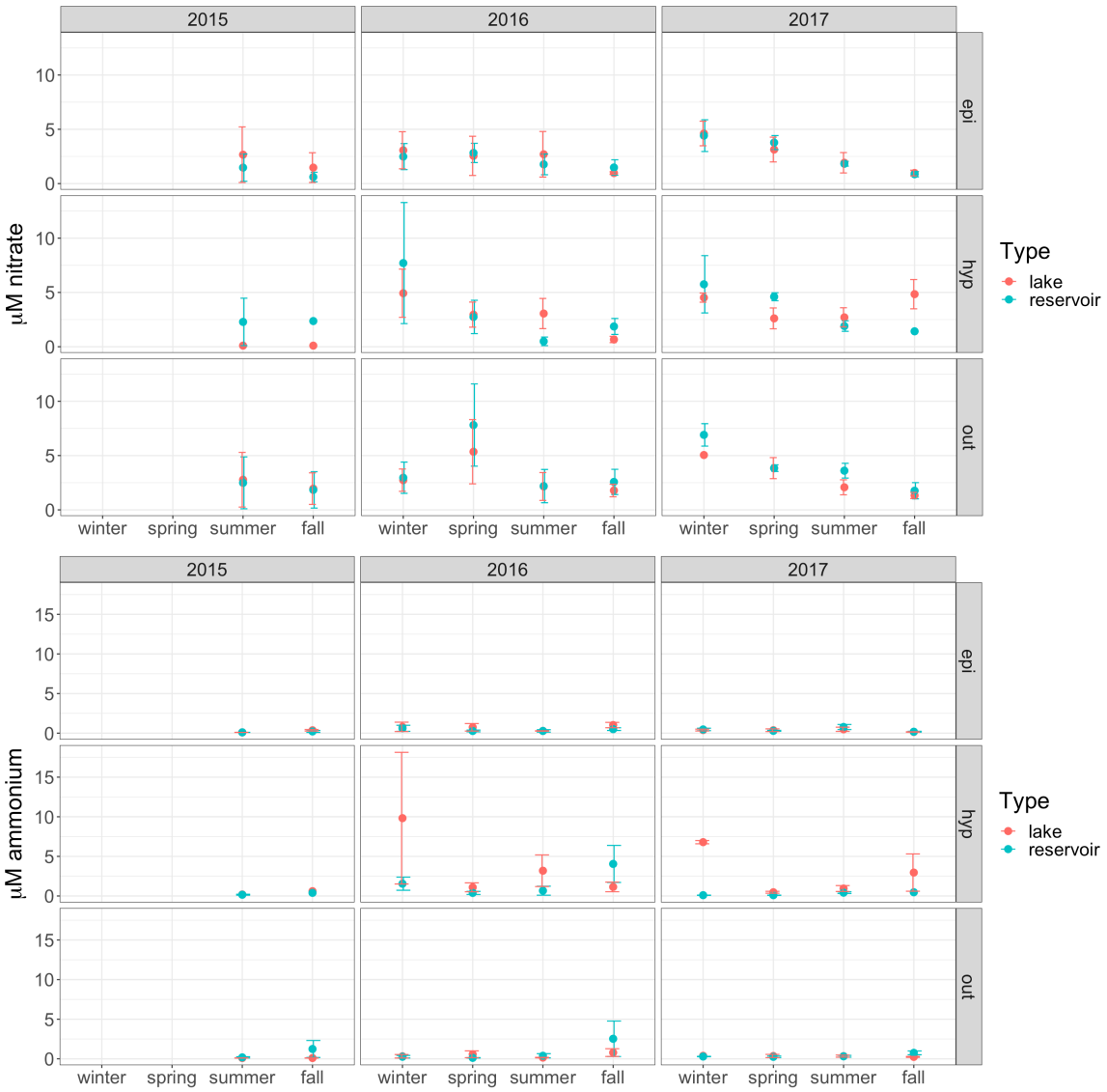

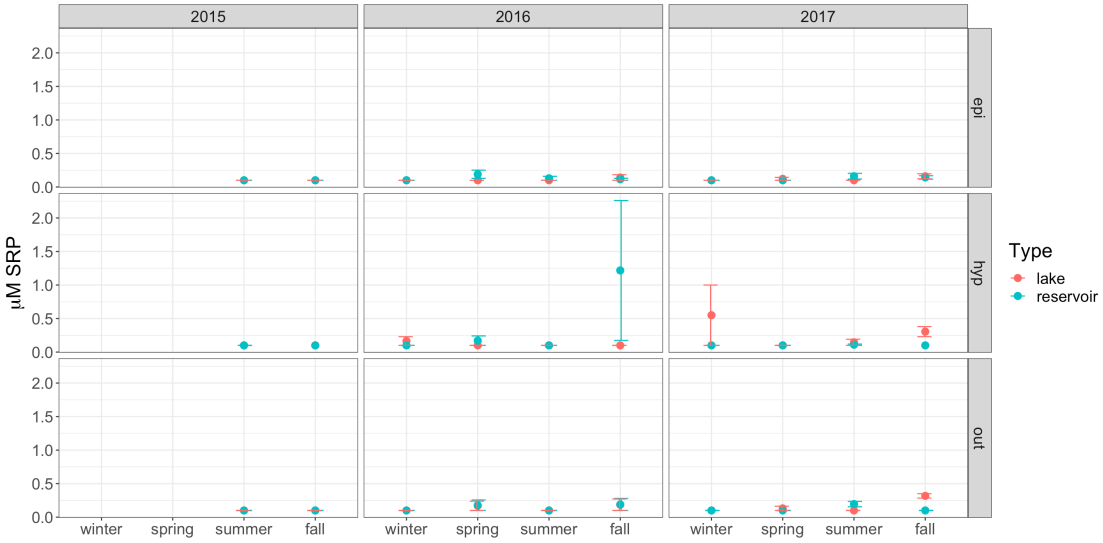
2015
2016
2017
epi
hyp
out
µM SRP
0.0
0.5
1.0
1.5
2.0
winter
spring
summer
fall
Type
lake
reservoir

Figure 6: Mean lake versus reservoir nutrient export ± 1 SE, averaged across dates, then years, for each season for each site. Significant differences are denoted with "*" (adjusted $p < 0.05$, Mann-Whitney U tests with Benjamini-Hochberg corrections). Top panel: nitrate concentration; middle panel: ammonium concentration; bottom panel: soluble reactive phosphorus concentration.

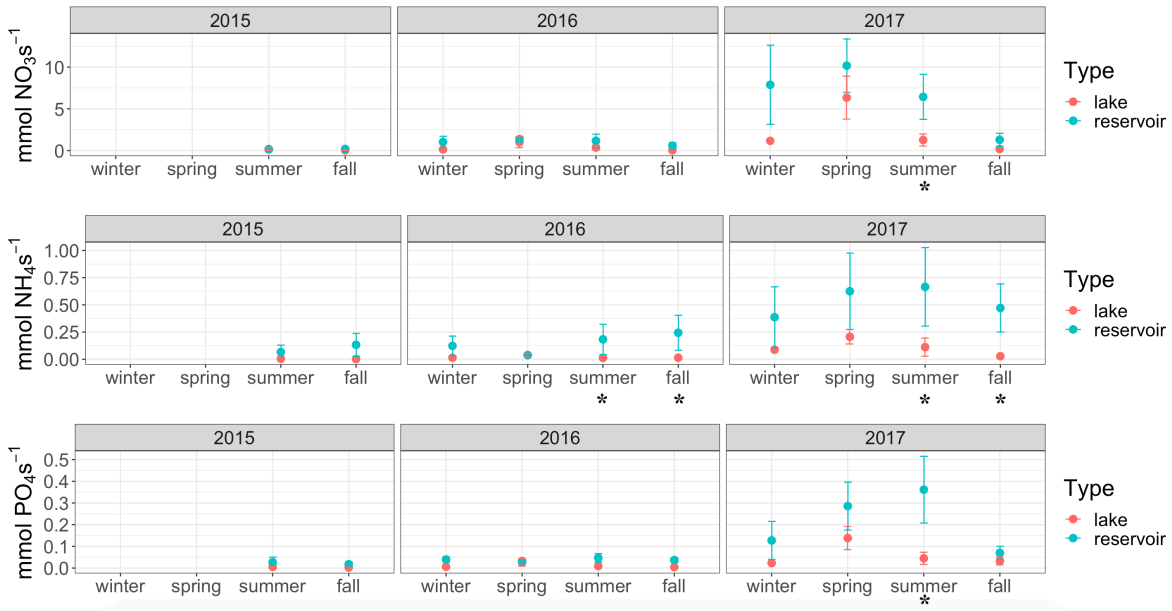

CHAPTER TWO

Relationships of nutrient chemistry and flow metrics to benthic macroinvertebrate assemblages in high elevation lake and reservoir outlet streams

Abstract

Although reservoirs are known to alter downstream flow and hydrochemical regimes and, hence, stream macroinvertebrate communities, almost no studies have compared invertebrate assemblages in the outlets of reservoirs versus natural lakes. In this study, I compared benthic macroinvertebrate communities in the outlet streams of high elevation natural lakes (n = 5) and hydropower storage reservoirs (n = 5) in the Sierra Nevada of California over three years (2015-2017) encompassing a wide range of flow regimes. Discharge from reservoirs over the study period were greater than from lakes in mean annual flow, 30 day minimum flow, baseflow, and, in one year, zero flow days, but other flow metrics, such as peak annual flow and the recession period, were similar between lake and reservoir outlets across years. Invertebrate community structure (richness, evenness, density, and composition) was similar between lake and reservoir outlets across seasons and years, despite flow metric differences, but varying annual snowpack and flow regimes drove interannual differences in invertebrate assemblages. Filter feeders (primarily *Prosimulium*) dominated in 2017, likely in response to elevated flow, whereas Ephemeroptera and Trichoptera (commonly *Baetis, Serratella, Rhyacophila*) and chironomids (Tanypodinae, Chironominae) were abundant throughout the study period. Non-metric multidimensional scaling (NMDS) showed that invertebrate communities were influenced by elevated flow (peak annual flow, ammonium export, annual mean flow), substrata sizes, and algal biomass (as chlorophyll *–a*), but not related to low flow metrics such as baseflow and minimum flows, which were greater below reservoirs. Reservoir management elevated ammonium export in summer and fall of two study years, but did not cause divergence of lake and reservoir invertebrate assemblages in those seasons. Although reservoir management altered

flow regimes and nutrient flux across years in these high elevation systems, interannual climactic variability outweighed the effects of flow management on benthic macroinvertebrate communities.

Introduction

The alteration of stream flows by human activities, such as the construction and management of dams, water diversions, and groundwater extraction, is recognized as a major source of ecological degradation (Poff et al., 1997; Rosenberg et al., 2000; Bunn and Arthington, 2002). To understand the effects of such activities on stream flows and, hence, biological communities, it is important to characterize biological responses to natural flow regimes then examine how these responses are affected by human-induced flow alterations. Hydroelectric dams, including those on high-elevation, headwater streams, often change the magnitude, variability, and timing of downstream flows (Poff et al., 2007; Schinegger et al., 2012), altering invertebrate density, diversity, community composition, and life history cycles (Céréghino and Lavandier, 1998; Weisberg et al., 1990; Rehn, 2009; Yarnell et al., 2010; Bruno et al., 2013; Kennedy et al., 2016; Quadroni et al., 2017). Hypolimnetic releases from reservoirs also can modify downstream water temperatures and chemistry, with potential repercussions for invertebrate assemblages (Hannan, 1979; Ward and Stanford, 1979; Jackson et al., 2007; Bona et al., 2008; Dickson et al., 2012; Bini et al., 2014).

Natural flow regimes are critical in maintaining the biological integrity of fluvial ecosystems by driving the physical habitat and connectivity conditions that native species are adapted to while preventing invasion by exotic species (Power et al., 1995; Bunn and Arthington, 2002; Lytle and Poff, 2004; Poff and Zimmerman, 2009). Natural, seasonal flow

intermittency can reduce longitudinal connectivity, initially increase invertebrate density, and ultimately result in the local extirpation of some species while favoring the dominance of drought-resistant taxa (Gasith and Resh, 1999; Rader and Belish, 1999; Donath and Robinson, 2001; Robinson and Matthaei, 2007; Vidal-Abarca et al., 2013; Datry et al., 2014; Robinson et al., 2015, 2016; Herbst et al., 2019). How biological communities respond to flow regimes altered by reservoir management in headwater, snowmelt streams that are characterized by high spring flows and zero or intermittent flows in the fall is less clear.

In contrast to many headwater hydroelectric reservoirs which dam river or glacial valleys, most high elevation reservoirs in California's Sierra Nevada originated as natural lakes that were enlarged to capture snowmelt flows. The dams on these enlarged lakes release water through the original stream channel to smaller reservoirs downstream, where water is removed for hydropower generation. Stored reservoir water is primarily discharged from hypolimnia, but surface flows overtopping the dam can occur in high snowpack and runoff years and year-round minimum flows (*sensu* Tennant, 1976) are often mandated to support downstream trout populations. Although most studies examining the ecological effects of dam construction and management have compared regulated and unregulated rivers (e.g. Rehn, 2009; Steel et al., 2018), this research compares abiotic conditions and benthic macroinvertebrate assemblages in the outlet streams of high Sierra reservoirs versus natural lakes.

The serial discontinuity concept (SDC) was initially developed for reservoirs (Ward and Stanford, 1983), but has been applied recently to lakes, because both reservoirs and lakes disrupt stream continua and impact downstream conditions (Wurtsbaugh et al., 2005; Marcarelli and Wurtsbaugh, 2007; Goodman et al., 2010). High elevation lake outlets can be

warmer, show less daily temperature variation, and have increased invertebrate richness and density compared to streams uninterrupted by lakes (Robinson and Minshall, 1990; Hieber et al., 2002), as well as exhibit altered nutrient uptake rates relative to inlets (Arp and Baker, 2007), demonstrating that outlet effects are not limited to reservoirs. Comparisons of lake and reservoir outlet streams rather than unregulated reaches and reservoir outlets allow the examination of abiotic conditions and biological communities below lakes and reservoirs with similar serial discontinuity. In this study, I measured flow and physical-chemical variables, and sampled benthic macroinvertebrate assemblages, in the outlet streams of high-elevation Sierra lakes and reservoirs across seasons during ice-free periods for three years to examine the responses of invertebrate assemblages to reservoir management and environmental variables.

I predicted that reservoirs would reduce flow intermittency, increase baseflows, and reduce peak flows relative to lakes through snowmelt storage and year-round hypolimnetic releases. Reduced peak flows and lower flow intermittency should favor sensitive taxa (i.e., Ephemeroptera, Plecoptera, Trichoptera (EPT)), whereas more tolerant taxa (Chironomidae) might be elevated in lake outlets. In addition, elevated ammonium, nitrate, and phosphorus concentrations in hypolimnia combined with increased reservoir discharge should result in increased nutrient export below reservoirs, which is expected to cause bottom-up effects increasing invertebrate abundance. Chlorophyll *a* (Chl-a) concentrations, here serving as a proxy for particulate organic matter (POM), may also be elevated in hypolimnia in response to seasonally elevated nutrient concentrations, contributing to increased POM flux out of reservoir than lake outlets, which should serve to sustain higher abundances of filterers, collector-gatherers, and their predators.

Methods

Five lake and five reservoir outlet streams were studied in the eastern Sierra Nevada, California, within or adjacent to protected wilderness areas (Chapter 1, Table 1). Beginning in summer 2015, three lake and two reservoir outlets were sampled, and the outlets of an additional two lakes and three reservoirs were added in spring 2016, then sampled through fall 2017. Although the design entailed sampling 5 lake and 5 reservoir outlets through 2016 and 2017, the actual number of sites sampled varied across seasons because several sites could not be accessed in spring during a high snowpack year (2017) and several outlet stream dried in the fall (Table 2). These sites occur at subalpine to alpine elevations near or above treeline, ranging from 2782 to 3383 m a.s.l. (Table 1), within recently-glaciated watersheds with poor soil development underlain primarily by granitic rock. These outlets are well-oxygenated, have consistently low conductivity (< 30 $\mu S\ cm^{-1}$), and most have minimal riparian cover, characteristic of streams at or above treeline (Ward, 1994). The reservoirs were constructed in the early 20th century (Ellery, 1927; Tioga, 1928; Saddlebag, 1921; South, 1910; Sabrina, 1908), and are currently managed for hydroelectric production and year-round minimum flow releases, with the exception of Ellery Reservoir where the outlet is allowed to cease flowing at any time. Eight reservoirs have been constructed in the eastern high Sierra (> 2500 m), five of which were selected for this study based on their year-round accessibility, allowing for the same-day processing of nutrient samples in the laboratory. The five lake outlets were selected for their similarity to study reservoirs in their elevations, landscape positions, and, hence, basin snow cover across years (Table 1). Introduced trout (*Oncorhynchus mykiss*, *Oncorhynchus mykiss aguabonita*, *Salvelinus fontinalis*, *Salmo*

trutta) were present at all sites, and were stocked annually in all reservoirs as well as one lake (Rock Creek).

Outlet benthic macroinvertebrate and water samples were collected across spring, summer, and fall at each sampled site from summer 2015 through fall 2017 (Table 2), roughly coinciding with upstream lake or reservoir spring mixing, summer stratification, and fall overturn. Lack of flow in fall, or deep snow cover in spring, prevented samples from being collected at some sites in each year (Table 2). Outlet grab water samples for nutrient analyses were filtered through 1.0 μm polycarbonate membranes (Nucleopore) < 6 hrs after collection into high density polyethylene bottles, then kept frozen, in the dark, until processing later the same day. Measurements of dissolved oxygen (DO) and temperature also were collected at each visit (Yellow Springs Instruments 2030, ± 0.2 mg DO L^{-1}, ± 0.3 °C). Stream bed particle size distributions were characterized by visually sorting particles into size classes, then computing the median particle size (cm; D_{50}; Wolman, 1954), in summer of 2016 and 2017.

Invertebrates were collected from riffles that were 50 m downstream of each lake or reservoir outlet with a D net (30 cm wide base, 500 μm mesh), by disturbing an area of 0.09 m^2 directly upstream of the net (3 samples per stream on each sampling date). Triplicate samples were combined and preserved in 90% ethanol in the field. All individual invertebrates were identified in each composite sample to genus or species for Ephemeroptera, Plecoptera, Trichoptera, and Coleoptera, whereas Chironomidae were identified to sub-family and other Diptera to genus. Taxa were then assigned to functional feeding groups (FFGs) using Merritt and Cummins (2008).

Nitrate, ammonium, and soluble reactive phosphorus (SRP) concentrations were measured on a Lachat Automated Ion Analyzer (Hach Company, Loveland, CO, USA), using cadmium reduction (detection limit = 0.3 μM, ±5%; Strickland and Parsons, 1972), indophenol red ammonia detection (detection limit = 0.3 μM, ±5%; Williason and Johnson, 1986), and phosphomolybdate methods (detection limit = 0.2 μM, ±10%; Grasshoff 1976), respectively. For July and August 2017 samples, the phosphomolybdate and fluorometric o-Phthalaldehyde methods (Taylor et al. 2007) were conducted within 24 hours of collection on filtered water that had not been frozen, which reduced detection limits for ammonium and SRP concentrations (ammonium detection limit = 0.1 μM, SRP detection limit = 0.1 μM). Chlorophyll-*a* (chl-a) samples were collected on 0.45 μm nitrocellulose filters (Millipore) and frozen for up to 1 month prior to analysis, then extracted in 90% acetone for 24 hours prior to analysis on an Abbott V-1100D spectrophotometer (Lorenzen, 1967; detection limit = 0.1 $\mu g\ L^{-1}$).

Discharge in reservoir outlets was recorded by the reservoir operator, Southern California Edison, and reported annually to the US Geologic Survey with the data being available as daily mean values on the National Water Information System (NWIS, nwis.waterdata.usgs.gov/nwis). At each lake outlet, pressure transducers were installed (Solinst Levelogger 3001 M5, ± 0.3 cm) with data compensated for local atmospheric pressure by the associated deployment of an atmospheric pressure logger (Solinst Barologger, ± 0.05 kPa; Spuller, Lower Gaylor lakes) or by using atmospheric pressure data obtained from the US Army Corps of Engineers Cold Regions Research and Engineering Laboratory and the University of California, Santa Barbara Energy Site at Mammoth Mountain (Bair et al. 2015, snow.ucsb.edu; used for Rock Creek, Ruby, Crystal lakes). Lake

outlet discharge was monitored manually during spring, summer, and fall for a minimum of eight times at each site from 2015 to 2017 by measuring outlet width, depths, and current velocities (using a Marsh McBirney Flo-Mate 2000 current meter) at 10 regularly spaced points along a cross-stream transect. Rating curves of relationships between measured discharge and pressure transducer data for each lake outlet were then used to compute 30 minute discharge values from pressure data, which were then averaged daily for comparison to reservoir outlet flow data.

Statistical analyses

Flow metrics were computed using daily discharge data for each outlet stream (Indicators of Hydrological Analysis, IHA, Richter et al., 1996). IHA group 2, 3, and 5 metrics were calculated, which encompassed the magnitude, duration, and timing of annual extreme (maximum, minimum) flow conditions, as well as the rate and frequency of daily flow changes. The rise and fall rates were calculated as the mean of all positive (rise rate) or negative (fall rate) differences for consecutive daily values at each site. Reversals were calculated by determining periods of two or more consecutive days when flow was rising or falling, then counting the number of times that flow shifted in direction (e.g., "rising" to "falling") during the water year. Two additional flow metrics, days since maximum flow (DSMF), and duration of snowmelt recession, were calculated. DSMF was computed as the number of days elapsed from the date of peak spring flow to the sampling date, whereas recession period was the number of days between peak spring flow and baseflow index (7-day minimum flow/mean annual flow) at each site. Discharge data were not collected from lakes until August 2015, so calculations of reservoir flow metrics did not begin until that time and 2015 data cannot be directly compared to 2016 and 2017 data.

Flow metrics were examined for collinearity using a correlation matrix (Pearson's r), with some inter-correlated metrics being removed prior to analyses to eliminate redundancy in hydrological information. Metrics removed were: 1, 3, 7, and 90 day minimum flow (related to 30 day minimum flow); 3, 7, 30, and 90 day maximum flow (related to 1 day maximum flow); rise and fall rate (related to 1 day maximum flow); and minimum flow date (related to 30 day minimum flow). The metrics retained for analyses were annual mean daily flow, mean 7 day discharge before sampling, 1 day maximum flow, 30 day minimum flow, zero flow days, baseflow, maximum flow date, recession period duration, DSMF, and reversals.

The benthic macroinvertebrate assemblage data were comprised of a matrix of relative abundances of all invertebrate taxa across all sampled sites and times. Dissimilarity between all pairs of site-times was computed using the Sørensen distance metric. Non-metric multidimensional scaling (NMDS) was used to visualize patterns in invertebrate assemblages across sites-times, grouped by season and water body type (lake or reservoir). Significant correlations (Pearson's r, $p < 0.01$) between NMDS axes and transformed abiotic variables ($\log_{10}$ for continuous measurements, $\log_{10} x + 1$ for counts), as well as the relative abundances of common invertebrate taxa (> 25% of samples), were also calculated. Paired t-tests were used with NMDS axis scores to distinguish significant differences in the multivariate invertebrate dataset among seasons and years. The multi-response permutation procedure (MRPP) was used to test for significant differences in multivariate distances among water body types.

Species richness data were rarified to the minimum number of invertebrates identified and counted across samples. Evenness was computed as $J = H/ln(S)$, where H = Shannon-

Weiner diversity and *S* is the total number of species in a sample. Statistical differences in rarified species richness, evenness, and total invertebrate density between lakes and reservoirs, grouped by season-year (e.g., spring 2017), were determined using Mann-Whitney U tests with corrections for comparisonwise error across all tests using Benjamini-Hochberg adjustments (Benjamini and Hochberg, 1995; false discovery rate = 0.05).

Statistical analyses were conducted in R, using the *vegan* and *ecodist* packages for NMDS, Sørensen distance computation, and rarefaction.

Results

Mean annual daily flow varied by two orders of magnitude across the study period and all sites, from 0.013 $m^3 s^{-1}$ at Lower Gaylor Lake in 2016 to 1.15 $m^3 s^{-1}$ at Sabrina reservoir in 2017. Mean annual reservoir discharge was significantly higher than lake discharge in 2016 and 2017 (t-test, Benjamini-Hochberg adjusted (B-H) $p < 0.001$) (Figure 1, Table 3). Mean daily discharge for the 7 days prior to sampling (7 Day Discharge) spanned 4 orders of magnitude across all sites and times, peaking at 4.5 $m^3 s^{-1}$ at Sabrina reservoir in spring 2017, but was not significantly different between lakes and reservoirs in any season-year (t-test, B-H adjusted p values > 0.05). The recession period ranged from 18 days (Saddlebag Reservoir, 2017) to 166 days (Rock Creek Lake, 2016), and was also not significantly different in lake and reservoir outlets in each year (t-test, B-H adjusted p values > 0.05). Reservoir baseflow and 30 day minimum flows were significantly greater than those in lakes in 2016 and 2017 (t-test, B-H adjusted p values < 0.05). Reservoir outlets had more zero flow days than lakes in 2016, driven by the Ellery Reservoir outlet, which was dry more than 250 days in that year, and year-round low but non-zero flows at Ruby and Rock Creek lakes. The remaining four reservoirs had no zero flow days through the entire study period. A

likely avalanche hit the surface of Ruby Lake in January 2017, accounting for the peak in discharge for lakes shown for that time in Figure 1.

Lake and reservoir outlet concentrations of ammonium and SRP ranged from below detection (ammonium 2015-2016 detection limit = 0.3 μM, 2017 = 0.1 μM; SRP 2015-2016 detection limit = 0.2 μM, 2017 = 0.1 μM), to 9.2 μM NH_4 and 0.46 μM PO_4, but were low (< 1 μM) in most samples (93% and 100%, respectively). Nitrate concentrations ranged from below detection limits (0.3 μM) to 13.4 μM, with values > 1 μM occurring in 70% of the samples. Nitrate export from both lakes and reservoirs was highest in spring and decreased through summer into fall, being most pronounced in 2017 when both concentration and flow were higher than in 2015 and 2016 (Figure 2). Ammonium and SRP export from lakes was low across seasons in 2015 and 2016, but exhibited a peak in spring 2017, then subsequently decreased through summer into fall 2017. Reservoir ammonium export increased through the ice free seasons of 2015 and 2016, but decreased slightly from spring to fall in 2017. SRP export from reservoirs was low throughout 2015 and 2016, but increased from spring into summer of 2017 before decreasing to 2015 and 2016 levels. Export of nitrate, ammonium, and SRP were higher out of reservoirs than lakes in summer 2017 and ammonium export also was significantly higher from reservoirs than lakes in the summer of 2016 and the autumns of 2016 and 2017 (t-tests, B-H adjusted p values < 0.05; Figure 2).

Water temperature in both lake and reservoir outlets followed a seasonal pattern of low temperatures in spring, increasing temperatures in summer, and decreases into fall, except for 2017 when temperatures were similar in summer and fall. Outlet temperatures were not significantly different between lake and reservoir outlets in any season-year (t-test, B-H adjusted p values > 0.05) (Figure 3). D_{50} values similarly were not significantly different

in lake (n = 5) and reservoir (n = 5) outlets (t-test, $p > 0.60$), nor did they consistently change across sites from 2016 to 2017 (paired t-test, p ca. 0.98). Outlet chl-a concentrations were low (all < 3 $\mu g\ L^{-1}$), but reservoir export was elevated in 2017, and was significantly higher than from lakes for each season that year ($p < 0.05$, B-H comparisonwise error adjustment) (Figure 4).

A total of 85 invertebrate taxa were identified, with samples being numerically dominated by four sub-families of Chironomidae (Chironominae, Orthocladiinae, Prodiamesinae, Tanypodinae) and a single Simuliidae genus (*Prosimulium*), but Ephemeroptera, Plecoptera, and Trichoptera also were commonly collected. Coleoptera (primarily the elmid beetle *Lara*) and Tipulidae (*Antocha*, *Pedicia*, *Tipula*) were present at low densities. Reservoir outlet invertebrate density increased from summer to fall in 2015, but decreased from summer to fall in 2016, reflecting temporal patterns in chironomid abundance. In 2017, total invertebrate, primarily Simuliidae, density increased from spring to summer, then decreased into fall (Figure 5). Lake and reservoir outlet rarified richness and evenness were relatively stable across seasons in 2017, but decreased in lakes from spring through fall in 2016. In 2015, richness remained stable, but evenness declined, from summer to fall in reservoir outlets, whereas richness declined and evenness increased in lake outlets. The proportion of total density made up of EPT species showed similar patterns as rarified richness, reflecting the importance of EPT species in determining total richness. Lake and reservoir evenness, richness, total density, chironomid density, the proportion of total density composed of EPT taxa, and Simuliidae density were not significantly different in any season-year (p's > 0.05, Mann Whitney U tests with B-H comparisonwise error adjustment applied for each response variable).

Invertebrate assemblages were numerically dominated by collector-filterers (primarily *Prosimulium*) in both lake and reservoir outlets in summer and fall 2017 and in reservoir outlets in summer 2016 (Figure 6), and densities of each functional feeding group were not different between lakes and reservoirs after B-H error adjustment (p's > 0.05, Mann Whitney U tests with B-H comparisonwise error adjustment). Shredders and scrapers were rare across all times in both lake and reservoir outlets, with the exception of scrapers in lake outlets in spring 2017. Functional feeding groups (FFGs) were more evenly distributed in lake than reservoir outlets in summer 2016, but by fall lake outlet assemblages were composed almost exclusively of predators and collector-filterers, whereas reservoir outlets still additionally contained collector-gatherers and shredders. In 2016, filterer densities were stable across seasons in lake outlets, but increased from spring into summer then decreased into fall in reservoir outlets.

NMDS analysis on the relative abundances of invertebrate taxa across all sites and times produced three axes accounting for 75% of the variation in the multivariate invertebrate dataset (stress = 17.1). The first and second NMDS axes accounted for 34.6% and 23.4% of the variation in the multivariate invertebrate dataset, respectively. Positive values of NMDS axes 1 and 2 were positively correlated with 1 day maximum flow, whereas D50 values were negatively related to NMDS axis 1 scores and positively related to NMDS axis 2 scores (Pearson's r, $p < 0.01$) (Figure 7). Positive values of NMDS 1 were associated with high relative abundances of the mayfly *Baetis* and the filter-feeding simuliid *Prosimulium*, whereas negative values were related to high relative abundances of the Chironomid sub-family Tanypodinae. Chironominae were positively related, and Tanypodinae, *Rhyacophila*, and *Serratella* were negatively related, to NMDS axis 2. NMDS

axis 3 accounted for 17.1% of the multivariate variation and was correlated positively with ammonium flux, mean annual flow, and chl-a export. Positive values of NMDS 3 were associated with *Isoperla* and negative values with *Prosimulium.*

Lake and reservoir NMDS scores were not significantly different along the three axes, in any season-year (t tests, p values > 0.05, B-H comparisonwise error adjustment). Along NMDS axis 2, spring and summer were significantly different from fall when averaging scores for each site across all years (paired t tests, $p < 0.05$, B-H comparisonwise error adjustment. NMDS axes 1 and 3 differentiated between 2016 and 2017, where scores were averaged across all seasons within individual years (paired t tests, $p < 0.01$, B-H comparisonwise error adjustment).

MRPP tests showed that multivariate distances between lakes and reservoirs combining all season-years were not significantly different ($p > 0.05$).

Discussion

Although baseflow, 30 day minimum flows, and mean annual flow were higher in reservoirs than lakes in 2016 and 2017, benthic macroinvertebrate assemblages did not differ between lake and reservoir outlets in any season-year, contrary to my initial hypothesis based on expected relationships between flow conditions and invertebrate communities. However, invertebrate community structure differed across season and years, likely in response to variable flow regimes, such as the elevated 1 day maximum flow, mean annual flow, and summer ammonium export in 2017 relative to other years. The results suggest, then, that lake and reservoir flow differences were not large enough to have a significant effect on invertebrate communities against a backdrop of large temporal changes in flow. Although other studies have shown that reservoirs affect water temperature via hypolimnetic releases

(e.g. Ward and Stanford, 1979), I did not observe temperature differences between lake and reservoir outlets in this study, possibly owing to insufficient temporal coverage. On the other hand, mean annual flow (2016, 2017), chl-a export (2017), and ammonium flux (summer, fall, 2016 and 2017) were higher out of reservoirs than lakes (Table 3, Figure 2), and were significantly correlated with community structure (Figure 7). Multivariate invertebrate responses to temporal changes in nutrient export and flow apparently outweighed the effects of flow alteration by reservoir management.

Both floods and drought disturbances can have large effects on stream community structure (Resh et al., 1988; Naiman et al., 2008; Herbst et al., 2019), but here only a 'flood' disturbance, 1 day maximum flow, was significantly correlated with community assemblages, though maximum flow was also associated with increased mean annual flow. Although baseflow or minimum flow metrics were not correlated with community structure in this study, lake outlet richness tended to be reduced in the falls versus summers of 2015 and 2016 (Figure 5), when reservoir outlet richness remained fairly constant, possibly as a step response to very low flows (< 0.01 m^3 s^{-1}), as has been observed in other streams (Lake, 2003; Herbst et al., 2019). This study coincided with the final year of a multi-year drought (2015), a nearly average snow pack year (2016), and a wet year (2017), so lower flows in 2015 and 2016 versus 2017 may have resulted in reduced fall richness in lake outlets, whereas reservoir fall richness remained higher owing to higher base and minimum flows effected through hypolimnetic release. The recession period was not related to invertebrate community structure in this study, despite covering a range of 60-115 days through the study period, contrasting with research in Sierra foothill streams showing that the snowmelt

recession period duration was positively associated with invertebrate diversity and richness (Steel et al. 2018).

The importance of flow regimes in structuring invertebrate communities in this study was confirmed by results showing that 2017 communities were different from 2016, and metrics related to flow (export, mean annual flow, 1 day maximum flow) were significantly related to invertebrate communities. Species evenness and rarified richness were more seasonally variable in 2016 than 2015 or 2017 (Figure 5), reflecting a notable decrease in reservoir chironomid density from spring through summer to fall in 2016 but not 2015 or 2017 and almost total disappearance of gatherers in fall in both lakes and reservoirs. Lake and reservoir outlet communities were not different in any season-year, again suggesting that the magnitude of flow alteration by reservoirs did not have an effect on invertebrate communities, even though overall temporal variation in flow did.

Ephemeroptera, Plecoptera, and Trichoptera (EPT) taxa as a proportion of total density (% EPT) declined from spring (2016) or summer (2015) to fall, but remained relatively constant through the seasons in 2017. Percent EPT also was not significantly different between lakes and reservoirs, contrary to my expectation that EPT taxa would be elevated below reservoirs. This again is likely due to lake-reservoir flow differences being outweighed by interannual variability, because flood disturbance was related to community assemblage structure. *Baetis* and simuliids, which are known to increase in response to disturbance (Wallace and Gurtz, 1986; Flecker and Feifarek, 1994) were significantly correlated with 1 day maximum flow (Figure 7). Other EPT taxa, *Rhyacophila* and *Serratella*, were significantly related instead to smaller substrata, which in these streams were cobbles or pebbles (as opposed to boulders) (Minshall, 1984), but as low NMDS axis 2 scores were

related to fall, this is more likely to be a seasonal effect, suggesting that *Rhyacophila* and *Serratella* were late ice-free season taxa.

Black flies, primarily *Prosimulium*, were common below lakes and reservoirs particularly during high flow, a common and well-known phenomenon generally attributed to flow and the flux of sestonic food from upstream (Richardson and Mackay, 1991). In this study chl-a export was used as a proxy for POM flux, but was negatively correlated with *Prosimulium* and positively correlated with the perlodid stonefly *Isoperla*. Given that *Prosimulium* was also strongly correlated with one-day maximum discharge, it is likely that the observed relationships were ultimately driven by increasing *Prosimulium* density with increasing flow and food flux.

Water temperature is often related to stream invertebrate community structure, including in alpine and Sierra foothill streams (Ward and Stanford, 1982; Hieber et al., 2005; Steel et al., 2018), but temperature was not related to any invertebrate metrics in this study, which may have been due to the infrequency of temperature measurements. Lake and reservoir outlet temperatures may not have differed during the ice-free season as hypolimnetic reservoir discharge continuously removed the coldest water from reservoirs resulting in warmer overlying water replacing hypolimnetic water, and the ice-free season was shortened due to high snowpack in 2017, which reduced the time available for stratification.

Elevated nitrate, phosphorus and ammonium concentrations in low-order streams are often related to invertebrate abundance (Hinterleitner-Anderson et al., 1992; Harvey et al., 1998; Benstead et al., 2005), through bottom up effects, increasing stream primary productivity which subsequently drives increases in invertebrate abundances. In this study, ammonium export was higher out of reservoirs than lakes in summer and fall 2016 and 2017,

and both SRP and nitrate export were higher out of reservoirs in summer 2017 (Figure 2), but only ammonium export was significantly correlated with community structure, which was also related to differences in flow (Figure 7). SRP concentrations were low or below detection limits during the study period, whereas nitrate concentrations and flux in high elevation streams usually peak before maximum flow (Melack et al., 1998) then steadily decrease into fall (Figure 2), thus effects of nitrate are likely collinear with flow. Ammonium concentrations and fluxes were generally low in the dry and average years (2015, 2016) with increases in late summer below reservoirs or rarely in early fall below lakes (Chapter 1), suggesting that ammonium export increased when invertebrate densities decreased in fall when flows were low.

Conclusions

Although mean annual flow, minimum flows, and ammonium export were higher in reservoir than lake outlets in 2016 and 2017, the structure of benthic macroinvertebrate assemblages did not differ between lake and reservoir outlets during the study period. Instead, aggregated lake and reservoir outlet community structure differed across seasons and years, with the summer and fall of 2017, a wet year, being different from other times. Because low or no flows are important determinants of invertebrate community structure in alpine streams (Herbst et al., 2019), outlet invertebrate assemblages may be expected to diverge in lake versus reservoir outlets during drought years (Weisberg et al., 1990), but no such significant effect was observed here after comparisonwise error adjustment. The effects of interannual flow variability on invertebrate communities apparently outweighed the importance of flow alteration by reservoirs, but reservoir management seasonally increased ammonium export from Sierra reservoirs (Chapter 1), which was significantly related to

community structure likely as a combined effect of seasonal patterns in flow and resource export. In addition, rain-on-snow extreme flow events are predicted to increase over the next century (Dettinger et al., 2009), which can have a significant effect on high Sierra stream invertebrate assemblages (Herbst and Cooper, 2010), but reservoir management (i.e., winter drawdown, runoff storage) may prevent such events from affecting reservoir outlet streams.

References

Arp, C.D., Baker, M.A., 2007. Discontinuities in stream nutrient uptake below lakes in mountain drainage networks. Limnology and Oceanography 52, 1978–1990. https://doi.org/10.4319/lo.2007.52.5.1978

Bair, E.H., Dozier, J., Davis, R.E., Colee, M.T., Claffey, K.J., 2015. CUES—a study site for measuring snowpack energy balance in the Sierra Nevada. Front. Earth Sci. 3. https://doi.org/10.3389/feart.2015.00058

Benstead, J.P., Deegan, L.A., Peterson, B.J., Huryn, A.D., Bowden, W.B., Suberkropp, K., Buzby, K.M., Green, A.C., Vacca, J.A., 2005. Responses of a beaded Arctic stream to short-term N and P fertilisation. Freshwater Biology 50, 277–290. https://doi.org/10.1111/j.1365-2427.2004.01319.x

Benjamini Y, Hochberg Y., 1995. Controlling the false discovery rate: a practical and powerful approach to multiple testing. Journal of the Royal statistical society: series B (Methodological). 57, 289-300. https://doi.org/10.1111/j.2517-6161.1995.tb02031.x

Bini, L.M., Landeiro, V.L., Padial, A.A., Siqueira, T., Heino, J., 2014. Nutrient enrichment is related to two facets of beta diversity for stream invertebrates across the United States. Ecology 95, 1569–1578. https://doi.org/10.1890/13-0656.1

Bona, F., Falasco, E., Fenoglio, S., Iorio, L., Badino, G., 2008. Response of macroinvertebrate and diatom communities to human-induced physical alteration in mountain streams. River Research and Applications 24, 1068–1081. https://doi.org/10.1002/rra.1110

Bruno, M.C., Siviglia, A., Carolli, M., Maiolini, B., 2013. Multiple drift responses of benthic invertebrates to interacting hydropeaking and thermopeaking waves. Ecohydrology 6, 511–522. https://doi.org/10.1002/eco.1275

Bunn, S.E., Arthington, A.H., 2002. Basic principles and ecological consequences of altered flow regimes for aquatic biodiversity. Environmental Management 30, 492–507. https://doi.org/10.1007/s00267-002-2737-0

Céréghino, R., Lavandier, P., 1998. Influence of hypolimnetic hydropeaking on the distribution and population dynamics of Ephemeroptera in a mountain stream. Freshwater Biology 40, 385–399. https://doi.org/10.1046/j.1365-2427.1998.00353.x

Datry, T., Larned, S.T., Tockner, K., 2014. Intermittent rivers: a challenge for freshwater ecology. BioScience 64, 229–235. https://doi.org/10.1093/biosci/bit027

Dettinger, M.D., Hidalgo León, H.G., Das, T., Cayan, D.R., Knowles, N., 2009. Projections of potential flood regime changes in California. California Climate Change Center, California Energy Commission, Sacramento CA. 54 pages.

Dickson, N.E., Carrivick, J.L., Brown, L.E., 2012. Flow regulation alters alpine river thermal regimes. Journal of Hydrology 464–465, 505–516. https://doi.org/10.1016/j.jhydrol.2012.07.044

Donath, U., Robinson, C.T., 2001. Ecological characteristics of lake outlets in Alpine environments of the Swiss Alps. Archiv für Hydrobiologie 207–225. https://doi.org/10.1127/archiv-hydrobiol/150/2001/207

Flecker AS, Feifarek B., 1994. Disturbance and the temporal variability of invertebrate assemblages in two Andean streams. Freshwater Biology. 2, 131-42.

Gasith, A., Resh, V.H., 1999. Streams in Mediterranean climate regions: abiotic influences and biotic responses to predictable seasonal events. Annual Review of Ecology and Systematics 30, 51–81.

Goodman, K.J., Baker, M.A., Wurtsbaugh, W.A., 2010. Mountain lakes increase organic matter decomposition rates in streams. Journal of the North American Benthological Society 29, 521–529. https://doi.org/10.1899/09-070.1

Grasshoff, K., 1976. Methods of Seawater Analysis. Verlag Chemie, 159-228. https://doi.org/10.1002/iroh.19850700232

Hannan, H.H., 1979. Chemical modifications in reservoir-regulated streams, in: Ward, J.V., Stanford, J.A. (Eds.), The Ecology of Regulated Streams. Springer US, Boston, MA, pp. 75–94. https://doi.org/10.1007/978-1-4684-8613-1_6

Harvey, C.J., Peterson, B.J., Bowden, W.B., Hershey, A.E., Miller, M.C., Deegan, L.A., Finlay, J.C., 1998. Biological responses to fertilization of Oksrukuyik Creek, a tundra stream. Journal of the North American Benthological Society 17, 190–209. https://doi.org/10.2307/1467962

Herbst, D.B., Cooper, S.D., 2010. Before and after the deluge: rain-on-snow flooding effects on aquatic invertebrate communities of small streams in the Sierra Nevada, California. Journal of the North American Benthological Society 29, 1354–1366. https://doi.org/10.1899/09-185.1

Herbst, D.B., Cooper, S.D., Medhurst, R.B., Wiseman, S.W., Hunsaker, C.T., 2019. Drought ecohydrology alters the structure and function of benthic invertebrate communities in mountain streams. Freshwater Biology 64, 886– 902. https://doi.org/10.1111/fwb.13270

Hieber, M., Robinson, C.T., Uehlinger, U., Ward, J.V., 2005. A comparison of benthic macroinvertebrate assemblages among different types of alpine streams. Freshwater Biology 50, 2087–2100. https://doi.org/10.1111/j.1365-2427.2005.01460.x

Hieber, M., Robinson, C.T., Uehlinger, U., Ward, J.V., 2002. Are alpine lake outlets less harsh than other alpine streams? Archiv für Hydrobiologie 154, 199–223. https://doi.org/10.1127/archiv-hydrobiol/154/2002/199

Hinterleitner-Anderson, D., Hershey, A.E., Schuldt, J.A., 1992. The effects of river fertilization on mayfly (Baetis sp.) drift patterns and population density in an arctic river. Hydrobiologia 240, 247–258. https://doi.org/10.1007/BF00013466

Jackson, H.M., Gibbins, C.N., Soulsby, C., 2007. Role of discharge and temperature variation in determining invertebrate community structure in a regulated river. River Research and Applications 23, 651–669. https://doi.org/10.1002/rra.1006

Kennedy, T.A., Muehlbauer, J.D., Yackulic, C.B., Lytle, D.A., Miller, S.W., Dibble, K.L., Kortenhoeven, E.W., Metcalfe, A.N., Baxter, C.V., 2016. Flow management for hydropower extirpates aquatic insects, undermining river food webs. BioScience 66, 561–575. https://doi.org/10.1093/biosci/biw059

Kownacka, M., Kownacki, A., 1968. The influence of ice cover on bottom fauna in the Tatra streams. Acta Hydrobiologica 10, 95–102.

Lake, P. S., 2003. Ecological effects of perturbation by drought in flowing waters. Freshwater Biology 48, 1161–1172. https://doi.org/10.1046/j.1365-2427.2003.01086.x

Lorenzen, C.J., 1967. Determination of chlorophyll and pheo-pigments: spectrophotometric equations. Limnology and Oceanography 12, 343–346. https://doi.org/10.4319/lo.1967.12.2.0343

Lusardi, R.A., Bogan, M.T., Moyle, P.B., Dahlgren, R.A., 2016. Environment shapes invertebrate assemblage structure differences between volcanic spring-fed and runoff rivers in northern California. Freshwater Science 35, 1010–1022. https://doi.org/10.1086/687114

Lytle, D.A., Poff, N.L., 2004. Adaptation to natural flow regimes. Trends in Ecology & Evolution 19, 94–100. https://doi.org/10.1016/j.tree.2003.10.002

Marcarelli, A.M., Wurtsbaugh, W.A., 2007. Effects of upstream lakes and nutrient limitation on periphytic biomass and nitrogen fixation in oligotrophic, subalpine streams. Freshwater Biology 52, 2211–2225. https://doi.org/10.1111/j.1365-2427.2007.01851.x

Melack, J., Sickman, J.O., Leydecker, A., Marrett, D., 1998. Comparative analyses of high-altitude lakes and catchments in the Sierra Nevada: susceptibility to acidification, final report (No. 032–188). University of California, Santa Barbara, California Air Resources Board.

Merritt, R.W., Cummins, K.W., 2008. An introduction to the aquatic insects of North America, 4th ed. Kendall Hunt Publishing Company, Dubuque, Iowa.

Minshall, G. W., 1984. Aquatic insect-substratum relationships. In: V. H. Resh and D. M. Rosenberg (eds.). The Ecology of Aquatic Insects, Praeger, New York, pp. 358–400.

Naiman, R.J., Latterell, J.J., Pettit, N.E., Olden, J.D., 2008. Flow variability and the biophysical vitality of river systems. Comptes Rendus Geoscience, Ecosystèmes et événements climatiques extrêmes 340, 629–643. https://doi.org/10.1016/j.crte.2008.01.002

Nakagawa, S., Johnson, P.C.D., Schielzeth, H., 2017. The coefficient of determination R^2 and intra-class correlation coefficient from generalized linear mixed-effects models revisited and expanded. J R Soc Interface 14. https://doi.org/10.1098/rsif.2017.0213

Null SE, Viers JH, Mount JF., 2010. Hydrologic response and watershed sensitivity to climate warming in California's Sierra Nevada. PLoS One, 5:e9932.

Poff, N.L., Allan, J.D., Bain, M.B., Karr, J.R., Prestegaard, K.L., Richter, B.D., Sparks, R.E., Stromberg, J.C., 1997. The natural flow regime. BioScience 47, 769–784. https://doi.org/10.2307/1313099

Poff, N.L., Olden, J.D., Merritt, D.M., Pepin, D.M., 2007. Homogenization of regional river dynamics by dams and global biodiversity implications. Proceedings of the National Academy of Sciences 104, 5732–5737.

Poff, N.L., Zimmerman, J.K.H., 2009. Ecological responses to altered flow regimes: a literature review to inform the science and management of environmental flows. Freshwater Biology 55, 194–205. https://doi.org/10.1111/j.1365-2427.2009.02272.x

Power, M.E., Sun, A., Parker, G., Dietrich, W.E., Wootton, J.T., 1995. Hydraulic food-chain models: an approach to the study of food-web dynamics in large rivers. BioScience 45, 159–167. https://doi.org/10.2307/1312555

Quadroni, S., Crosa, G., Gentili, G., Espa, P., 2017. Response of stream benthic macroinvertebrates to current water management in Alpine catchments massively developed for hydropower. Science of The Total Environment 609, 484–496. https://doi.org/10.1016/j.scitotenv.2017.07.099

Rader, R.B., Belish, T.A., 1999. Influence of mild to severe flow alterations on invertebrates in three mountain streams. Regulated Rivers: Research & Management 15, 353–363.

https://doi.org/10.1002/(SICI)1099-1646(199907/08)15:4<353::AID-RRR551>3.0.CO;2-U

Rehn, A.C., 2009. Benthic macroinvertebrates as indicators of biological condition below hydropower dams on west slope Sierra Nevada streams, California, USA. River Research and Applications 25, 208–228. https://doi.org/10.1002/rra.1121

Resh, V.H., Brown, A.V., Covich, A.P., Gurtz, M.E., Li, H.W., Minshall, G.W., Reice, S.R., Sheldon, A.L., Wallace, J.B., Wissmar, R.C., 1988. The role of disturbance in stream ecology. Journal of the North American Benthological Society 7, 433–455. https://doi.org/10.2307/1467300

Richter, B.D., Baumgartner, J.V., Powell, J., Braun, D.P., 1996. A method for assessing hydrologic alteration within ecosystems. Conservation Biology 10, 1163–1174. https://doi.org/10.1046/j.1523-1739.1996.10041163.x

Richardson, J., & Mackay, R., 1991. Lake outlets and the distribution of filter feeders: an assessment of hypotheses. Oikos, 62, 370-380. doi:10.2307/3545503

Robinson, C., Minshall, G., 1990. Longitudinal development of macroinvertebrate communities below oligotrophic lake outlets. Great Basin Naturalist 50, 303-311.

Robinson, C.T., Alther, R., Leys, M., Moran, S., Thompson, C., 2015. A note on the trophic structure of alpine streams in the Wind River Mountains, Wyoming, USA. Fundamental and Applied Limnology/Archiv für Hydrobiologie 187, 43-54. https://doi.org/info:doi/10.1127/fal/2015/0730

Robinson, C.T., Matthaei, S., 2007. Hydrological heterogeneity of an alpine stream–lake network in Switzerland. Hydrological Processes 21, 3146–3154. https://doi.org/10.1002/hyp.6536

Robinson, C.T., Tonolla, D., Imhof, B., Vukelic, R., Uehlinger, U., 2016. Flow intermittency, physico-chemistry and function of headwater streams in an Alpine glacial catchment. Aquatic Science 78, 327–341. https://doi.org/10.1007/s00027-015-0434-3

Rosenberg, D.M., McCully, P., Pringle, C.M., 2000. Global-scale environmental effects of hydrological alterations: Introduction. BioScience 50, 746–751. https://doi.org/10.1641/0006-3568(2000)050[0746:GSEEOH]2.0.CO;2

Schinegger, R., Trautwein, C., Melcher, A., Schmutz, S., 2012. Multiple human pressures and their spatial patterns in European running waters. Water and Environment Journal 26, 261–273. https://doi.org/10.1111/j.1747-6593.2011.00285.x

Steel, A.E., Peek, R.A., Lusardi, R.A., Yarnell, S.M., 2018. Associating metrics of hydrologic variability with benthic macroinvertebrate communities in regulated and unregulated snowmelt-dominated rivers. Freshwater Biology 63, 844–858. https://doi.org/10.1111/fwb.12994

Strickland, J.D., Parsons, T.R., 1972. A practical handbook of seawater analysis. Fisheries Research Board of Canada, 310 pages.

Taylor, B.W., Keep, C.F., Hall, R.O., Koch, B.J., Tronstad, L.M., Flecker, A.S., Ulseth, A.J., 2007. Improving the fluorometric ammonium method: matrix effects, background fluorescence, and standard additions. Journal of the North American Benthological Society 26, 167–177. https://doi.org/10.1899/0887-3593(2007)26[167:ITFAMM]2.0.CO;2

Tennant, D.L., 1976. Instream flow regimens for fish, wildlife, recreation and related environmental resources. Fisheries 1, 6–10. https://doi.org/10.1577/15488446(1976)001<0006:IFRFFW>2.0.CO;2

Vidal-Abarca, M.R., Sánchez-Montoya, M.M., Guerrero, C., Gómez, R., Arce, M.I., García-García, V., Suárez, M.L., 2013. Effects of intermittent stream flow on macroinvertebrate community composition and biological traits in a naturally saline Mediterranean stream. Journal of Arid Environments 99, 28–40. https://doi.org/10.1016/j.jaridenv.2013.09.008

Wallace JB, Gurtz M., 1986. Response of Baetis mayflies (Ephemeroptera) to catchment logging. American Midland Naturalist 1, 25-41.

Ward, J.V., 1994. Ecology of alpine streams. Freshwater Biology 32, 277–294. https://doi.org/10.1111/j.1365-2427.1994.tb01126.x

Ward, J.V., Stanford, J.A., 1983. The serial discontinuity concept of lotic ecosystems, in: Dynamics of Lotic Ecosystems, Fontaine, T., Bartell, S. (Eds.). Ann Arbor Science Publishers, Michigan pp. 29–42.

Ward, J.V., Stanford, J.A., 1982. Thermal responses in the evolutionary ecology of aquatic insects. Annual Review of Entomology 27, 97–117. https://doi.org/10.1146/annurev.en.27.010182.000525

Ward, J.V., Stanford, J.A., 1979. Ecological factors controlling stream zoobenthos with emphasis on thermal modification of regulated streams, in: Ward, J.V., Stanford, J.A. (Eds.), The Ecology of Regulated Streams. Springer US, Boston, MA, pp. 35–55. https://doi.org/10.1007/978-1-4684-8613-1_4

Weisberg, S.B., Janicki, A.J., Gerritsen, J., Wilson, H.T., 1990. Enhancement of benthic macroinvertebrates by minimum flow from a hydroelectric dam. Regulated Rivers: Research & Management 5, 265–277. https://doi.org/10.1002/rrr.3450050307

Willason, S.W., Johnson, K.S., 1986. A rapid, highly sensitive technique for the determination of ammonia in seawater. Mar. Biol. 91, 285–290. https://doi.org/10.1007/BF00569445

Wolman, M.G., 1954. A method of sampling coarse river-bed material. Eos, Transactions American Geophysical Union 35, 951–956. https://doi.org/10.1029/TR035i006p00951

Wurtsbaugh, W.A., Baker, M.A., Gross, H.P., Brown, P.D., 2005. Lakes as nutrient "sources" for watersheds: a landscape analysis of the temporal flux of nitrogen through sub-alpine lakes and streams. SIL Proceedings, 1922-2010 29, 645–649. https://doi.org/10.1080/03680770.2005.11902758

Yarnell, S., Peek, R., Epke, G., Lind, A., 2016. Management of the spring snowmelt recession in regulated systems. JAWRA Journal of the American Water Resources Association 52, 723–736. https://doi.org/10.1111/1752-1688.12424

Yarnell, S.M., Viers, J.H., Mount, J.F., 2010. Ecology and management of the spring snowmelt recession. BioScience 60, 114–127. https://doi.org/10.1525/bio.2010.60.2.6

Table 1: Locations and characteristics of study streams, with annual maximum snow water equivalent (SWE) for each basin in each year. “L” and “R” denote lake and reservoir. The first year of sampling is indicated below the site name. The bottom row indicates if there were significant differences between lake and reservoir outlet characteristics (Mann-Whitney U tests with Benjamini-Hochberg (B-H) corrections).

Site	***Latitude***	***Longitude***	***Elevation (m)***	***Watershed Area (ha)***	***2015 SWE (cm)***	***2016 SWE (cm)***	***2017 SWE (cm)***
Crystal (L) (2016)	37° 35' 39" N	119° 01' 07" W	2932	95	NA	103	208
Spuller (L) (2016)	37° 56' 55" N	119° 17' 05" W	3124	137	NA	69	164
Lower Gaylor (L) (2015)	37° 54' 50" N	119° 16' 06" W	3155	99	3.8	72	138
Rock Creek (L) (2015)	37° 27' 14" N	118° 44' 13" W	2957	3116	1.3	19	80
Ruby (L) (2015)	37° 24' 55" N	118° 46' 01" W	3383	449	12.7	49	132
Sabrina (R) (2015)	37° 12' 35" N	118° 36' 50" W	2782	4334	2.5	34	61
Saddlebag (R) (2016)	37° 58' 01" N	119° 16' 06" W	3068	1801	NA	69	164
South (R) (2016)	37° 10' 07" N	118° 34' 12" W	2977	3277	NA	34	61
Tioga (R) (2015)	37° 55' 35" N	119° 15' 10" W	2937	980	3.8	72	138
Ellery (R) (2015)	37° 56' 07" N	119° 14' 07" W	2901	4139	15.2	70	160
p-values, L or R greater			0.10	**0.026 (R>L)**	0.87	0.92	0.38

Table 2: Sites sampled in each season and year. Lack of flow occasionally prevented sampling in fall and deep snow cover precluded sampling in spring for some sites. Five additional sites were sampled in 2016: Ellery, Saddlebag, South, Crystal, and Spuller.

Year	*Season*	*Lakes sampled*	*Reservoirs sampled*	*Lakes not sampled*	*Reservoirs not sampled*
2015	Summer	Gaylor, Rock, Ruby	Tioga, Sabrina	-	Ellery
	Fall	Rock, Ruby	Tioga, Sabrina	Gaylor	Ellery
2016	Spring	Gaylor, Rock, Ruby, Crystal, Spuller	Sabrina, South, Saddlebag, Tioga, Ellery	-	-
	Summer	Gaylor, Rock, Ruby, Crystal, Spuller	Sabrina, South, Saddlebag, Tioga, Ellery	-	-
	Fall	Rock, Crystal, Ruby	Sabrina, South, Saddlebag, Tioga	Spuller, Gaylor	Ellery
2017	Spring	Rock, Gaylor, Crystal	Sabrina, South, Saddlebag, Tioga, Ellery	Spuller, Ruby	-
	Summer	Gaylor, Rock, Ruby, Crystal, Spuller	Sabrina, South, Saddlebag, Tioga, Ellery	-	-
	Fall	Rock, Crystal, Ruby, Spuller	Sabrina, South, Saddlebag, Tioga	Gaylor	Ellery

Table 3: Mean annual lake and reservoir (2015: lakes, n = 3, reservoirs n = 3; 2016-2017: lakes, n = 5, reservoirs, n = 5) flow metrics, computed for each water year. Where lake and reservoir metrics were significantly different (t tests, B-H adjusted $p < 0.05$), values are presented in bold.

Flow Metric	***2015***	***2016***	***2017***	***Type***
1 Day Max	0.06	0.44	3.49	lake
(m^3s^{-1})	0.49	1.36	4.67	reservoir
30 Day Min	0.04	**0.01**	**0.02**	lake
(m^3s^{-1})	0.24	**0.12**	**0.23**	reservoir
Baseflow	0.48	**0.04**	**0.03**	lake
(m^3s^{-1})	0.75	**0.34**	**0.26**	reservoir
Zero flow days	17	**47**	57	lake
(days)	11	**59**	48	reservoir
Max. Flow Date	220	176	179	lake
(Julian day)	228	218	191	reservoir
Reversals	4	38	69	lake
(count)	15	51	41	reservoir
Mean Annual Flow	0.043	**0.069**	**0.221**	lake
(m^3s^{-1})	0.392	**0.363**	**0.92**	reservoir
Recession Period	33.6	95.4	115	lake
(days)	34.5	60.0	78	reservoir

Figure 1: Mean daily discharge averaged across all lakes (red) and reservoirs (blue) throughout the study period, August 2015- September 2017. Shaded areas represent ± 1 SE.

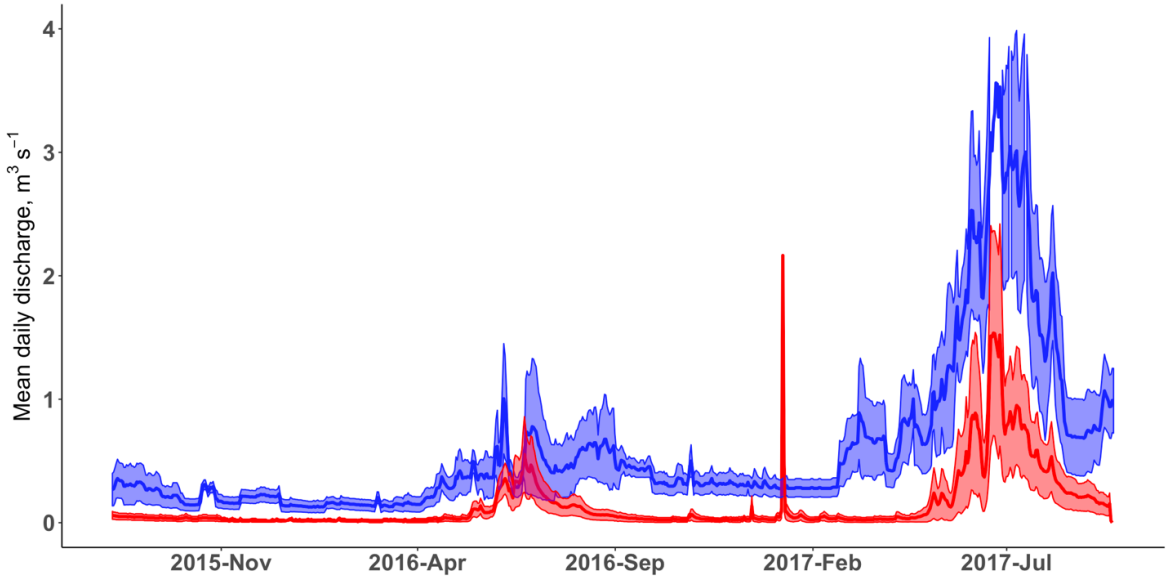

Figure 2: Lake and reservoir mean nutrient export rates (+ 1 SE) across seasons and years. No samples were collected in spring 2015. Significant differences between lakes and reservoirs are denoted with "*" (t-test, B-H adjusted $p < 0.05$).

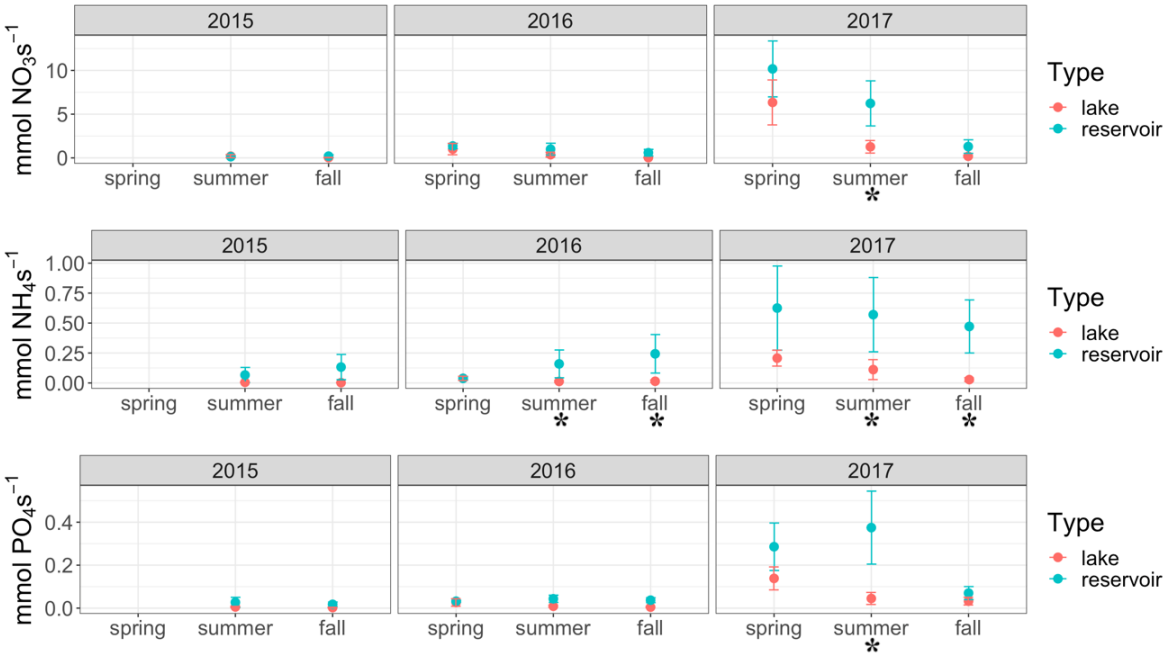

Figure 3: Mean lake and reservoir outlet temperatures (± 1 SE) across seasons and years. No significant differences were observed between lake and reservoir temperatures for any season in any year (t-tests, B-H adjusted p's > 0.05).

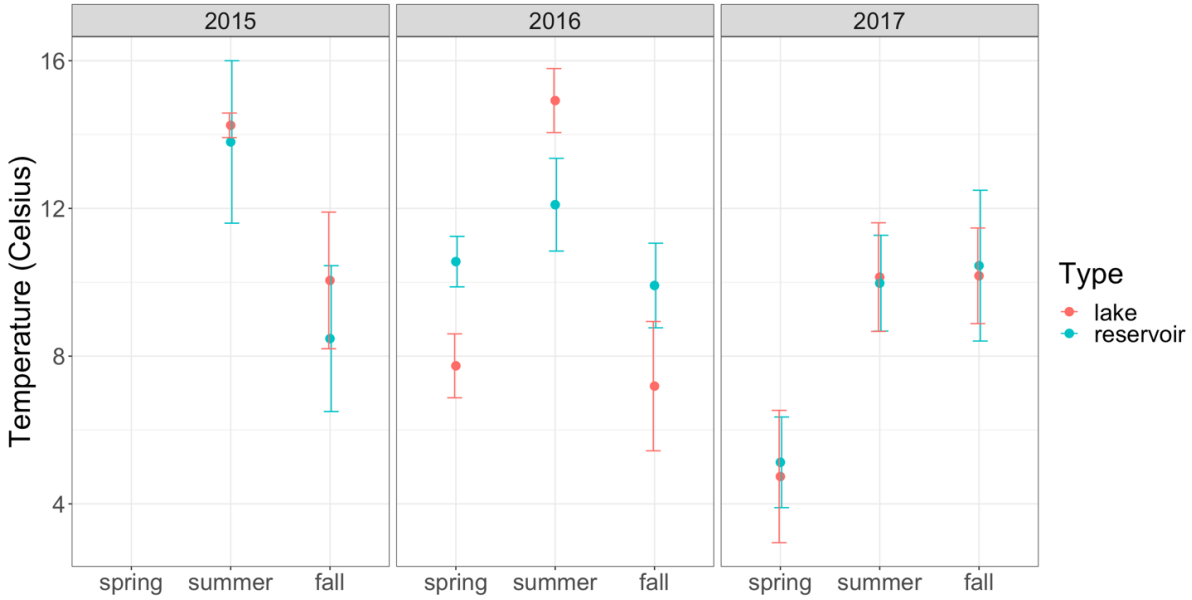

Figure 4: Mean lake and reservoir outlet chlorophyll-*a* export (mg s^{-1}) (± 1 SE) across seasons and years. Significant differences are denoted with "*" (t-tests, B-H adjusted p < 0.05).

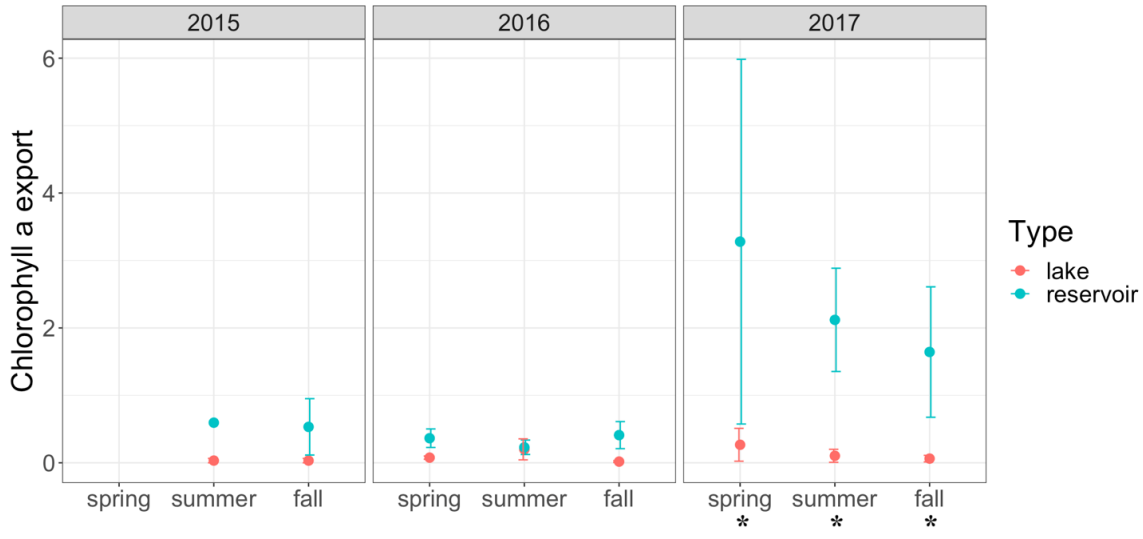

Figure 5: Mean benthic macroinvertebrate taxa evenness index, rarified richness (species), total density (indv. m^{-2}), chironomid density (indv. m^{-2}), EPT (Ephemeroptera, Plecoptera, Trichoptera) taxa as a percent of total abundance, and Simuliidae density (indv. m^{-2}) ($\pm$ 1 SE) in lakes vs. reservoirs across seasons and years. No samples were collected in spring 2015. Lake and reservoir values were not significantly different for any invertebrate metric in any season-year (Mann Whitney U test, adjusted $p > 0.05$).

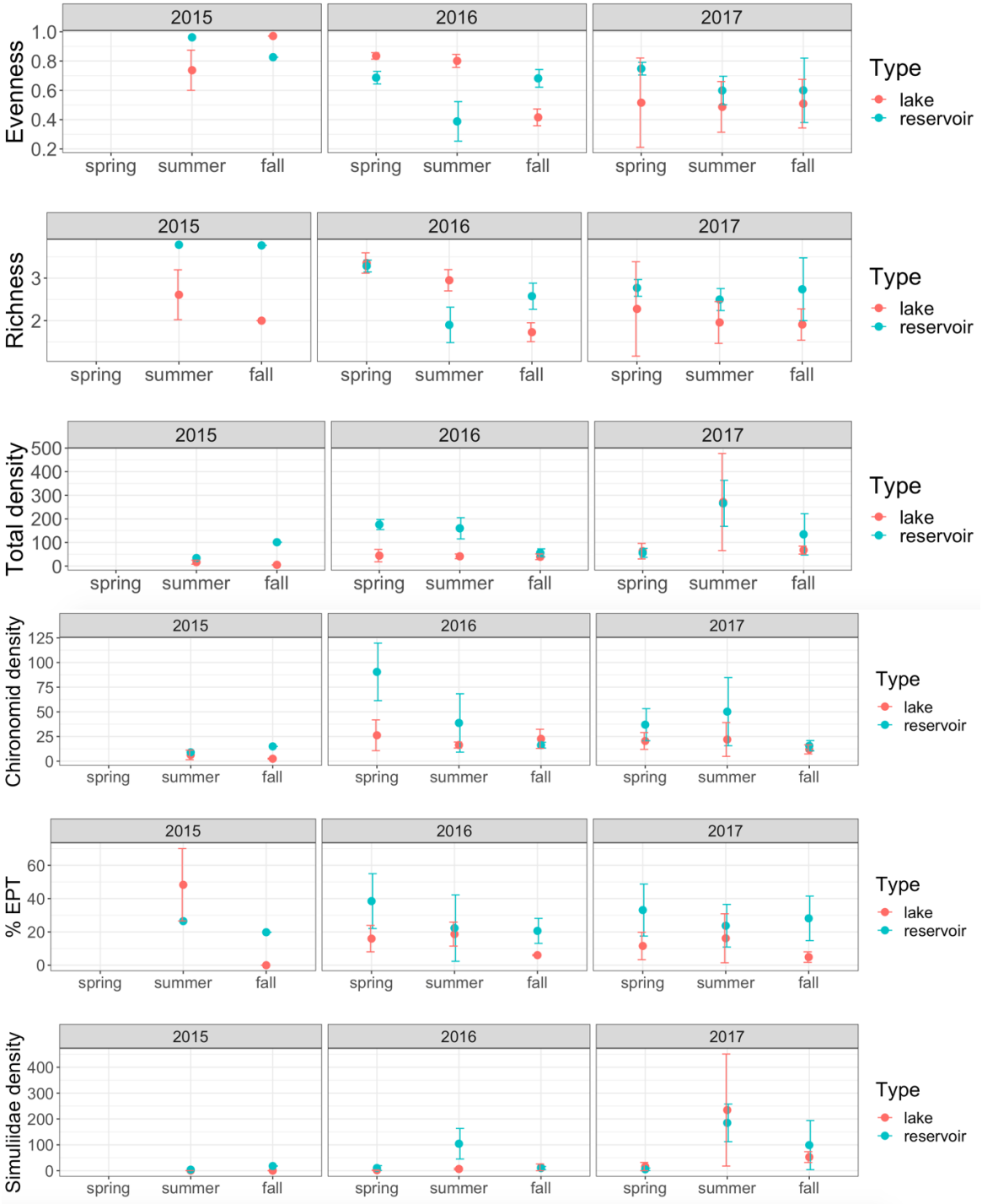

Figure 6: Mean invertebrate functional feeding group densities for lakes (top panel) and reservoirs (bottom panel). No samples were collected in spring 2015. Lake and reservoir functional feeding group densities were not significantly different in any season-year (Mann Whitney U test, adjusted $p > 0.05$).

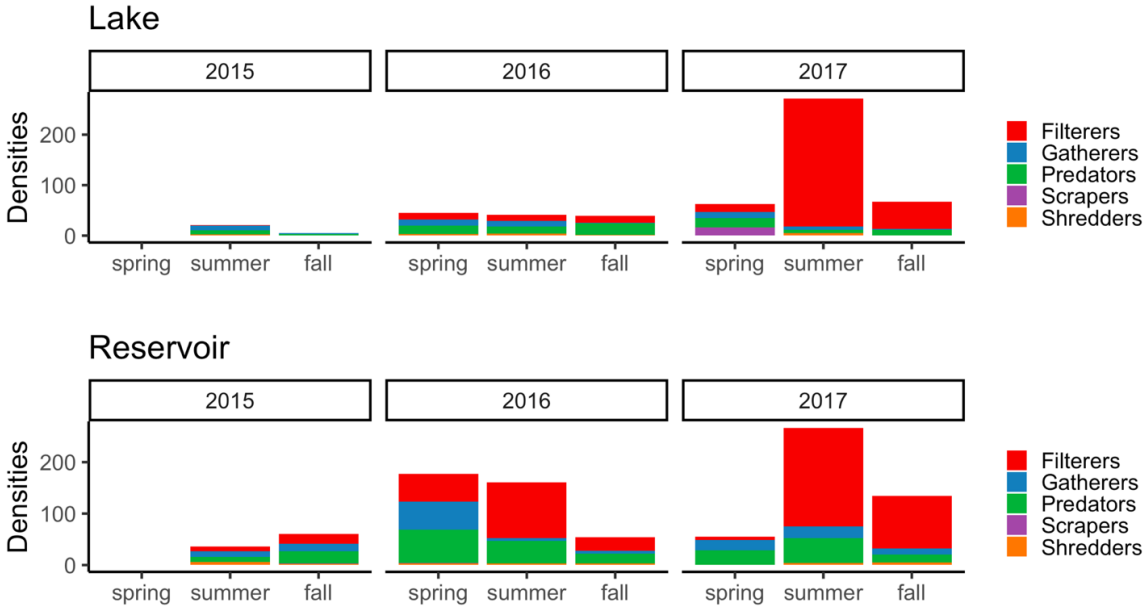

Figure 7: Ordination plots of nonmetric multidimensional scaling (NMDS) analysis on relative abundances of benthic macroinvertebrate taxa across sites during spring (triangles), summer (squares), fall (circles) in 2015 (red), 2016 (green), and 2017 (blue). Top panel: NMDS axis 1 versus NMDS axis 2. Bottom panel: NMDS axis 1 versus NMDS axis 3. The variation in the invertebrate dataset explained by each NMDS axis is displayed with the axis labels. The stress of the 3-dimensional NMDS solution is shown in the top panel. Correlation coefficients (Pearson's *r*) of common taxa (occurring in >1/4 of samples) significantly related ($p < 0.01$) to each NMDS axis are shown next to axes. Transformed (log_{10} for measured continuous data, $log_{10}x+1$ for counts) environmental variables significantly ($p < 0.01$) correlated with NMDS axes are shown on the left side of both plots, where: *1MAX* = mean 1 day maximum flow (m^3s^{-1}) , *NH4F* = ammonium export rate (mmol NH_4 s^{-1}) , *ANNQ* = annual mean flow (m^3 s^{-1}) , *D50* = median particle size (mm), *chla* = chlorophyll-a concentration (µg L^{-1}) .

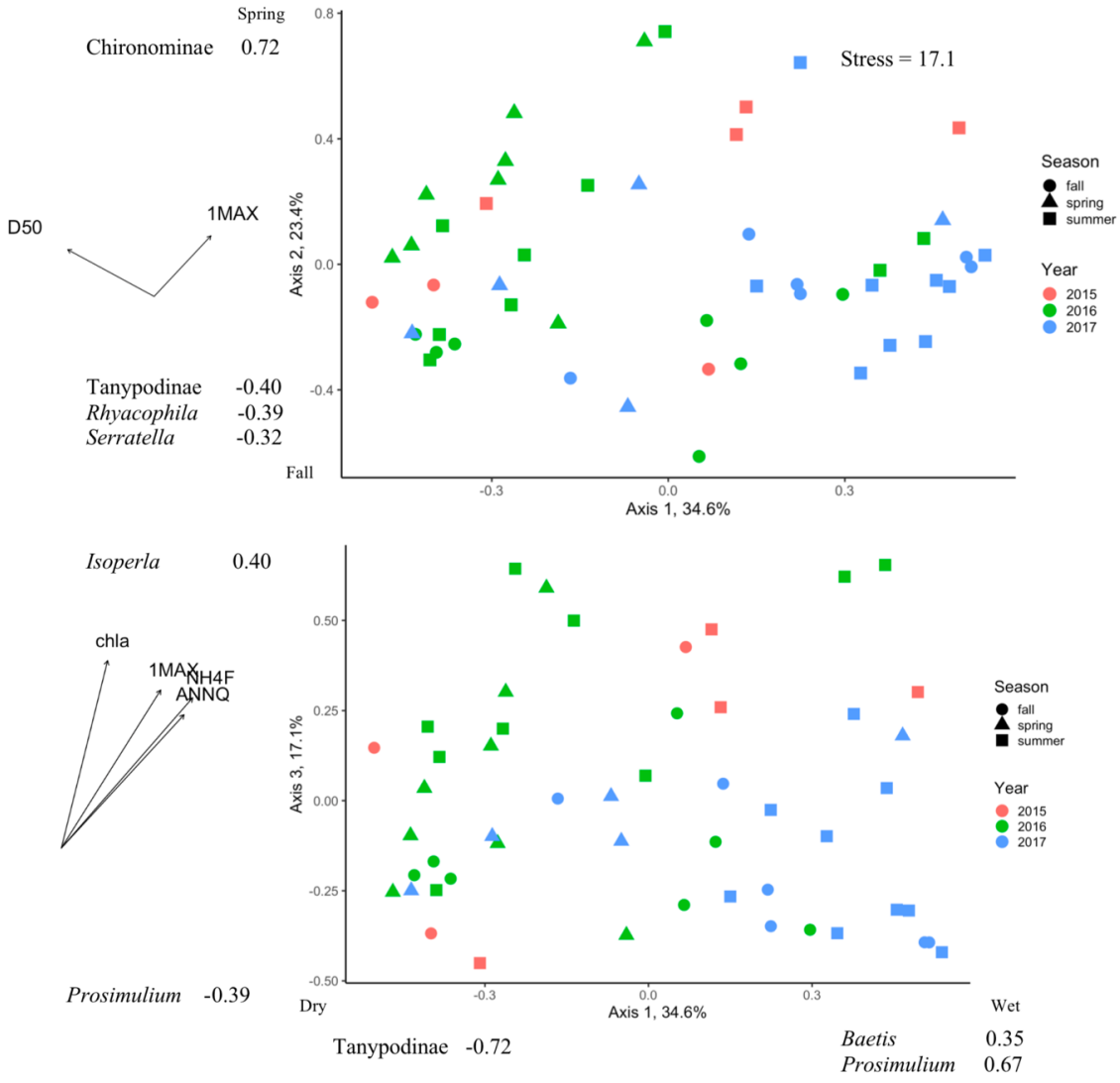

Figure 8: Ordination plots of nonmetric multidimensional scaling (NMDS) analysis on relative abundances of benthic macroinvertebrate taxa across sites, identical to figure 7, but where lakes (red) and reservoirs (blue) are shown in addition to season. Top panel: NMDS axis 1 versus NMDS axis 2. Bottom panel: NMDS axis 1 versus NMDS axis 3. The variation in the invertebrate dataset explained by each NMDS axis is displayed with the axis labels. The stress of the 3-dimensional NMDS solution is shown in the top panel. Correlation coefficients (Pearson's *r*) of common taxa (occurring in >1/4 of samples) significantly related ($p < 0.01$) to each NMDS axis are shown next to axes. Transformed (log_{10} for measured continuous data, $log_{10}x+1$ for counts) environmental variables significantly ($p < 0.01$) correlated with NMDS axes are shown on the left side of both plots, where: *1MAX* = mean 1 day maximum flow (m^3s^{-1}) , *NH4F* = ammonium export rate (mmol NH_4 s^{-1}) , *ANNQ* = annual mean flow (m^3 s^{-1}) , *D50* = median particle size (mm), *chla* = chlorophyll-a concentration (µg L^{-1}) .

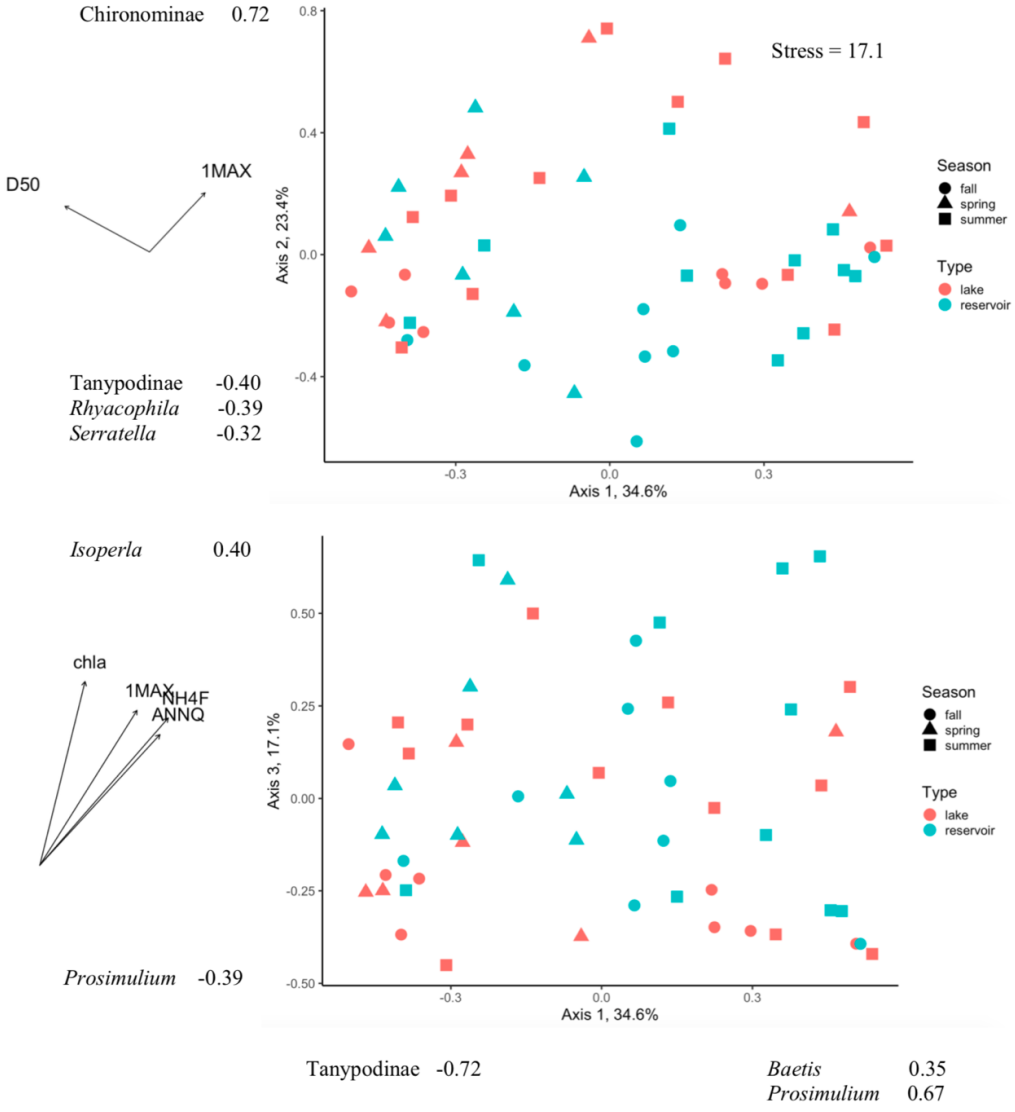

CHAPTER THREE

Carbon dioxide supersaturation in high-elevation oligotrophic lakes and reservoirs in the Sierra Nevada, California

Abstract

To better understand the contribution of alpine lakes to global CO_2 emissions, carbon dioxide concentrations and fluxes to the atmosphere were measured in five high-elevation lakes and five reservoirs in the Sierra Nevada, California. Median summer surface concentrations of dissolved CO_2 (reservoirs: 21.1 μM, lakes: 23.7 μM) were supersaturated for most of the ice-free season. Median diffusive flux of CO_2 was low as compared to other inland waters (lakes: 260 mg CO_2 m^{-2} d^{-1}, reservoirs: 192 mg CO_2 m^{-2} d^{-1}). Linear mixed modeling demonstrated that the length of ice cover, persisting for 5-9 months and allowing for accumulation of under-ice CO_2, was a strong predictor of summer surface CO_2. During the ice-free period, surface evasion of CO_2 was highest for the first 40 days after ice-off when carbon dioxide that had accumulated during winter was released, though supersaturation and evasion continued until fall at most sites despite low rates of ecosystem metabolism. This study suggests that the contribution of high-elevation, oligotrophic lakes and reservoirs in the Sierra to global CO_2 emissions are small despite persistent supersaturation, and are primarily driven by the duration of ice-cover.

Introduction

Supersaturation of CO_2 is common in inland waters (Cole et al. 1994), from the arctic (Kling et al. 1992) to tropical wetlands (Melack 2016), and many lakes and reservoirs release CO_2 to the atmosphere (Cole et al. 2007; Raymond et al. 2013). Studies on high-elevation aquatic emissions are less common, and often focus on hydropower reservoirs (Del Sontro et al. 2010, Diem et al. 2012). Though unproductive, high elevation lakes have been found to be supersaturated in CO_2 (Jonnson et al. 2003; Pighini et al. 2018).

In seasonally ice-covered lakes, summer supersaturation of CO_2 at the lake surface can be a result of under-ice conditions, as CO_2 produced by decomposition during winter is trapped under ice and retained into the ice-free season (MacIntyre et al. 2018). Winter CO_2 accumulation can account for 3-80% of total annual CO_2 flux in northern lakes (Ducharme-Riel et al. 2015), and 11-55% of annual flux can occur during the initial ice thaw (Karlsson et al. 2013), which can occur in pulses rather than a single event, as spring mixing brings gases to the surface (Denfeld et al. 2018). Measuring the rate of CO_2 evasion during those periods can be accomplished in a variety of ways, including eddy covariance and floating chambers (Podgrajsek et al. 2014); chambers are portable and readily deployed in remote areas.

Reservoirs greater than ~15 years old generally emit CO_2 at an areal rate similar to that of lakes (Barros et al. 2011), but in the Austrian and Italian Alps, Pighini et al. (2018) found that mean summer surface CO_2 concentrations were lower in reservoirs than natural lakes despite ubiquitous supersaturation. However, they found no significant correlations between surface dissolved CO_2 and temperature, dissolved oxygen, elevation, surface area, and depth, leaving the primary drivers of pCO_2 and the mechanism of reduced pCO_2 in reservoirs unclear.

California's Sierra Nevada contain more than 10,000 lakes and several dozen reservoirs, which are oligotrophic, primarily at high elevations (>2700 m), and are ice-covered for some portion of the year. Little work has been done to characterize seasonal or spatial control of Sierra lake pCO_2, and to date no data have been published on CO_2 within the high-elevation reservoirs throughout this range. For high elevation lakes within the Sierra, watershed snow water equivalent (SWE) determines the timing of ice-off in spring (Sadro et al. 2019), which sets the length of time during which CO_2 can accumulate under

ice. In addition, SWE is negatively correlated with summer dissolved organic carbon (DOC) concentrations (Sadro et al. 2018), and an increase in DOC inputs was observed to shift a southern Sierra lake to net heterotrophy (Sadro et al. 2011a) by increasing allochthony. Late summer pCO_2 across a latitudinal gradient of lakes throughout the Sierra in 2014 (S. Sadro, personal communication) show surface under saturation of CO_2 as low as 7%, and hypolimnetic supersaturation of up to 590%, indicating that local factors will play an additional role in determining summer CO_2 concentrations. Earlier work on Emerald Lake in the southern Sierra Nevada demonstrates that a typical high-elevation Sierra lake is net autotrophic during the ice-free season (Sadro et al. 2011a), suggesting that net autotrophy should contribute to the summer drawdown of CO_2. However, metabolic rates are variable seasonally and with depth (Sadro et al. 2011b), and periods of net heterotrophy may contribute to the CO_2 pool even after ice-off.

This study examined concentrations and fluxes of CO_2 from five lakes and five reservoirs in the Sierra Nevada across a gradient of watershed characteristics, lake morphologies (Table 1), and ice-covered periods (Table 2), in order to understand controls on summer pCO_2 in seasonally ice-covered, oligotrophic systems, while also providing the first characterization of CO_2 emissions from reservoirs in the region. By quantifying CO_2 concentrations under ice and through the ice-free season, in conjunction with measurements of surface CO_2 flux and metabolic rates, the results of this work should provide a better understanding of how environmental factors and aquatic productivity interact to determine CO_2 retention in these unproductive lakes.

Accumulation of CO_2 and resultant supersaturation in late winter was expected at all sites as a result of ice cover, and under-ice CO_2 was hypothesized to be positively related to

the duration of ice cover allowing for a longer period of accumulation, while negatively correlated with dissolved oxygen concentrations, which should act as a proxy for overwinter respiration rates. Summer surface CO_2 concentrations were expected to decrease rapidly after ice-off as a result of diffusive flux and net autotrophy, while summer hypolimnetic concentrations were expected decrease more slowly due to net heterotrophy at depth, and stratification reducing vertical flux.

Methods

Ten sites were sampled in the eastern Sierra Nevada, California, within or adjacent to protected wilderness areas from June to September 2017 (Figure 1). The sites are subalpine to alpine, ranging from 2782 to 3383 m a.s.l. (Table 1) in recently glaciated watersheds with poor soil development underlain primarily by granitoids and sporadic metasedimentary and metavolvanic rocks. Five of these sites are storage reservoirs constructed in the early 1900s managed for recreation, hydropower generation, domestic use, and irrigation. Of the eight high elevation eastern Sierra reservoirs, five were selected based on their year-round accessibility allowing for same-day processing of samples in the laboratory; high flows in 2017 closed access to the remaining three reservoirs. The five lakes were selected for their proximity to the reservoirs (Figure 1) and to span a range of characteristics comparable to that of the selected reservoirs (Table 1). Southern Sierra April 1 snow water equivalent (SWE) was ~200% of the 1966-2015 average in 2017 (California Cooperative Snow Surveys), causing an extended ice-covered season particularly at higher elevations.

Sites were sampled at least three times during the ice-free season: immediately following ice-off, during midsummer stratification, and during fall overturn. Under-ice CO_2

samples were collected once from Spuller, Lower Gaylor, Tioga, Ellery, Rock Creek, Sabrina, and South lakes. Under ice samples were not collected from Crystal, Saddlebag, and Ruby lakes as access was delayed due to the deep snowpack. Water was collected from each outlet stream and from a boat over the deepest point of each lake on each sampling date in the midmorning or early afternoon, with hypolimnetic samples also collected when lakes were stratified. Stratification was first observed in profiles 2-4 weeks after ice-off, and lakes were mixed on final fall sampling dates, which was inferred from observed isothermy through each water column. Profiles of dissolved oxygen (DO), temperature, and specific conductivity were also collected at 1 m intervals at each visit with probes (Yellow Springs Instruments 2030, $\pm$ 0.2 mg DO L^{-1}, $\pm$ 0.3 °C, $\pm$ 1 $\mu S\ cm^{-1}$), which were calibrated for DO in 0 and 100% saturation solutions in April, June, and September, as well as calibration for altitude and temperature prior to sampling at each site.

Surface water samples were collected at ~0.20 m depth in high density polyethylene bottles and hypolimnetic samples were collected 2 m below the thermocline using a Kemmerer bottle. Headspace equilibration was performed in the field by transferring the sampled water to a syringe, drawing in ambient air, and shaking vigorously for two minutes. Headspace gas was then injected directly into evacuated vials. Ambient air samples were also collected at each visit. Vials were stored at room temperature in the dark until analysis, within 24 hours of collection. All gas samples were analyzed using a PP Systems EGM-4 portable IRGA, calibrated at 0 and 10,000 ppm and standards of 300, 800, 5,000 and 10,000 ppm were run prior to sample injection. Dissolved CO_2 was calculated with Henry's law, using the concentration of CO_2 in air, CO_2 solubility in water, and local air pressure and temperature (Weiss 1974; Benson and Krause 1984).

Chlorophyll-a (chl-a) samples were collected on 0.45 μm porosity nitrocellulose filters (Millipore), and extracted in 90% acetone for 24 hours prior to analysis on an Abbott V-1100D spectrophotometer. DOC samples were filtered through precombusted (2 hours, 500°C) 0.7 μm nominal pore size Whatman GF/F filters (Wilde et al. 2014) into precombusted (12 hours, 500°C) 40 mL borosilicate vials with Teflon-coated septa. DOC samples were acidified with hydrochloric acid to pH <2, and analyzed using the high temperature combustion method on a Shimadzu TOC-V (± 1.5% measured concentration)

Lake volumes were obtained in three ways: for reservoirs, elevation-storage tables were provided by the reservoir operator, Southern California Edison (SCE); for three sites (Spuller, Ruby, Crystal), volumes were obtained from Melack et al. (1998); for the remaining two sites (Lower Gaylor, Rock Creek), bathymetric maps were generated through depth measurements taken with a Lowrance Hook-5 sonar system along transects across these lakes in 2016. Depth and location data were then used to calculate hypsometric curves in QGIS 3.2. Watershed area was calculated from 1/3 arc-second resolution digital elevation models (3D Elevation Program, USGS), lake area from the California Department of Fish and Wildlife California Lakes GIS product, and land cover was determined from CALVEG (Region 5, Existing Vegetation). Watershed, lake, and land cover areas were calculated in ArcMap 10.2. Basin April 1 SWE was obtained from the California Cooperative Snow Survey using stations nearest to each site and at similar elevations.

Ice-on and ice-off dates for all sites were determined visually from Landsat 7 and 8 satellite imagery (landlook.usgs.gov); ice-on and ice-off could be determined with ± 4 day uncertainty. The date recorded was chosen as the midpoint between images before and after ice-on or ice-off, and adjusted when direct observation during sample collection allowed.

Reservoir outlet discharge is reported annually by USGS on the National Water Information System (NWIS). At each lake outlet, pressure transducers were installed (Solinst Levelogger 3001 M5, ± 0.3 cm), which were adjusted for atmospheric pressure by data from an atmospheric pressure logger (Solinst Barologger, ± 0.05 kPa), or atmospheric pressure data obtained from the US Army Corps of Engineers Cold Regions Research and Engineering Laboratory and the University of California, Santa Barbara Energy Site (Bair et al. 2015, snow.ucsb.edu), depending on the distance from each submerged pressure transducer. Transducers were installed at Lower Gaylor, Ruby, and Rock Creek lakes in August 2015, after which discharge was measured at a minimum nine times at each site over the ice-free seasons of 2015, 2016, and 2017. Two additional transducers were installed in June 2016 at Crystal and Spuller lakes, where discharge was measured at a minimum seven times during the ice-free seasons of 2016 and 2017. Discharge was calculated using measurements of stream depth, width, and current velocity, the latter measured with a current meter (Marsh McBirney Flo-Mate 2000), to develop discharge rating curves for each lake outlet pressure transducer.

Flux chamber construction, deployment, and resulting calculation of CO_2 flux were performed following Bastviken et al. (2015). Infrared CO_2 sensors (Senseair K33 ELG, ± 3% measured value) were installed within plastic containers on the interior of plastic tubs (6.85 L volume, 29.5 cm diameter at water surface). A dozen 2 cm diameter holes were drilled in the small plastic containers to allow airflow while minimizing the potential for lake water to wet the sensors. The rate of increase of CO_2 within the chamber was calculated by fitting a linear regression to the chamber data, which was used to calculate flux by:

$$\text{Flux} = \frac{\Delta C}{\Delta t} \cdot \frac{\text{volume}}{\text{area}} \cdot \frac{p_{atm}}{R \cdot T}$$

where $\Delta C/\Delta t$ = fitted slope of CO_2 increase within chamber ($R^2 > 0.98$), volume of chamber = 6.85 L, area of chamber at water surface = 684 cm^2, p_{atm} = local atmospheric pressure, in atm, R = gas constant 0.08205746 L atm K^{-1} mol^{-1}, T = water surface temperature, in Kelvin. Flux chambers were deployed for ~1 hour during each visit at a measurement interval of 30 seconds, over the deepest part of each lake or reservoir.

To measure metabolism, optical dissolved oxygen loggers (D-opto, Zebratech, ±0.02 mg DO L^{-1}) were deployed for 24 h at two lakes and two reservoirs in late July to mid-August and at one lake and one reservoir in late August to mid-September. Instruments were calibrated in 0% and 100% saturation solutions prior to deployment. Loggers were deployed at two to four depths, dependent on maximum lake depth, and recorded DO every 10 minutes. A variation of the mass balance method (Odum 1956; Sadro et al. 2011a) was used to calculate metabolic rates from data averaged hourly. Net ecosystem production (NEP) was calculated for each hourly average as NEP = ΔDO + F_{DO}/MLD, where NEP (g m^{-3}) is the net change in dissolved oxygen that is attributed to biological processes, ΔDO (g m^{-3}) is the change in dissolved oxygen as measured directly by each logger, F_{DO} (g m^{-2}) is flux across the air-water interface, and MLD (m) is the mixed layer depth. Flux of oxygen into or out of the lake or reservoir due to atmospheric gas exchange was calculated as: $F_{DO} = k_{DO}(C_w - C_{aq})$, where k_{DO} (m h^{-1}) is the coefficient of gas exchange of oxygen at given temperature, C_w (g m^{-3}) is the concentration of dissolved oxygen at the water surface, and C_{aq} (g m^{-3}) is the saturation concentration of dissolved oxygen at the water surface. C_{aq} was calculated from measured water surface temperature and local atmospheric pressure (Garcia and Gordon, 1992). k_{DO} was estimated from k_{600} as modeled from wind speed (Cole and Caraco, 1998) and Schmidt numbers were calculated for oxygen based on surface water temperature

(Wanninkhof 2014), which were used to compute the gas transfer coefficient of oxygen from the relationship between Schmidt numbers (Jahne et al. 1987). Wind speeds were obtained from the California Data Exchange Center (CDEC), from California Department of Water Resources meteorological stations nearest to each lake or reservoir, which were 0.5 km (Rock Creek), 0.9 km (Lower Gaylor), 1.6 km (Tioga), and 6 km (Saddlebag) from each site. At Rock Creek Lake in July, wind speed data from a station 13 km away were used because repairs were being conducted at the nearer station. Wind data from these stations introduces error into the estimate of O_2 flux, but provide approximations of local high-elevation wind conditions.

Calculated NEP hourly averages were summed across each 24 h deployment to determine daily rates of NEP; community respiration (CR) was determined by summing calculated nighttime NEP and dividing by the duration of night to obtain an hourly rate of CR, which was used for the full deployment. GPP was then calculated from the difference of NEP and CR where CR is treated as a negative value. Whole-lake areal rates of metabolism were computed by multiplying volumetric metabolic rates by the volume of water at each logger depth, summing those rates for all depths, and dividing by the surface area of the lake.

To determine the drivers of ice-free season surface CO_2 concentrations across all sites while accounting for the non-independence of CO_2 concentrations during repeat sampling, linear mixed models were developed, with date of sample collection and site treated as random effects. Explanatory variables were checked for collinearity then scaled by centering around 0, and observed CO_2 concentrations were log-transformed to meet assumptions of normality, before model fitting. The function ‘dredge’ in *MuMIn* was used to test all possible combinations of an initial linear mixed model that included all random and fixed effects:

*log(μM) ~ Site Type + Lake Network Number + Ice period + Days since ice-off + Elevation + Water residence time + surface area + DOC + N^2 + PBare + PMeadow + Maximum Storage + Depth*Season + 1|Site + 1|Sample Date*. The best five models as determined by the Akaike information criterion (AIC) are discussed, and the best model overall is presented. Visual inspection of the residual plots did not reveal any deviations from normality.

Nonparametric Spearman's rho was used to compute correlations, and the independent 2-group Mann-Whitney U was used for means comparisons of lakes and reservoirs. Statistical analyses were performed using R, in RStudio, with the base *stats* package. Linear mixed models were developed in R using the packages *MuMIn* and *lme4*.

Results

During the ice-free season in the lakes and reservoirs, dissolved CO_2 concentrations ranged from 15 to 107 μM (Table 3), corresponding to 82-590% saturation. 80% of calculated concentrations were below 50 μM; the highest 20% of the measured concentrations occurred in the early summer, shortly after ice-off (Figure 2). The lowest computed CO_2 saturation (83% of saturation) occurred in late September. Under-ice concentrations ranged from 44.6 μM to 438.6 μM CO_2, corresponding to 250 and 338% saturation, respectively. The median surface CO_2 concentration over the ice-free period was 25.8 μM (median absolute deviation 'MAD' = 7.6, mean = 27.6 μM), which was lower than hypolimnetic concentrations in both lakes (median = 42.8μM, MAD = 22.1, mean = 47.4 μM) and reservoirs (median = 48.7 μM, MAD = 36.9, mean = 49.3 μM), which were not significantly different (p = 0.81; Table 2).

Dates of ice-on and ice-off, and resultant ice-covered periods, varied across sites. In 2016, ice-on occurred as early as Oct. 15 (Spuller) and as late as Dec. 24 (Sabrina, South). Ice-off dates ranged from May 15 (Sabrina) to Aug. 1 (Spuller), corresponding to a range in the period of ice-cover across sites of 148 days (Sabrina: 142 days, Spuller: 290 days) (Table 2).

Surface water temperatures over the period of this study ranged from 0°C under ice at all sites to 15.8°C in midsummer (Tioga reservoir, 7/29/17). Dissolved oxygen ranged from 0 mg L^{-1} (Lower Gaylor, midsummer) to 10.5 mg L^{-1} (Ellery, 6/4/17) in surface waters under ice. DO decreased throughout the period of study as temperature increased. DO was typically near saturation, though there were several exceptions in hypolimnetic waters (<5.3 mg L^{-1}, <5.3°C). Median summer chl-a was 0.35 μg L^{-1} (MAD = 0.3) and below 1 μg L^{-1} for 80% of samples. Summer DOC concentrations ranged from 44.5 μM to 281 μM (Supplement 1). Reservoir discharge during sampling peaked at 5.9 $m^3 s^{-1}$ (Sabrina), while lake discharge peaked at 2.6 $m^3 s^{-1}$ (Rock Creek), and reservoir discharge was higher than lake discharge for the duration of summer 2017.

Maximum buoyancy frequency (N^2) was computed from temperature profiles collected at each visit. N^2 ranged from 0 s^{-2}, where lakes were isothermal, to 5 x 10^{-3} s^{-2} in midsummer. Maximum N^2 briefly decreased after ice off, but increased in summer as stratification developed before falling again in early autumn. Seasons within each waterbody are defined by their stratification, as ice-off dates varied widely; “winter” corresponds to under-ice samples, “spring” to the unstratified period following ice-off, “summer” to ice-free stratified waters, and “fall” corresponds to the second isothermal period reached upon the breakdown of summer stratification.

The rate of CO_2 evasion decreased rapidly after ice-off (Figure 3), with a maximum flux of 1.3 mmol CO_2 m^{-2} hr^{-1} at Crystal Lake in spring (Table 4). Midsummer flux during the stratified period was <0.3 mmol CO_2 m^{-2} hr^{-1} (median: 0.2 mmol CO_2 m^{-2} hr^{-1}, MAD = 0.13, mean = 0.1 mmol CO_2 m^{-2} hr^{-1}), with two observations of negative flux (South and Sabrina, 8/16/17), indicating reservoir uptake of CO_2. An additional two observations of uptake occurred in fall (Rock Creek, Ruby lakes), resulting from undersaturation of CO_2. Midsummer positive and negative fluxes independently were detectably different from zero, but overall were not statistically different from zero ($p = 0.38$). Flux could not be determined with this method in three cases (Spuller lake in spring, summer, and fall) where rates of emission and uptake were too low to detect over a 1 h deployment. Overall fluxes of from lakes (0.2 mmol CO_2 m^{-2} hr^{-1}, MAD = 0.26, mean = 0.4 mmol CO_2 m^{-2} hr^{-1}) and reservoirs (median = 0.2 mmol CO_2 m^{-2} hr^{-1}, MAD = 0.25, mean = 0.2 mmol CO_2 m^{-2} hr^{-1}) were not significantly different ($p = 0.317$). For broader comparisons, daily values of flux were computed by applying hourly values over a 24 h period, yielding a median flux of 260 mg CO_2 m^{-2} d^{-1} (mean = 415 CO_2 m^{-2} d^{-1}) from lakes, and 192 CO_2 m^{-2} d^{-1} (mean = 176 CO_2 m^{-2} d^{-1}) from reservoirs.

Median summer reservoir outlet CO_2 concentration was 31.1 μM (MAD = 11.5), and median summer lake outlet concentration of CO_2 was 28.8 μM (MAD = 10.2), not significantly different from each other ($p = 0.08$).

The five best mixed models were selected using AIC, in which several predictors were dominant: an interactive effect, Depth*Season, and days since ice-off (DSIO) occurred in all five. Length of the ice-covered period and percent of the watershed that is bare were included in four of the five best models. Averaged over the best five models, the effect of

DSIO ($p = 0.0048$) was highly significant, and both Depth*Season ($p = 0.052$) and the ice-covered period ($p = 0.058$) were nearly significant.

The best model as determined by AIC included DSIO, ice-covered period, and Depth*Season as fixed effects, and sample date as a random factor: *log(μM) ~ Days since ice off + Length of winter ice cover + Depth*Season + 1|Sample Date* (R^2 conditional = 0.92, R^2 marginal = 0.66, AIC = 99.1) (Figure 4). In this case, each of the predictors was statistically significant (DSIO, $p = 0.00071$; ice-period, $p = 0.0035$; Depth*Season, $p = 0.028$).

In the ice-covered season, here described as "winter" but extending into late July at Spuller, Tioga, Saddlebag, and Lower Gaylor, epilimnetic and outlet CO_2 concentrations were not significantly correlated with any of the explanatory variables (Table 5). Within the hypolimnion, the day of year, basin SWE, length of ice-covered period, days before ice-off, and watershed area were strongly and significantly correlated with CO_2.

Ice-free season surface, hypolimnion, outlet, and winter surface CO_2 concentrations were not significantly different ($p > 0.05$) between lakes and reservoirs (Table 6). Summer outlet export of CO_2 was significantly higher from reservoirs than lakes ($p = 0.004$).

Net ecosystem production was variable between net autotrophy and net heterotrophy, across depth, site, and time. Volumetric rates of NEP (Table 7) ranged from -9.2 μmol L^{-1} day^{-1} (Rock Creek, 2 m depth, September) to 10.9 μmol L^{-1} day^{-1} (Tioga, 5 m depth, August). Volumetric rates of CR and GPP generally increased with depth, ranging from -0.8 to -21.2 μmol L^{-1} day^{-1} and 0.2 to 20.7 μmol L^{-1} day^{-1}, respectively. Areal estimates of NEP (Table 8) also varied between net heterotrophy and net autotrophy, from -14.2 mmol m^{-2} day^{-1} (Rock Creek, September) to 33.9 mmol m^{-2} day^{-1} (Tioga, August).

Discussion

Concentrations of CO_2 were highest under ice and decreased rapidly after ice-off (Figure 2), a decline observed in other seasonally ice-covered lakes (Denfeld et al. 2018). Chamber deployments were not frequent enough to determine whether most spring gas evasion in these lakes and reservoirs occurs primarily during brief pulses, but flux decreased rapidly in the first 40 days after ice-off (Figure 3). Slight supersaturation and CO_2 evasion persisted at most sites into autumn, suggesting that supersaturation can be maintained by periods of heterotrophy, terrestrial inputs, and sediment respiration. By August, near-surface CO_2 had decreased to below 200% of saturation at all sites, resulting in low positive fluxes, or negative fluxes when surface water was undersaturated in CO_2.

Rising water temperatures cause a decrease in gas solubility, which contributed to the observed decrease of CO_2 and dissolved oxygen. The effect of biological productivity could not explain the decrease, as computed NEP was nearly balanced, and positive in some cases. Though temperature was not included in the mixed modeling due to collinearity with other variables, in years when Sierra snowpack was high, such as 2017 when April 1 SWE was ~200% of normal, Sierra lake temperature rose 1 °C $month^{-1}$ slower than in a drought year, and peaked at a slightly lower temperature than in low snow years (Sadro et al. 2018b). Thus in drought years, higher temperatures will drive gas solubility lower than in a high snowpack year, which would cause additional evasion, but this is mediated by the length of the ice-covered period, a direct result of SWE. Positive correlations between temperature and dissolved CO_2 are apparent at continental scales (Kosten et al. 2010), but this occurs as the result of increasing net heterotrophy, which was not observed here. Similarly, late-season observations of CO_2 undersaturation might be the result of cooling rather than biological

activity, as net heterotrophy was observed during the fall metabolism deployment, and concentrations of chl-a were similar to those in the mid-summer.

Though allochthonous DOC inputs are predicted to influence aquatic CO_2 concentrations (Jonsson et al. 2003; Lapierre et al. 2013), DOC did not emerge as a strong predictor of dissolved CO_2 in this study. Sierra lakes are oligotrophic (Sadro et al. 2012) and can be driven to net heterotrophy during intervals of high DOC input (Sadro et. al 2011b), but these short periods of heterotrophy typically occur in late spring and early summer, when gas evasion was found to be highest. Although brief 'fertilizing' effects of allochthonous DOC on Sierra lake metabolism can drive periods of heterotrophy (Sadro and Melack, 2012), this may be outweighed by evasion of accumulated winter CO_2.

Spatial and temporal variability of metabolic rates calculated from measurements of free-water dissolved oxygen suggest a weak relationship between aquatic pCO_2 and metabolism. A total of six deployments in two lakes and two reservoirs allowed calculation of NEP, CR, and GPP (Tables 7, 8). Differences in metabolism between lakes and reservoirs in three adjacent basins which span a small range of characteristics including watershed area, bare and wet meadow area, and minimum elevation (Table 1), measured over a 3-day stratified period in August, suggest lake-specific characteristics which were not quantified here are a major control on metabolism, including benthic respiration rates in both littoral and pelagic habitats. One reservoir (Tioga) and a lake (Lower Gaylor) were net heterotrophic in mid-August, while a second reservoir (Saddlebag) was net autotrophic at the same period. Although both CR and GPP generally increased with depth across all three sites, NEP varied from net heterotrophy to net autotrophy with no clear relationship to depth. This suggests that the contribution of aquatic metabolism to pCO_2 can be more complex than would be

expected where NEP shifts from net autotrophy near the surface to net heterotrophy below the thermocline as observed by Sadro et al. (2011a). In both lakes and reservoirs, summer hypolimnetic CO_2 was elevated relative to the surface, which cannot be explained by pelagic metabolism as net autotrophy was often observed. All sites were stratified in midsummer, and an interactive effect of season and depth was a significant predictor of CO_2, suggesting the persistence of elevated CO_2 at depth in summer is more strongly controlled by reduced vertical flux across the thermocline. That buoyancy frequency (as a measure of the strength of stratification) was a poor predictor of summer dissolved CO_2 may suggest that stratification is sufficiently high at all sites in midsummer to reduce vertical diffusion, and instead vertical flux is mediated by the depth at which hypolimnetic CO_2 has accumulated. More frequent sampling of pCO_2 in conjunction with long-term measurements of metabolism would be required to determine its control on the gradual decrease of CO_2 observed here.

Under-ice concentrations of CO_2 in late spring were not correlated with DO, suggesting that water column community respiration (CR) is not the primary source of winter CO_2 accumulation. In most cases, DO under ice remained at or near saturation despite supersaturation of CO_2. Inflow streams may provide some CO_2 to the lakes as a result of upstream processing (Crawford et al. 2015; Weyhenmeyer et al. 2012) but this cannot be quantified as inflows were not sampled. In Rocky Mountain National Park, Crawford et al. (2015) found that high mountain headwater streams were supersaturated in CO_2 even in winter, suggesting that inflow streams could be sources of CO_2 to high Sierra lakes. However, the lack of a statistically significant correlation between winter pCO_2 and lake network number suggests upstream processing is not a major winter contributor. A lake's position within a chain of lakes (lake network number, LNN) can partially explain its

chemistry (Sadro et al. 2012), but in this case, lake network number was not a significant predictor of ice-free season CO_2 nor was it included in the best mixed models, and additionally had no significant correlation with under-ice CO_2 (Table 5). Similarly, the proportion of each watershed that is bare (PBare, as rock or ice) or wet meadow were expected to be negatively and positively related with summer pCO_2, respectively. These expectations were based on previous work which found that across 11 lake-chain catchments throughout the Sierra, shrub cover explained 42% of the variability in lake surface DOC (Sadro et al. 2012), a pattern also observed in the north-central United States (Gergel et al. 1999), and the Rocky Mountains (Hood et al. 2005). Wet meadows are known to be a particularly important contributor of DOC to downstream lakes (Gergel et al. 1999; Hood et al. 2005), though their significance was not examined in the Sierra (Sadro et al. 2012). The lack of a significant relationship between DOC and CO_2 in this study might explain the lack of an association between CO_2 and watershed meadow proportion, which was expected to represent differences in DOC inputs from each catchment. However, PBare was present in four of the five best models of summer CO_2, which may reflect a combination of watershed elevation, soil cover, and possibly local variation in SWE not captured by the station data used here. LNN and watershed area were poor predictors of summer surface pCO_2, which may be partially explained by the timing of ice-off, where time since ice-off outweighed any effect of the watershed on lake chemistry, particularly as lower LNN lakes are necessarily higher in the catchments, and here thawed much later than lower elevation sites.

Benthic respiration is likely the major contributor to high-elevation Sierra lake CO_2. At Emerald Lake in the southern Sierra, benthic CR during the ice-free season is on average 37.3 ± 15.8 mmol O_2 m^2 day^{-1}, a rate which declines with decreasing temperature but results

in a consistently net heterotrophic benthos (Sadro et al. 2011b); this is common in lake sediments (Gudasz et al. 2010). In the Arctic, where MacIntyre et al. (2018) incubated benthic lake sediments at ambient under-ice temperatures, respiration rates ranged from 9 to 24 mmol O_2 m^2 day^{-1}. Under-ice temperatures of bottom water in the Arctic are no different than in the Sierra (4° C), thus despite differences in organic carbon content of sediments, the winter rates found in the Arctic may be similar to those in the Sierra. Applying the low end of this range over the duration of ice-cover found for lakes and reservoirs in this study, total winter accumulation of CO_2 from benthic respiration, assuming a respiratory quotient of 1, would range from 1.8 to 2.6 mmol m^{-2}. Winter near-bottom DO was <5 mg L^{-1} in some lakes and less frequently in reservoirs, while remained fully saturated in the upper water column, suggesting that under-ice benthic respiration contributes a substantial portion of accumulated hypolimnetic CO_2. However, under-ice CO_2 remained high in South and Tioga reservoirs, despite a fully oxygenated hypolimnion, potentially reflecting advection of bottom waters via the dam outlet. Benthic organic matter quality and quantity influences respiration rates (den Heyer and Kalff, 1998), and thus differences in substrate may aid in explaining the differences in winter hypolimnetic CO_2 accumulation, but little work has been done to characterize benthic substrates in Sierra lakes (Melack et al. 1998; Sadro et al. 2011b).

Winter hypolimnetic CO_2 had a strong, positive and significant correlation with day of year, length of the ice covered period, and local SWE (Table 5). An extended period of ice cover allows CO_2 to continue to accumulate before fluxes to the atmosphere can begin, although the reservoirs examined in this study are managed such that they discharge stored water from the base of their impounding dam, year round. Importantly, time since ice-off and the length of the ice-covered period were the strongest and most important predictors of

summer surface CO_2 concentrations, reflecting evasion after ice-off, but also the accumulation of CO_2 described above. Time since ice-off and the ice-covered period can both be determined via satellite imagery as described in the methods, thus CO_2 concentrations during summer could potentially be predicted with a smaller model that requires no physical sampling. Using only remotely sensed predictors to fit a new mixed model to the CO_2 concentrations observed in this study, with sample date as a random effect : *log(μM) ~ DSIO + Ice period + 1|Sample Date* (R^2 marginal = 0.53, R^2 conditional = 0.70), DSIO remains highly significant (p = <0.001) and ice-period nears significance (p = 0.074), which should allow for reasonable approximations of summer lake surface CO_2 in the high Sierra without the need for sample collection.

The reservoirs in this study release water from the base of the dam that impounds them, and though overflow from the reservoir surfaces is possible, it occurs rarely and contributes only a small portion to downstream flow. Thus, while most of the natural lake outlets in this study stop flowing in winter, reservoirs continue to release water from under ice, as SCE manages flow for various purposes downstream. Summer reservoir outlet concentrations were slightly higher (median 31.1 μM) than lakes (median 22.8 μM), though this difference was not significant (p = 0.08). Concentrations of CO_2 were elevated in both lake and reservoir bottom waters, particularly under ice and for a brief period following spring thaw. Elevated CO_2 in reservoir outlet streams reflects the release of hypolimnetic water, whereas the natural lakes discharge water from their surface.

Export of CO_2 in outlet streams, computed from discharge and outlet concentration, for reservoirs in summer (30 mmol CO_2 s^{-1}) was significantly higher than from lakes (4.5 mmol CO_2 s^{-1}, p = 0.004). Although median reservoir outlet concentrations were only slightly

higher, discharge was higher below reservoirs than lakes, especially prior to peak snowmelt. In Canadian seasonally frozen reservoirs, discharge of water from depth alters the seasonality of CO_2 emissions rather than the total annual flux, by releasing gases that would otherwise be trapped under-ice and released after ice-off as in natural lakes (Roehm and Tremblay, 2006). This finding suggests that in the Sierra, the elevated export of CO_2 in winter and spring from reservoir outlets relative to lakes should be offset by reduced summer fluxes from reservoirs. However, median reservoir fluxes (0.2 mmol CO_2 m^{-2} hr^{-1}) were similar to lake median fluxes (0.2 mmol CO_2 m^{-2} hr^{-1}), and the difference was insignificant ($p = 0.317$). In the Sierra, it is thus unclear whether spring reservoir export of hypolimnetic CO_2 shifts the timing of emissions without altering the total, or whether combined reservoir export and flux is greater than that of similar lakes.

Comparing the results of this study to other regions, median summer surface concentrations of 23.7 μM for lakes and 21.1 μM for reservoirs were lower than lakes and reservoirs in the Alpine region of Europe (Pighini et al. 2018; Diem et al. 2012) and non-arctic North American lakes (Cole et al. 1994), and more than an order of magnitude lower than tropical reservoirs and lakes (Abril et al. 2006; Melack 2016). Given the low DOC concentrations, relatively low temperatures, and low metabolic rates, but combined with 6-9 months of ice cover allowing for accumulation, weak supersaturation of surface CO_2 would be expected in subalpine and alpine systems where benthic respiration contributes CO_2 to the overlying system.

Median summer fluxes of CO_2 from lakes (260 mg CO_2 m^{-2} d^{-1}) and reservoirs (191 mg CO_2 m^{-2} d^{-1}) were not significantly different ($p = 0.317$) and are an order of magnitude lower than fluxes from North American temperate reservoirs (Barros et al. 2011), and about a

fifth that of European Alpine reservoirs (Diem et al. 2012). Previous work has shown subalpine and alpine reservoir contribution to global CO_2 emissions to be small (Diem et al. 2012), and this study confirms that high elevation alpine reservoirs as well as natural alpine lakes are likely small overall contributors to global emissions.

References

Abril, G., S. Richard, and F. Guérin. 2006. In situ measurements of dissolved gases (CO_2 and CH_4) in a wide range of concentrations in a tropical reservoir using an equilibrator. Sci. Total Environ. 354: 246–251. doi:10.1016/j.scitotenv.2004.12.051

Bair, E. H., J. Dozier, R. E. Davis, M. T. Colee, and K. J. Claffey. 2015. CUES—a study site for measuring snowpack energy balance in the Sierra Nevada. Front. Earth Sci. 3. doi:10.3389/feart.2015.00058

Barros, N., J. J. Cole, L. J. Tranvik, Y. T. Prairie, D. Bastviken, V. L. M. Huszar, P. del Giorgio, and F. Roland. 2011. Carbon emission from hydroelectric reservoirs linked to reservoir age and latitude. Nat. Geosci. 4: 593–596. doi:10.1038/ngeo1211

Bastviken, D., I. Sundgren, S. Natchimuthu, H. Reyier, and M. Gålfalk. 2015. Technical Note: Cost-efficient approaches to measure carbon dioxide (CO2) fluxes and concentrations in terrestrial and aquatic environments using mini loggers. Biogeosciences 12: 3849–3859. doi:10.5194/bg-12-3849-2015

Benson, B. B., and D. Krause. 1984. The concentration and isotopic fractionation of oxygen dissolved in freshwater and seawater in equilibrium with the atmosphere. Limnol. Oceanogr. 29: 620–632. doi:10.4319/lo.1984.29.3.0620

Cole, J. J., Y. T. Prairie, N. F. Caraco, and others. 2007. Plumbing the global carbon cycle: integrating inland waters into the terrestrial carbon budget. Ecosystems 10: 172–185. doi:10.1007/s10021-006-9013-8

Cole, J. J., and N. F. Caraco. 1998. Atmospheric exchange of carbon dioxide in a low-wind oligotrophic lake measured by the addition of SF6. Limnol. Oceanogr. 43: 647–656. doi:10.4319/lo.1998.43.4.0647

Cole, J. J., N. F. Caraco, G. W. Kling, and T. K. Kratz. 1994. Carbon dioxide supersaturation in the surface waters of lakes. Science (80). 265: 1568–1570. doi:10.1126/science.265.5178.1568

Crawford, J. T., M. M. Dornblaser, E. H. Stanley, D. W. Clow, and R. G. Striegl. 2015. Source limitation of carbon gas emissions in high-elevation mountain streams and lakes. J. Geophys. Res. Biogeosciences 120: 952–964. doi:10.1002/2014JG002861

DelSontro, T., D. F. McGinnis, S. Sobek, I. Ostrovsky, and B. Wehrli. 2010. Extreme methane emissions from a Swiss hydropower reservoir: contribution from bubbling sediments. Environ. Sci. Technol. 44: 2419–2425. doi:10.1021/es9031369

Denfeld, B. A., H. M. Baulch, P. A. del Giorgio, S. E. Hampton, and J. Karlsson. 2018. A synthesis of carbon dioxide and methane dynamics during the ice-covered period of northern lakes. Limnol. Oceanogr. Lett. 3: 117–131. doi:10.1002/lol2.10079

Diem, T., S. Koch, S. Schwarzenbach, B. Wehrli, and C. J. Schubert. 2012. Greenhouse gas emissions (CO_2, CH_4, and N_2O) from several perialpine and alpine hydropower reservoirs by diffusion and loss in turbines. Aquat. Sci. 74: 619–635. doi:10.1007/s00027-012-0256-5

Ducharme-Riel, V., D. Vachon, P. A. del Giorgio, and Y. T. Prairie. 2015. The relative contribution of winter under-ice and summer hypolimnetic CO2 accumulation to the annual CO2 emissions from northern lakes. Ecosystems 18: 547–559. doi:10.1007/s10021-015-9846-0

Garcia, H. E., and L. I. Gordon. 1992. Oxygen solubility in seawater: Better fitting equations. Limnol. Oceanogr. 37: 1307–1312. doi:10.4319/lo.1992.37.6.1307

Gergel, S. E., M. G. Turner, and T. K. Kratz. 1999. Dissolved organic carbon as an indicator of the scale of watershed influence on lakes and rivers. Ecol. Appl. 9: 1377–1390. doi:10.1890/1051-0761(1999)009[1377:DOCAAI]2.0.CO;2

Gudasz, C., D. Bastviken, K. Steger, K. Premke, S. Sobek, and L. J. Tranvik. 2010. Temperature-controlled organic carbon mineralization in lake sediments. Nature 466: 478–481. doi:10.1038/nature09186

Heyer, C. den, and J. Kalff. 1998. Organic matter mineralization rates in sediments: A within- and among-lake study. Limnol. Oceanogr. 43: 695–705. doi:10.4319/lo.1998.43.4.0695

Hood, E., M. W. Williams, and D. M. McKnight. 2005. Sources of dissolved organic matter (DOM) in a Rocky Mountain stream using chemical fractionation and stable isotopes. Biogeochemistry 74: 231–255. doi:10.1007/s10533-004-4322-5

Jähne, B., K. O. Münnich, R. Bösinger, A. Dutzi, W. Huber, and P. Libner. 1987. On the parameters influencing air-water gas exchange. J. Geophys. Res. Ocean. 92: 1937–1949. doi:10.1029/JC092iC02p01937

Jonsson, A., J. Karlsson, and M. Jansson. 2003. Sources of carbon dioxide supersaturation in clearwater and humic lakes in northern Sweden. Ecosystems 6: 224–235.

Karlsson, J., R. Giesler, J. Persson, and E. Lundin. 2013. High emission of carbon dioxide and methane during ice thaw in high latitude lakes. Geophys. Res. Lett. 40: 1123–1127. doi:10.1002/grl.50152

Kling, G. W., G. W. Kipphut, and M. C. Miller. 1991. Arctic lakes and streams as gas conduits to the atmosphere: implications for tundra carbon budgets. Science (80-.). 251: 298–301.

Kling, G. W., G. W. Kipphut, and M. C. Miller. 1992. The flux of CO2 and CH4 from lakes and rivers in arctic Alaska. Hydrobiologia 240: 23–36. doi:10.1007/BF00013449

Kosten, S., F. Roland, D. M. L. D. M. Marques, E. H. Van Nes, N. Mazzeo, L. da S. L. Sternberg, M. Scheffer, and J. J. Cole. 2010. Climate-dependent CO2 emissions from lakes. Global Biogeochem. Cycles 24. doi:10.1029/2009GB003618

Lapierre, J.-F., F. Guillemette, M. Berggren, and P. A. del Giorgio. 2013. Increases in terrestrially derived carbon stimulate organic carbon processing and CO_2 emissions in boreal aquatic ecosystems. Nat. Commun. 4: 2972. doi:10.1038/ncomms3972

MacIntyre, S., A. Cortés, and S. Sadro. 2018. Sediment respiration drives circulation and production of CO2 in ice-covered Alaskan arctic lakes. Limnol. Oceanogr. Lett. 3: 302–310. doi:10.1002/lol2.10083

Melack, J. M. 2016. Aquatic Ecosystems, p. 119–148. *In* L. Nagy, B.R. Forsberg, and P. Artaxo [eds.], Interactions Between Biosphere, Atmosphere and Human Land Use in the Amazon Basin. Springer Berlin Heidelberg.

Melack, J., J. O. Sickman, A. Leydecker, and D. Marrett. 1998. Comparative analyses of high-altitude lakes and catchments in the Sierra Nevada: susceptibility to acidification, final report, contract 032-188. Calif. Air Resour. Board.

Odum, H. T. 1956. Primary production in flowing waters. Limnol. Oceanogr. 1: 102–117. doi:10.4319/lo.1956.1.2.0102

Pighini, S., M. Ventura, F. Miglietta, and G. Wohlfahrt. 2018. Dissolved greenhouse gas concentrations in 40 lakes in the Alpine area. Aquat. Sci. 80: 32. doi:10.1007/s00027-018-0583-2

Podgrajsek, E., E. Sahlée, D. Bastviken, J. Holst, A. Lindroth, L. Tranvik, and A. Rutgersson. 2014. Comparison of floating chamber and eddy covariance measurements of lake greenhouse gas fluxes. Biogeosciences 11: 4225–4233. doi:https://doi.org/10.5194/bg-11-4225-2014

Raymond, P. A., J. Hartmann, R. Lauerwald, and others. 2013. Global carbon dioxide emissions from inland waters. Nature 503: 355–359. doi:10.1038/nature12760

Roehm, C., and A. Tremblay. 2006. Role of turbines in the carbon dioxide emissions from two boreal reservoirs, Québec, Canada. J. Geophys. Res. Atmos. 111. doi:10.1029/2006JD007292

Sadro, S., and J. M. Melack. 2012. The effect of an extreme rain event on the biogeochemistry and ecosystem metabolism of an oligotrophic high-elevation lake. Arctic, Antarct. Alp. Res. 44: 222–231. doi:10.1657/1938-4246-44.2.222

Sadro, S., J. M. Melack, and S. MacIntyre. 2011. Depth-integrated estimates of ecosystem metabolism in a high-elevation lake (Emerald Lake, Sierra Nevada, California). Limnol. Oceanogr. 56: 1764–1780. doi:10.4319/lo.2011.56.5.1764

Sadro, S., J. M. Melack, and S. MacIntyre. 2011. Spatial and temporal variability in the ecosystem metabolism of a high-elevation lake: integrating benthic and pelagic habitats. Ecosystems 14: 1123–1140.

Sadro, S., J. M. Melack, J. O. Sickman, and K. Skeen. 2019. Climate warming response of mountain lakes affected by variations in snow. Limnol. Oceanogr. Lett. 4: 9–17. doi:10.1002/lol2.10099

Sadro, S., C. E. Nelson, and J. M. Melack. 2012. The influence of landscape position and catchment characteristics on aquatic biogeochemistry in high-elevation lake-chains. Ecosystems 15: 363–386.

Sadro, S., J. O. Sickman, J. M. Melack, and K. Skeen. 2018. Effects of climate variability on snowmelt and implications for organic matter in a high-elevation lake. Water Resour. Res. 54: 4563–4578. doi:10.1029/2017WR022163

Survey, C. C. S. 2018. Snow Course Measurements for April 2017. Calif. Data Exch. Cent.

Wanninkhof, R. 2014. Relationship between wind speed and gas exchange over the ocean revisited. Limnol. Oceanogr. Methods 12: 351–362. doi:10.4319/lom.2014.12.351

Weiss, R. F. 1974. Carbon dioxide in water and seawater: the solubility of a non-ideal gas. Mar. Chem. 2: 203–215. doi:10.1016/0304-4203(74)90015-2

Weyhenmeyer, G. A., P. Kortelainen, S. Sobek, R. Müller, and M. Rantakari. 2012. Carbon dioxide in boreal surface waters: A comparison of lakes and streams. Ecosystems 15: 1295–1307. doi:10.1007/s10021-012-9585-4

Wilde, F. D., M. W. Sandstrom, and S. C. Skrobialowski. 2014. Chapter A2. Selection of Equipment for Water Sampling. U.S. Geological Survey.

Table 1: Characteristics of each sampled lake (L) or reservoir (R); location (‘latitude’, ‘longitude’), elevation above sea level (m), maximum depth (m), water surface area (ha), watershed area (ha), lake network number (‘LNN’), percent of the watershed that is bare rock (‘Bare’) and percent of the watershed that is wet meadow (‘Meadow’).

Site	***Latitude***	***Longitude***	***Elevation (m)***	***Maximum Depth (m)***	***Surface Area (ha)***	***Watershed Area (ha)***	***LNN***	***Bare***	***Meadow***
Crystal (L)	37° 35' 39" N	119° 01' 07" W	2932	19	5	95	0	25.2	0
Ellery (R)	37° 56' 07" N	119° 14' 07" W	2901	4	25	4139	5	45.5	3.2
Lower Gaylor (L)	37° 54' 50" N	119° 16' 06" W	3155	13	9.5	99	1	36.7	17.8
Rock Creek (L)	37° 27' 14" N	118° 44' 13" W	2957	24	23	3116	9	55.7	0.46
Ruby (L)	37° 24' 55" N	118° 46' 01" W	3383	34	15	449	1	84.7	0
Sabrina (R)	37° 12' 35" N	118° 36' 50" W	2782	19	76	4334	6	49.1	0.85
Saddlebag (R)	37° 58' 01" N	119° 16' 06" W	3068	22	124	1801	4	51.1	2.4
South (R)	37° 10' 07" N	118° 34' 12" W	2977	10	69	3277	5	55.7	0.08
Spuller (L)	37° 56' 55" N	119° 17' 05" W	3124	5.5	1.9	137	0	68.2	0
Tioga (R)	37° 55' 35" N	119° 15' 10" W	2937	16	29	980	0	48.9	8.79

Table 2: Dates of ice-on, ice-off, ice-covered period, and April 1 snow water equivalent 'SWE' for study sites. Ice-on and ice-off dates were obtained with ±4 day accuracy, from Landsat imagery. Ice-off dates confirmed to ±1 day in the field at Tioga, Spuller, Lower Gaylor, Saddlebag, and Ruby. Ice-covered period is the length of time between ice-on in 2016 and ice-off in 2017. April 1 SWE (mm) is obtained from California Cooperative Snow Survey measurement sites nearest to each lake or reservoir.

Site	*Ice-on 2016*	*Ice-off 2017*	*Ice-covered period (days)*	*April 1 SWE (mm)*
Ellery	11/24/16	6/12/17	200	160
Tioga	11/24/16	7/4/17	222	138
Spuller	10/15/16	8/1/17	290	164
Gaylor	11/24/16	7/22/17	240	138
Saddlebag	12/10/16	7/22/17	224	164
Crystal	12/2/16	6/30/17	210	208
Ruby	12/2/16	7/14/17	224	132
Rock Creek	12/11/16	6/2/17	173	80
Sabrina	12/23/16	5/10/17	138	61
South	12/23/16	6/3/17	162	61

Table 3: All CO_2 concentration data collected for this study during winter, spring, summer, and fall of 2017. 'Season' describes individual stratification conditions of lake or reservoir rather than calendar dates: winter is under ice, spring is mixing after ice-off, summer is the stratified period after spring mixing, and fall is the mixed period after the breakdown of summer stratification. 'Location' describes depth of sampling: epilimnion is 0.2 m during both stratified and mixed periods, hypolimnion is 2 m below thermocline during stratified periods, and outlet is the lake or reservoir outlet stream. Percent saturation (%) is computed from local water temperature, air pressure, and CO_2 concentration.

Sample Date	***Site***	***Season***	***Location***	***Type***	***μM CO_2***	***% Sat***
7/2/17	Crystal	spring	epilimnion	lake	67.3	377
7/2/17	Crystal	spring	outlet	lake	38.5	216
7/23/17	Crystal	summer	epilimnion	lake	36.4	204
7/23/17	Crystal	summer	outlet	lake	27.6	154
8/15/17	Crystal	summer	epilimnion	lake	27.2	152
8/15/17	Crystal	summer	hypolimnion	lake	28.0	157
8/15/17	Crystal	summer	outlet	lake	25.8	145
9/18/17	Crystal	fall	epilimnion	lake	23.7	130
9/18/17	Crystal	fall	outlet	lake	22.8	125
6/4/17	Ellery	winter	epilimnion	reservoir	131.7	760
7/3/17	Ellery	spring	epilimnion	reservoir	28.6	160
7/3/17	Ellery	spring	outlet	reservoir	30.0	168
7/18/17	Ellery	summer	epilimnion	reservoir	17.6	98

7/18/17	Ellery	summer	outlet	reservoir	24.0	134
8/19/17	Ellery	summer	hypolimnion	reservoir	25.5	143
8/19/17	Ellery	summer	outlet	reservoir	34.5	193
9/20/17	Ellery	fall	epilimnion	reservoir	21.1	115
7/3/17	Gaylor	winter	epilimnion	lake	78.9	441
7/3/17	Gaylor	winter	outlet	lake	68.7	384
7/12/17	Gaylor	spring	epilimnion	lake	91.3	511
7/12/17	Gaylor	spring	outlet	lake	88.1	493
7/24/17	Gaylor	summer	epilimnion	lake	48.2	270
7/24/17	Gaylor	summer	hypolimnion	lake	56.3	315
8/20/17	Gaylor	summer	epilimnion	lake	15.9	89
9/21/17	Gaylor	fall	epilimnion	lake	17.0	93
8/20/17	Gaylor	summer	hypolimnion	lake	27.9	156
8/20/17	Gaylor	summer	outlet	lake	15.2	85
6/1/17	Rock Creek	winter	epilimnion	lake	100.8	581
6/1/17	Rock Creek	winter	hypolimnion	lake	235.7	1359
7/4/17	Rock Creek	spring	epilimnion	lake	21.9	123
7/4/17	Rock Creek	spring	outlet	lake	15.5	87
7/17/17	Rock Creek	summer	epilimnion	lake	19.2	107
7/17/17	Rock Creek	summer	outlet	lake	15.7	88
8/10/17	Rock Creek	summer	outlet	lake	21.3	119
8/21/17	Rock Creek	summer	hypolimnion	lake	50.6	283
9/19/17	Rock Creek	fall	epilimnion	lake	15.1	83
9/19/17	Rock Creek	fall	hypolimnion	lake	67.8	371
7/27/17	Ruby	summer	epilimnion	lake	28.1	158

7/27/17	Ruby	summer	hypolimnion	lake	35.1	196
7/27/17	Ruby	summer	outlet	lake	34.6	194
9/19/17	Ruby	fall	epilimnion	lake	19.6	107
9/19/17	Ruby	fall	outlet	lake	15.9	87
9/19/17	Ruby	fall	hypolimnion	lake	86.3	473
6/2/17	Sabrina	winter	epilimnion	reservoir	50.7	292
6/2/17	Sabrina	winter	hypolimnion	reservoir	52.3	302
6/2/17	Sabrina	winter	outlet	reservoir	48.3	279
7/5/17	Sabrina	spring	epilimnion	reservoir	15.1	84
7/5/17	Sabrina	spring	outlet	reservoir	27.5	154
7/14/17	Sabrina	summer	outlet	reservoir	18.1	101
9/17/17	Sabrina	fall	epilimnion	reservoir	16.6	91
7/7/17	Saddlebag	spring	epilimnion	reservoir	22.3	125
7/7/17	Saddlebag	spring	outlet	reservoir	38.2	214
7/18/17	Saddlebag	summer	epilimnion	reservoir	45.9	257
7/18/17	Saddlebag	summer	outlet	reservoir	55.8	312
8/19/17	Saddlebag	summer	outlet	reservoir	33.6	188
8/20/17	Saddlebag	summer	epilimnion	reservoir	16.3	91
8/20/17	Saddlebag	summer	hypolimnion	reservoir	77.7	435
9/21/17	Saddlebag	fall	epilimnion	reservoir	18.6	102
9/21/17	Saddlebag	fall	outlet	reservoir	18.1	99
6/2/17	South	winter	outlet	reservoir	59.7	344
6/2/17	South	winter	epilimnion	reservoir	115.8	668
6/2/17	South	winter	hypolimnion	reservoir	133.2	768
7/5/17	South	summer	epilimnion	reservoir	22.8	127

7/5/17	South	summer	outlet	reservoir	107.8	590
7/14/17	South	summer	epilimnion	reservoir	23.7	133
7/14/17	South	summer	outlet	reservoir	50.8	284
9/17/17	South	fall	epilimnion	reservoir	20.3	111
9/17/17	South	fall	hypolimnion	reservoir	22.2	121
9/17/17	South	fall	outlet	reservoir	30.1	165
7/7/17	Spuller	winter	epilimnion	lake	44.6	250
7/7/17	Spuller	winter	outlet	lake	28.2	158
7/29/17	Spuller	spring	epilimnion	lake	24.3	136
7/29/17	Spuller	spring	hypolimnion	lake	27.2	152
7/29/17	Spuller	summer	outlet	lake	28.4	159
9/20/17	Spuller	fall	outlet	lake	17.7	97
9/20/17	Spuller	fall	epilimnion	lake	15.1	83
6/4/17	Tioga	winter	epilimnion	reservoir	52.9	305
6/4/17	Tioga	winter	hypolimnion	reservoir	438.6	338
7/3/17	Tioga	spring	outlet	reservoir	42.9	240
7/3/17	Tioga	spring	epilimnion	reservoir	48.1	180
7/18/17	Tioga	summer	outlet	reservoir	32.1	124
7/29/17	Tioga	summer	epilimnion	reservoir	22.2	403
7/29/17	Tioga	summer	hypolimnion	reservoir	72.0	127
8/9/17	Tioga	summer	outlet	reservoir	22.7	102
9/20/17	Tioga	fall	epilimnion	reservoir	18.6	269
9/20/17	Tioga	fall	outlet	reservoir	17.5	96

Table 4: Lake and reservoir CO_2 flux (mmol CO_2 m^{-2} hr^{-1}) measured from floating chamber deployments, summer 2017. 'NA' is given where fluxes were too small to be computed. Positive values indicate flux out of the lake or reservoir, negative values indicate uptake into the lake or reservoir.

Date	*Site*	*Type*	*Flux (mmol CO_2 m^{-2} hr^{-1})*
7/2/17	Crystal	lake	0.3
8/15/17	Crystal	lake	0.2
9/18/17	Crystal	lake	1.3
7/3/17	Ellery	reservoir	1.1
7/12/17	Lower Gaylor	lake	0.2
7/24/17	Lower Gaylor	lake	1.2
8/3/17	Lower Gaylor	lake	0.9
8/20/17	Lower Gaylor	lake	0.1
7/4/17	Rock Creek	lake	0.2
7/17/17	Rock Creek	lake	0.2
8/23/17	Rock Creek	lake	-0.5
9/18/17	Rock Creek	lake	1.1
7/28/17	Ruby	lake	0.3
9/15/17	Ruby	lake	-0.4
7/5/17	Sabrina	reservoir	0.4
8/16/17	Sabrina	reservoir	-0.5
9/17/17	Sabrina	reservoir	0.1

7/18/17	Saddlebag	reservoir	0.2
8/20/17	Saddlebag	reservoir	NA
7/5/17	South	reservoir	0.5
8/16/17	South	reservoir	-0.5
9/17/17	South	reservoir	0.1
7/29/17	Spuller	lake	NA
8/24/17	Spuller	lake	NA
9/20/17	Spuller	lake	NA
7/29/17	Tioga	reservoir	0.2
8/24/17	Tioga	reservoir	0.3

	Temperature	DOY	DO	LNN	SWE	Ice-period	DBIO	Elev-ation	Discharge	WRT	Depth	SA	Watershed Area	DOC	Proportion bare	Proportion meadow	Total Volume
Epilimnion	-0.14	-0.33	0.41	0.42	-0.16	-0.32	0.29	-0.11	0.46	0.14	-0.25	0.18	0.32	-0.04	-0.34	0.18	0.32
Hypolimnion	-0.8	0.95*	0.4	-0.4	0.95*	0.98**	0.97*	0.2	-0.8	-0.6	0.06	-0.8	-0.97*	-0.4	-0.32	0.4	-0.8
Outlet	-0.4	-0.32	0.11	0.2	-0.32	-0.2	0.2	0.4	-0.4	0.4	0.4	0.2	-0.4	-0.95	-0.8	0.8	0.4

Table 5: Spearman's rho correlations between winter lake and reservoir epilimnion, hypolimnion, and outlet stream dissolved CO_2 concentrations (μM), to temperature (°C), day of year 'DOY', dissolved oxygen 'DO'(mg L^{-1}), lake network number 'LNN", basin snow water equivalent 'SWE' (mm), length of ice-covered period (days), days before ice-off 'DBIO' (days), elevation (m), discharge (m^3 s^{-1}), water residence time 'WRT' (days), maximum depth (m), water body surface area 'SA' (ha), watershed area (ha), dissolved organic carbon 'DOC' (μM), proportion of the watershed that is bare rock, proportion of watershed that is wet meadow, and water body volume (m^3). Asterisks denote p-value significance levels: * = p <0.05; ** = p < 0.01.

Table 6: Lake and reservoir median dissolved CO_2 concentrations (μM), lake and reservoir summer outlet export (mol s^{-1}) computed from discharge*concentration, and p-values determined from Mann-Whitney U nonparametric mean comparisons.

	Lake Median	***Reservoir Median***	***p-value***
Summer surface concentration	24	21	0.43
Summer hypolimnion concentration	43	49	0.81
Summer outlet concentration	23	31	0.08
Winter surface concentration	79	84	0.63
Summer outlet export	4	30	0.004

Table 7: Computed volumetric net ecosystem productivity (NEP), community respiration (CR), gross primary productivity (GPP) rates (μmol O_2 $L^{-1}day^{-1}$), and the ratio of volumetric gross primary productivity to community respiration, by location, date, and depth (m).

Site	***Date***	***Depth (m)***	***Volumetric NEP (μmol $L^{-1}day^{-1}$)***	***Volumetric CR (μmol $L^{-1}day^{-1}$)***	***Volumetric GPP (μmol $L^{-1}day^{-1}$)***	***GPP:R***
Rock Creek	Jul. 26	0.1	-0.5	-21.2	20.7	1.0
Rock Creek	Jul. 26	2	1.2	-16.2	17.4	1.1
Tioga	Aug. 17	0.1	-1.1	-4.8	3.7	0.8
Tioga	Aug. 17	2	-6.2	-13.3	7.1	0.5
Tioga	Aug. 17	5	-0.1	-17.0	16.9	1.0
Gaylor	Aug. 18	0.1	0.2	-3.3	3.6	1.1
Gaylor	Aug. 18	2	-8.8	-14.5	5.6	0.4
Gaylor	Aug. 18	5	-0.9	-8.2	7.2	0.9
Saddlebag	Aug. 19	0.1	3.7	-1.0	4.7	4.7
Saddlebag	Aug. 19	2	1.3	-3.3	4.6	1.4
Tioga	Aug. 24	0.1	-0.6	-0.8	0.2	0.3
Tioga	Aug. 24	2	0.7	-2.0	2.7	1.4
Tioga	Aug. 24	5	10.9	-3.8	14.7	3.9
Rock Creek	Sept. 18	0.1	1.4	-0.8	2.2	2.8
Rock Creek	Sept. 18	2	-9.2	-12.6	3.6	0.3
Rock Creek	Sept. 18	5	1.8	-1.3	3.1	2.4
Rock Creek	Sept. 18	9	-0.9	-18.0	17.1	1.0

Table 8: Computed areal net ecosystem productivity (NEP), community respiration (CR), gross primary productivity (GPP) rates (mmol O_2 m^{-2} day^{-1}), and the ratio of gross primary productivity to community respiration during the ice-free season of 2017, by site and date, determined from volumetric metabolic rates and water body bathymetry.

Site	*Date*	*Areal NEP (mmol m^{-2} day^{-1})*	*Areal CR (mmol m^{-2} day^{-1})*	*Areal GPP (mmol m^{-2} day^{-1})*	*GPP:CR*
Rock Creek	Jul. 26	1.2	-73.7	74.9	1.0
Tioga	Aug. 17	-14.2	-83.7	69.5	0.8
Gaylor	Aug. 18	-11.8	-32.6	20.8	0.6
Saddlebag	Aug. 19	8.9	-8.3	17.2	2.1
Tioga	Aug. 24	33.9	-16.3	50.2	3.1
Rock Creek	Sept. 18	-13.1	-96.4	80.3	0.8

Figure 1: Study site locations within the Sierra Nevada, California. Background topography was obtained from USGS digital elevation models, park boundaries from the US Forest Service, roads from Tiger Roads, and water bodies from the National Hydrography Dataset.

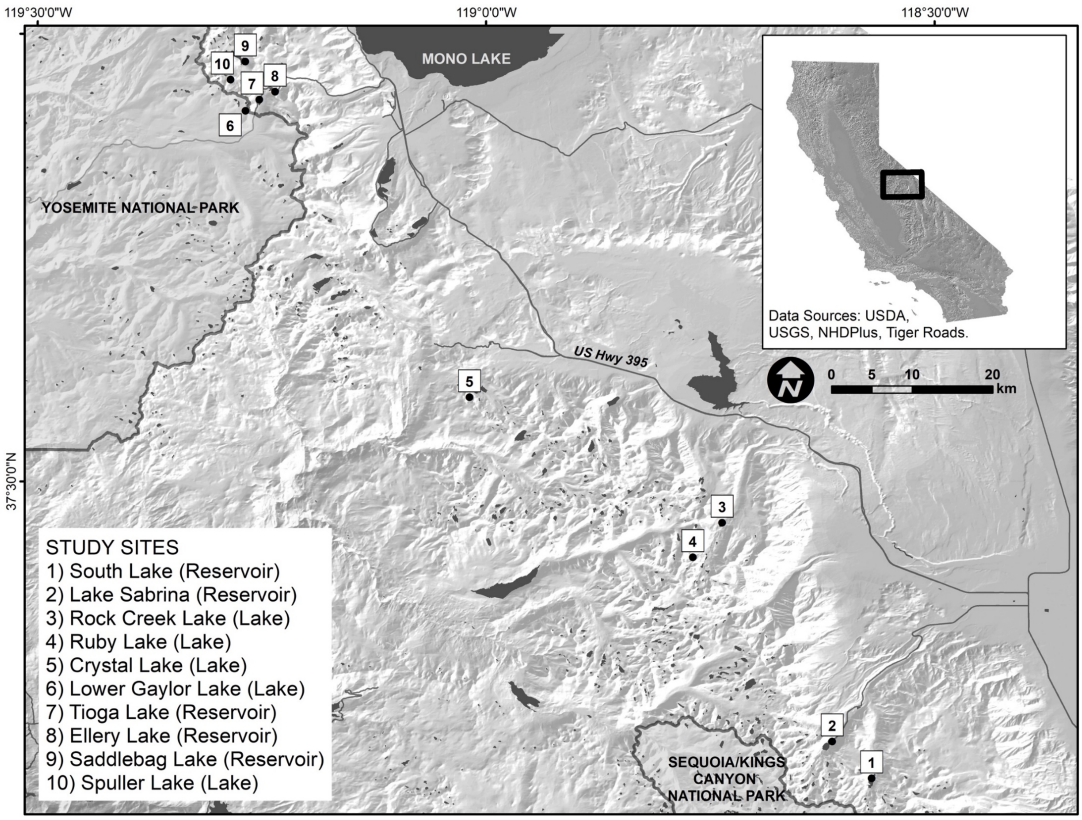

Figure 2: Relationship of lake and reservoir surface CO_2 concentrations (μM) and days since ice-off in 2017 as determined by Landsat 7 & 8 imagery, at all sites, where '0' marks the date of ice-off, and points before '0' are under ice.

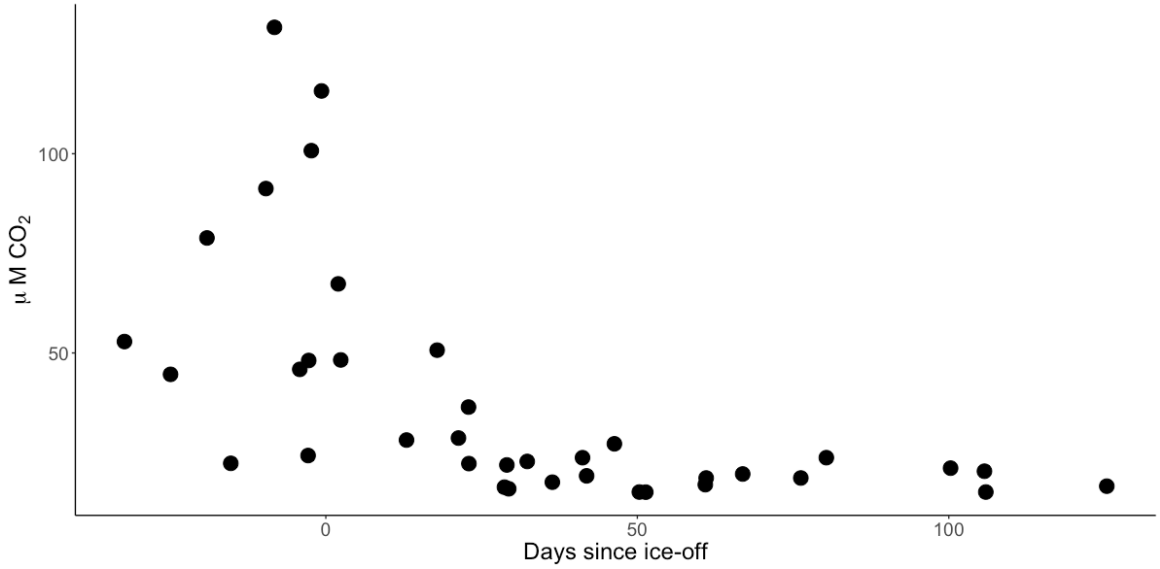

Figure 3: Relationship of lake and reservoir CO_2 fluxes (mmol CO_2 m^{-2} h^{-1}) and days since ice-off. Days since ice-off were determined from Landsat 7 & 8 imagery, where '0' marks the date of ice-off. Lake and reservoir (filled circles and filled triangles, respectively) CO_2 flux (mmol CO_2 m^{-2} hr^{-1}) was measured from floating chamber deployments, summer 2017. Positive values indicate flux emissions from the lake or reservoir, negative values indicate uptake into the lake or reservoir.

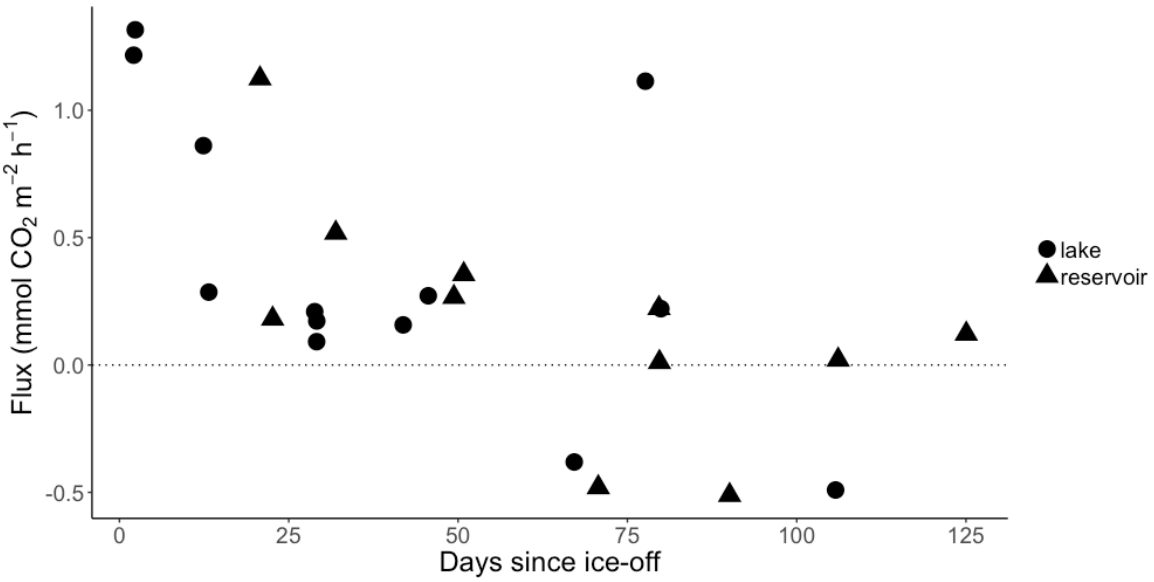

Figure 4: Linear mixed model predicted concentrations of log-transformed CO_2 and observed log-transformed CO_2 concentrations, for surface samples across all seasons in 2017, where *log(μM) ~ Days since ice off + Length of winter ice cover + Depth*Season + 1|Sample Date* (R^2 conditional = 0.92, R^2 marginal = 0.66, AIC = 99.1). Solid line indicates location of 1:1 relationship.